HOST KINASES IN CHLAMYDIA TRACHOMATIS

DEVELOPMENT AND INTERACTIONS OF

INCLUSION MEMBRANE PROTEIN CT226

By

PRAKASH SAH

Bachelor of Science in Microbiology
Tribhuvan University
Kathmandu, Nepal
2007

Master of Science in Microbiology
Tribhuvan University
Kathmandu, Nepal
2012

Submitted to the Faculty of the
Graduate College of the
Oklahoma State University
in partial fulfillment of
the requirements for
the Degree of
DOCTOR OF PHILOSOPHY
December, 2020

HOST KINASES IN CHLAMYDIA TRACHOMATIS

DEVELOPMENT AND INTERACTIONS OF

INCLUSION MEMBRANE PROTEIN CT226

Dissertation Approved:

Dr. Erika Lutter

Dissertation Adviser

Dr. Jeffery Hadwiger

Dr. Marianna Patrauchan

Dr. Karen Wozniak

Dr. Clinton Jones

ACKNOWLEDGEMENTS

I would like to begin by expressing my sincere gratitude to my advisor, Dr. Erika Lutter for providing me with an opportunity to pursue my doctoral study in her laboratory. Coming from antimicrobial resistance research background, when I first approached her to join the lab, I was naturally, interested in the antimicrobial resistance project in the lab. However, I am eternally thankful to her that she encouraged me take on the challenges of studying an intracellular pathogen. I am thankful to her for mentorship and continuous support, both professionally and personally, throughout my stay in her lab.

I would like to thank all my committee member, Dr. Jeff Hadwiger, Dr. Marianna Patrauchan, Dr. Karen Wozniak, and Dr. Clinton Jones for their suggestions and guidance during my doctoral research. I would also like to thank previous committee members, Dr. Ed Shaw and Dr. Jennifer Shaw, for their guidance.

I would like to thank the Department of Microbiology and Molecular Genetics, all the faculty members, staffs, and fellow graduate students. I would also like to thank Lutter lab members for their cooperation and support. I am thankful to Nirakar Adhikari for all his help with moving-in to the Stillwater.

I would like to thank Dr. Kenneth Fields, (University of Kentucky) for sharing plasmids and protocols for the generation of CT226 mutant.

I would like to thank my friends for always being there. A special thanks to my friends, Aawarta and Rita.

I would like to thank my family for their unconditional love and support. I am eternally grateful to my parents for I would not be here, if not for their sacrifices and love. Finally, I am thankful to my wife, Pramila, and my son, Reyansh whose love and support has been my motivation.

Name: PRAKASH SAH

Date of Degree: DECEMBER, 2020

Title of Study: HOST KINASES IN CHLAMYDIA TRACHOMATIS DEVELOPMENT AND INTERACTIONS OF INCLUSION MEMBRANE PROTEIN CT226

Major Field: MICROBIOLOGY, CELL AND MOLECULAR BIOLOGY

Abstract: *Chlamydia trachomatis* is an obligate intracellular pathogen that causes sexually transmitted infections and blinding trachoma. Inside the host cell, *C. trachomatis* replicates within a vacuole called the inclusion. Many of the Host-*Chlamydia* interactions occur at the inclusion membrane where chlamydial inclusion membrane proteins (Incs) as well as several host proteins localize. This study aimed to study the role of host kinases recruited at the inclusion and characterize host interactions of Inc, CT226. In this study, we showed that several isoforms of the host protein kinase C (PKC) are recruited at the inclusion microdomains, PKC substrates localize to the periphery of the inclusion and this recruitment is limited to *C. trachomatis* serovars. PKC substrates were phosphorylated differentially during infection. Pharmacological inhibition of PKC resulted in a modest decrease in infectious progeny production by *C. trachomatis*. Protein kinase A catalytic subunit α (PKA-Cα) and regulatory subunit II α (PKA-RIIα) were found to co-localize with the Golgi marker, golgin-97, close to the inclusion. PKA substrates were found to be recruited to the inclusion periphery in a time dependent manner. Phosphorylation of PKA substrates including glycogen synthase kinase-3β (GSK-3β) increased over time during *C. trachomatis* infection. Pharmacological inhibition of PKA resulted in a decrease in extrusion production by *C. trachomatis*. Investigation of CT226 interactions by co-immunoprecipitation assay showed CT226 interacts with FLII, LRRFIP1, and TMOD3. Recruitment of FLII, LRRFIP1, LRRFIP2, and TMOD3 was observed at the *C. trachomatis* inclusion. Deletion of CT226 resulted in loss of FLII recruitment, altered recruitment of LRRFIP1 and TMOD3, while no effect was seen on LRRFIP2 recruitment. Our data indicate FLII may be the primary host protein interacting with CT226.

TABLE OF CONTENTS

Chapter Page

Chapter Page

LIST OF TABLES

Table Page

LIST OF FIGURES

Figure Page

CHAPTER I

INTRODUCTION AND LITERATURE REVIEW

1.1. Burden of *Chlamydia trachomatis* infections

Chlamydia trachomatis is a Gram-negative intracellular bacterium that causes infections of ocular and genital tract epithelium (Belland, et al. 2004). Different biovars and serovars exhibit distinct tissue tropism. The trachoma biovar comprised of serovars A-C cause trachoma, an ocular infection that is the leading infectious cause of preventable blindness (Resnikoff, et al. 2004). Genital tract biovars comprised of serovars D-K cause sexually transmitted infections (STIs) and are the most frequently reported bacterial STIs in the United States (US) (CDC 2019). Majority of infections are asymptomatic which facilitates transmission of this pathogen. Repeated infections often lead to complications such as pelvic inflammatory disease, ectopic pregnancy and infertility. Furthermore, chlamydial infections can facilitate HIV transmission and have been associated with an increased risk of cervical cancer (Malhotra, et al. 2013; Zhu, et al. 2016). Lymphogranuloma venereum (LGV) biovars comprised of serovars L1-L3 cause invasive infections of the urogenital tract (Malhotra, et al. 2013). Inflammatory response invoked in the host plays an important role in the pathology of the *Chlamydia* infections (Stephens 2003). Although treatable with antibiotics, *C. trachomatis* infections represent a significant economic burden and no effective vaccines exists thus far.

1.2. *C. trachomatis* developmental cycle

C. trachomatis has a unique biphasic developmental cycle (Figure 1.1) consisting of alternation between two distinct forms: the infectious elementary bodies (EBs) and the non-infectious, intracellular reticulate bodies (RBs) (Moulder 1991; Abdelrahman and Belland 2005). Upon contact with host cell, EBs mediate uptake by the host and form a membrane bound compartment called inclusion which are non-fusogenic to lysosomes (Fields and Hackstadt 2002). EBs then transitioned to RBs which replicate inside the inclusion. About mid-way though the life cycle RBs asynchronously start to re-differentiate into EBs. At the end of the life cycle, about 48-72 hours, EBs are released from the host cell via lysis or extrusion to infect neighboring cells (Hybiske and Stephens 2007).

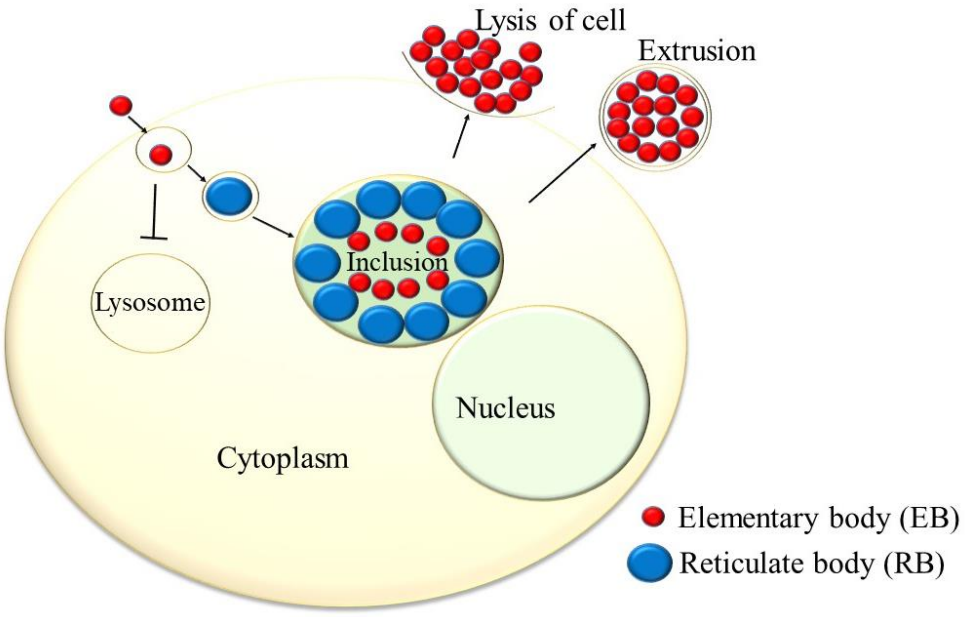

Figure 1.1. Life cycle of *Chlamydia trachomatis*. The infectious EB is internalized into host, upon contact, into a vacuole called inclusion. The inclusion segregates from lysosomal pathway and traffics to peri-Golgi region. EBs convert into RBs which multiply inside the

inclusion and midway through the life cycle re-differentiate into EBs. At the end of 48-72 hours, EBs leave the cells by lysis or extrusion.

1.3. *C. trachomatis* usurps host cell processes for its growth and development

C. trachomatis has a reduced genome lacking genes for proteins in several metabolic pathways and thus depends on the host for its many metabolic requirements (Stephens, et al. 1998). From entry and intracellular development to exit from the host, *C. trachomatis* usurps many host cell processes by expressing an array of effector proteins and maintains contacts with host cell organelles (Bastidas, et al. 2013; Elwell, et al. 2016).

Entry into host cells requires actin remodeling after which the nascent inclusion is transported along microtubules to the microtubule organizing center (MTOC)(Carabeo, et al. 2002; Grieshaber, et al. 2003). As the inclusion develops, it is actively remodeled by the recruitment of host proteins and bacterial effectors on the inclusion membrane (Bastidas, et al. 2013). Vesicular fusion is regulated via recruitment of several host Rab GTPases and soluble N-ethylmaleimide-sensitive factor attachment protein receptors (SNARE) proteins thus avoiding fusion with lysosomes and promoting fusion with nutrient rich exocytic vesicles (Damiani, et al. 2014; Elwell, et al. 2016). *C. trachomatis* rely on host lipids for its intracellular growth and development and has evolved several mechanisms to acquire host derived lipids, recruitment of lipid modifying enzymes and activating signal transduction pathways. Chlamydial strategies to acquire host derived lipids include hijacking vesicular as well as non-vesicular trafficking pathways, recruiting lipid modifying enzymes and activating host signaling pathways (Elwell and Engel 2012). The inclusion maintains a close contact with smooth endoplasmic reticulum (ER) forming an ER-inclusion membrane contact

site (MCS) which may facilitate lipid transport and form a signaling platform (Derre, et al. 2011; Elwell, et al. 2011; Derre 2015). Although *C. trachomatis* inclusions do not associate with mitochondria, depletion of translocase of inner membrane-translocase of outer membrane (TIM-TOM) complex disrupts chlamydial infection (Matsumoto, et al. 1991; Gurumurthy, et al. 2014). Recently, it was shown that mitochondrial dynamics is targeted by *C. trachomatis* for its intracellular survival (Kurihara, et al. 2019). Golgi apparatus is re-organized into mini-stacks that surrounds inclusion in a microtubule-dependent manner, likely increasing the supply of lipids (Heuer, et al. 2009; Al-Zeer, et al. 2014). The growing inclusion is stabilized by a dynamic actin and intermediate filament scaffold as well as a microtubule cage around the inclusion (Kumar and Valdivia 2008; Dumoux, Nans, et al. 2015).

As an intracellular pathogen, it is important for *Chlamydia* to keep its host alive for optimal growth. It is no surprise that *C. trachomatis* infected cells are resistant to pro-apoptotic stimuli and are mediated via activating pro-survival signaling, downregulating pro-apoptotic proteins, upregulating or stabilizing pro-survival proteins and sequestering pro-apoptotic proteins at inclusion (Sharma and Rudel 2009; Elwell, et al. 2016). Recently, it has been shown that under pro-apoptotic conditions, cell death in *Chlamydia*-infected cells shifts from apoptosis to an atypical form of necrosis (Sixt, et al. 2019).

Exit from the host cell is achieved by two mutually exclusive pathways: lysis or extrusion (depicted in Figure 1.1). Lytic exit is preceded by permeabilization of the inclusion membrane followed by the nuclear and plasma membrane leading to host cell death (Hybiske and Stephens 2007). Lytic exit requires actin depolymerization that is regulated by the chlamydial plasmid (Yang, et al. 2015). Extrusion is a packaged release mechanism leaving

the host cell intact. It involves pinching of the inclusion followed by protrusion out of the cell and finally abscission from the host cell (Hybiske and Stephens 2007). Extrusion requires actin polymerization, myosin II, Rho GTPase, host abscission proteins, septins and is also regulated by inclusion membrane proteins (Incs) CT228 and MrcA (Hybiske and Stephens 2007; Chin, et al. 2012; Lutter, et al. 2013; Nguyen, et al. 2018; Zuck and Hybiske 2019).

1.4. Role of host kinases in *C. trachomatis* development and infection

Several host kinases have been shown to be activated and recruited to *C. trachomatis* inclusion that play a role in entry, inclusion development, nutrient acquisition, regulating apoptosis and host cell exit. *C. trachomatis* has its own two serine/threonine kinases, Pkn1 and PknD. Pkn1 has been shown to phosphorylate IncG *in vitro*, although IncG is likely to be phosphorylated by host kinases *in vivo* (Scidmore and Hackstadt 2001; Verma and Maurelli 2003). Translocated actin-recruiting phosphoprotein (TarP) and translocated early phosphoprotein (TepP) are two other examples of chlamydial proteins phosphorylated by host kinases *in vivo* (Clifton, et al. 2004; Chen, et al. 2014). The role of phosphorylation in the function of IncG is not clear while phosphorylation of TarP and TepP is important for entry and inclusion development. Inc-human interactome mapping showed several host kinases potentially interact with Incs while Proteome analysis of the *C. trachomatis* inclusion also showed many host kinases associating with inclusion (Aeberhard, et al. 2015; Mirrashidi, et al. 2015). A phosphoproteome analysis of *C. trachomatis* infected cells showed several chlamydial proteins, mainly Incs, to be phosphorylated by host kinases. The kinases predicted to phosphorylate chlamydial proteins were protein kinase A (PKA), protein kinase C (PKC), casein kinase 2 (CSK2), and glycogen synthase kinase 3 (GSK3) among other host kinases (Zadora, et al. 2019).

Active Src family kinases (SFKs), non-receptor membrane associated tyrosine kinases, co-localize with at least 9 Incs (IncB, IncC, CT101, CT222, CT223, CT224, CT228, CT288, and CT850) at discrete sites called microdomains on *C. trachomatis* inclusion (Mital, et al. 2010; Lutter, et al. 2013; Weber, et al. 2015). SFKs regulate microtubule dependent trafficking of the nascent inclusion to the MTOC and intracellular development (Mital and Hackstadt 2011a). Src kinase, a member of SFKs, is also responsible for phosphorylation of Tarp and TepP effectors (Jewett, et al. 2008; Carpenter, et al. 2017). In addition, TarP is also phosphorylated by Abl, Syk kinases (Elwell, et al. 2008; Mehlitz, et al. 2008). Fyn, another SFKs member, has been shown to be important for sphingolipid acquisition by *C. trachomatis* (Mital and Hackstadt 2011b). Myosin light chain kinase (MLCK) is recruited to inclusion microdomains along with other proteins of myosin pathway to regulate extrusion (Lutter, et al. 2013; Nguyen, et al. 2018; Shaw, et al. 2018).

C. trachomatis binds to receptor tyrosine kinases (RTKs) to regulate binding and invasion, replication, and activate host survival pathways. Platelet derived growth factor receptor (PDGFR) is important in binding and internalization of *C. trachomatis* (Elwell, et al. 2008). Interaction with fibroblast growth factor receptor (FGFR) and its ligand FGF2 contributes to bacterial invasion (Kim, et al. 2011). Epidermal growth factor receptor (EGFR) activation is required for chlamydial development and has been implicated in F-actin assembly around the inclusion (Patel, et al. 2014). *C. trachomatis* also binds to Ephrin receptor A2 (EPHA2) leading to activation of phosphoinositide 3-kinase (PI3K) which is required for chlamydial development and host cell survival (Subbarayal, et al. 2015). Several other studies have also shown activation of PI3K and its downstream kinase Akt/protein kinase B (PKB) during *C. trachomatis* infection to regulate invasion (Lane, et al. 2008),

apoptosis resistance, bacterial replication (Verbeke, et al. 2006; Rajalingam, et al. 2008; Gurumurthy, et al. 2010), dampening of host immune response (Carpenter, et al. 2017), and sphingolipid acquisition (Capmany, et al. 2019). *C. trachomatis* also activates MAP/ERK signaling during infection to regulate apoptosis, lipid acquisition, cytokine production, and induce epithelial-to-mesenchymal transition (EMT) (Su, et al. 2004; Buchholz and Stephens 2007; Elwell, et al. 2008; Rajalingam, et al. 2008; Chen, et al. 2010; Mehlitz, et al. 2010; Kim, et al. 2011; Chumduri, et al. 2013; Kun, et al. 2013; Du, et al. 2018; Zadora, et al. 2019). *C. trachomatis* induced EMT has been implicated in molecular pathogenesis of sequelae associated with chronic infection and association of *C. trachomatis* as a risk factor in the development of cervical cancer (Igietseme, et al. 2015).

1.5. Interactions of inclusion membrane proteins

C. trachomatis encodes a type 3 secretion system (T3SS) to secrete effector proteins that localize into host cytosol or inclusion membrane (Stephens, et al. 1998; Betts-Hampikian and Fields 2010). Incs are a unique family of T3SS secreted effectors that are translocated across and inserted into inclusion membrane. They share a bilobed hydrophobic domain and are exposed to host cytosol, thus making them ideally positioned for interacting with host proteins (Bannantine, et al. 2000; Rockey, et al. 2002; Dehoux, et al. 2011; Lutter, et al. 2012). Incs share little to no similarity with other Incs or other known proteins thus limiting *in silico* analysis to predict their function. Over 50 Incs have been predicted in *C. trachomatis* and 36 of them has been identified as bona fide Incs (Dehoux, et al. 2011; Lutter, et al. 2012; Bugalhao and Mota 2019). Gene expression analysis during *C. trachomatis* developmental cycle showed that Incs are expressed at different times during the life cycle (Shaw, et al. 2000; Belland, et al. 2003; Nicholson, et al. 2003; Almeida, et al.

2012). Three classes of Incs have been identified based on timing of their expression: early, mid-cycle and late-cycle Incs suggesting Incs function at distinct times during the *C. trachomatis* developmental cycle (Shaw, et al. 2000). Although several Inc-host/Inc-Inc interactions have been characterized, the functions and host interactions of many of the Incs remain unknown. A global Inc-human interactome study and proteome analysis of the *C. trachomatis* inclusion have revealed putative host binding partners for many of the Incs (Aeberhard, et al. 2015; Mirrashidi, et al. 2015). This has been further complemented by proximity labelling based proteomics of the inclusion (Dickinson, et al. 2019; Olson, et al. 2019). With the advancements in chlamydial genetics and identification of putative host binding partners of several Incs, the field is very well poised to identify functions of more Incs in chlamydial development and infection.

Incs were first identified in *C. psittaci* and soon homologues of IncA/CT119, IncB/CT232, and IncC/CT233 were identified in the *C. trachomatis* genome (Rockey, et al. 1995; Stephens, et al. 1998; Bannantine, et al. 2000). Additional 4 Incs (IncD/CT115, IncE/CT116, IncF/CT117 and IncG/CT118) encoded in an operon were identified and characterized soon after (Scidmore-Carlson, et al. 1999). IncA shares similarity with SNAREs and is involved in homotypic fusion of chlamydial inclusions (Hackstadt, et al. 1999; Suchland, et al. 2000; Delevoye, et al. 2008; Johnson and Fisher 2013). *Chlamydia* lacking IncA form non-fusogenic inclusions (Suchland, et al. 2000). IncA also interacts with host SNAREs, vesicle-associated membrane protein-3 (VAMP-3), VAMP-7 and VAMP-8, and inhibits endocytic SNARE-mediated fusion (Delevoye, et al. 2008; Paumet, et al. 2009). Infections with *C. trachomatis* harboring *IncA* mutations are associated with milder symptoms and lower bacterial load (Geisler, et al. 2001). Although IncA is predicted to have

two SNARE like domains, determination of the 3D structure of IncA revealed it to be different from SNAREs (Delevoye, et al. 2008; Cingolani, et al. 2019). IncB localizes at inclusion microdomains and has been implicated in inclusion membrane biogenesis (Mital, et al. 2010; Mital, et al. 2013). IncC plays a role in inclusion membrane stability as deletion of IncC results in premature inclusion membrane lysis (Weber, et al. 2017). IncG was the first Inc shown to interact with a host protein, 14-3-3β (Scidmore and Hackstadt 2001). Further study revealed 14-3-3β sequesters B cell lymphoma (BCL2) associated agonist of death (BAD) on the inclusion membrane to promote host cell survival (Verbeke, et al. 2006). CpoS/CT229 was initially shown to interact with Rab GTPase, Rab4 (Rzomp, et al. 2006) followed by other studies that showed interactions with several other Rab GTPases (Sixt, et al. 2017; Faris, et al. 2019). Accordingly, CpoS is important in regulating vesicular trafficking and has been also implicated in stability of the inclusion and host cell survival (Sixt, et al. 2017; Faris, et al. 2019). InaC/CT813 interacts with 14-3-3 proteins, ADP ribosylating factors (ARFs) 1 and 4, and VAMPs 7 and 8 (Delevoye, et al. 2008; Kokes, et al. 2015; Wesolowski, et al. 2017). InaC is important for F-actin assembly around the inclusion and its interaction with ARFs plays a role in Golgi redistribution around the inclusion. IncD interacts with ceramide transporter (CERT) participating in ER-Inclusion MCS for lipid acquisition (Derre, et al. 2011; Agaisse and Derre 2014b). CT228 interacts with myosin phosphatase target subunit 1 (MYPT1) at inclusion microdomains to regulate extrusion (Lutter, et al. 2013; Shaw, et al. 2018). CT850 interacts with dynein light chain Tctex-type 1 (DYNLT1) at inclusion microdomains and plays a role in positioning of the inclusion at the MTOC (Mital, et al. 2015). IncE interacts with sorting nexins, SNX5 and 6 and IncE-SNX5 interaction has been further verified at the structural level (Mirrashidi, et al. 2015; Elwell, et

al. 2017; Paul, et al. 2017; Sun, et al. 2017). IncE-SNX5 interaction may help *Chlamydia* subvert host retromer mediated pathogen growth restriction (Aeberhard, et al. 2015; Mirrashidi, et al. 2015). Ectopic expression of inclusion protein acting on microtubules (IPAM)/CT223 in mammalian cells was shown to block cytokinesis (Alzhanov, et al. 2009). Later, IPAM/CT223 was shown to interact with centrosomal protein 170 (CEP170) to modulate host microtubule organization (Dumoux, Menny, et al. 2015). IncV/CT005 contains a FFAT (two phenylalanines, FF, in acidic tract) motif and interacts with VAMP-associated proteins A and B (VAPA/B). Like IncD, the IncV-VAPA/B interaction plays a role in formation of ER-inclusion MCS for lipid acquisition (Stanhope, et al. 2017). CT288 interacts with coiled-coil domain-containing protein 146 (CCDC146) and may modulate the function of this host protein (Almeida, et al. 2018). MrcA/CT101 localizes at inclusion microdomains where it interacts with inositol 1,4,5-triphosphate receptor type 3 (ITPR3) to regulate extrusion formation (Nguyen, et al. 2018). CT226 was shown to interact with leucine rich repeat interacting protein 1 (LRRFIP1). However, LRRFIP1 knockdown did not significantly affect infectious progeny production (Dickinson, et al. 2019; Olson, et al. 2019). Incs are also involved in Inc:Inc homo/heterotypic interactions. CT222 was shown to interact with CT850 at inclusion microdomain (Mital, et al. 2010). Bacterial two hybrid analysis of Inc:Inc interactions identified several homotypic as well as heterotypic Inc:Inc interaction. IncV, IncD, IncF, IncA, CT22 was among several Incs that showed homotypic interaction. Heterotypic interactions of IncF (with IncA, IncC, IncD, IncG, IncV, CT249 and CT850) and CT222 (with IncD, IPAM, CT224 and CT850) were identified as well (Gauliard, et al. 2015). which has been suggested to be important for inclusion stability or organizing the function of other Incs interacting with host proteins (Mital, et al. 2013; Gauliard, et al. 2015).

1.6. Genetic manipulation of *C. trachomatis*

The obligate intracellular nature of this bacterium makes it very difficult to apply molecular genetic tools for genetic manipulation (Hooppaw and Fisher 2015; Bastidas and Valdivia 2016). The genetic recalcitrance of *C. trachomatis* has been a major impediment in characterizing chlamydial virulence factors which has mainly relied on heterologous system (Sixt and Valdivia 2016). However, significant progress in genetic manipulation of *C. trachomatis* has been made in last decade. Tools adapted to *C. trachomatis* include chemical mutagenesis, targeted mutagenesis by TargeTron system or allelic exchange, and more recently transposon mutagenesis.

Random chemical mutagenesis using ethyl methanesulfonate (EMS) or N-ethyl-N-nitrosourea (ENU) followed by the screening of mutants for a specific phenotype or desired mutation has been used for *C. trachomatis*. These approaches rely on whole genome sequencing, genetic linkage analysis, and mapping of mutant alleles using mismatch-specific endonucleases. (Kari, et al. 2011; Nguyen and Valdivia 2012; Kokes, et al. 2015). Recently, transposon mutagenesis using himar 1 Tn system has also been applied to *C. trachomatis* (Fischer, et al. 2017; LaBrie, et al. 2019). However, low transposon insertion efficiency, as well as low transformation efficiency, of *Chlamydia* are limiting factors in transposon mutagenesis (LaBrie, et al. 2019).

Targeted mutagenesis in *C. trachomatis* has relied on transformation of a shuttle plasmid. First report of the successful but transient transformation of recombinant DNA into *C. trachomatis* by electroporation was reported in 1994 (Tam, et al. 1994). Wang et al. reported $CaCl_2$-based stable transformation of *C. trachomatis* in 2011 and has since been

widely adopted. A shuttle plasmid containing plasmid pL2 from *C. trachomatis* serovar L2 and elements of *E. coli* plasmid (pBR325) was used by Wang et al indicating that an intact chlamydial plasmid backbone was required for stable transformation (Wang, et al. 2011). Subsequently, a series of hybrid shuttle plasmids were generated using pL2 and pSW2 backbone. These shuttle plasmids allow for constitutive or inducible expression, expression from native promoter, tagging with various fluorescent proteins, and selection with different resistance markers such as penicillin resistance (*bla*), chloramphenicol acetyltransferase (*cat*), aminoglycoside 3' adenyltransferase (*aadA*), and blasticidin S deaminase (*bsd, ble*) (Agaisse and Derre 2013; Ding, et al. 2013; Wickstrum, et al. 2013; Xu, et al. 2013; Bauler and Hackstadt 2014). Leveraging on the development of shuttle plasmids, a suicide vector, pDFFT3-*bla* was created in an adapted TargeTron system for targeted mutagenesis in *C. trachomatis*. This was first report of targeted mutagenesis in *C. trachomatis* and was based on the mobilization of group II intron along with a *bla* marker into a target gene (Johnson and Fisher 2013). As a proof of principle, IncA was targeted for mutation successfully and since then it has been used by other investigators to generate chlamydial mutants (Sixt, et al. 2017; Weber, et al. 2017; Almeida, et al. 2018; Nguyen, et al. 2018; Shaw, et al. 2018). Limitations of this method include a restricted number of positions within a gene to target the group II intron and the possibility of polar effects. Fluorescence reported allelic exchange mutagenesis (FRAEM) has been reported for *C. trachomatis* in which several genes (*trpA*, *ctl0063*, *ctl0064*, and *ctl0065*) were shown to be deleted as proof of principle (Mueller, et al. 2016). Homology regions were cloned into a conditionally replicating vector, pSUmC followed by transformation into *C. trachomatis*. Transformants that have undergone allelic exchange can be monitored by fluorescence microscopy (Mueller, et al. 2016; Wolf, et al.

2019). Leveraging on FRAEM and Cre-LoxP genome editing, a method for markerless gene deletion, floxed cassette allelic exchange mutagenesis (FLAEM) has been developed in order to overcome cassette induced polar effects (Keb, et al. 2018). These developments in chlamydial genetics have helped researchers to better characterize the functions of chlamydial proteins. However, limitations such as low transformation efficiency, the whole process being time consuming and laborious, and inability to target essential genes still needs to be overcome (Bastidas and Valdivia 2016; Rahnama and Fields 2018).

CHAPTER II

CHLAMYDIA TRACHOMATIS RECRUITS PROTEIN KINASE C DURING INFECTION

This chapter is reproduced with slight modification from the following publication:

Prakash Sah, Nicholas H Nelson, Jennifer H Shaw, Erika I Lutter, *Chlamydia trachomatis* recruits protein kinase C during infection, *Pathogens and Disease*, Volume 77, Issue 6, October 2019, ftz061, https://doi.org/10.1093/femspd/ftz061. Reprinted with permission.

2.1. Introduction

Chlamydia trachomatis is a Gram negative, obligate intracellular pathogen causing a variety of infections in humans. The genus consists of distinct serovars categorized into three biovars based on tissue tropisms. Serovars A-C cause trachoma, which is the leading infectious cause of preventable blindness worldwide (Burton and Mabey 2009). Serovars D-K represent the most common sexually transmitted infection in United States and are associated with sequelae such as infertility, ectopic pregnancy, and pelvic inflammatory diseases (Gerbase, et al. 1998; Da Ros and Schmitt Cda 2008). Serovars L1, L2 and L3 cause invasive urogenital infections termed lymphogranuloma venereum (Schachter 1999). Infections with *C. trachomatis* have also been associated with increased risk for cervical cancer (Zhu, et al. 2016).

The chlamydial developmental cycle involves alternation between two morphologically and physiologically distinct forms, elementary bodies (EBs) and reticulate bodies (RBs). EBs are the highly infectious form that historically were defined as metabolically inactive; however, this paradigm is gradually shifting towards EBs having some metabolic activity (Omsland, et al. 2012; Cosse, et al. 2018). RBs on the other hand are non-infectious, replicating and metabolically active form. EBs, upon endocytosis into the host cell, convert into RBs that replicate by polarized cell division (Abdelrahman, et al. 2016) and the phagosome is rapidly modified by *Chlamydia*-encoded proteins to form a parasitophorous vacuole referred to as an inclusion (Moulder 1991; Wyrick 2000; Coombes and Mahony 2002; Abdelrahman and Belland 2005). Chlamydial development occurs exclusively inside the inclusion and as the infection proceeds, RBs convert back to EBs. At the end of the life cycle, EBs are released via cell lysis and/or extrusion to infect neighboring cells (Hybiske and Stephens 2007).

As an intracellular pathogen *C. trachomatis* manipulates several host signaling networks including kinase pathways and governs these activities at the inclusion membrane, the key host cell-pathogen interface. Active Src family kinases are recruited to inclusion membrane microdomains throughout the infection process and are important for inclusion development and infectious progeny formation (Mital, et al. 2010; Mital and Hackstadt 2011a). Src kinases are known to regulate the phosphatidylinositol 3-kinase (PI3K) signaling cascade, which is associated with increased host survival via AKT/protein kinase B activation during *C. trachomatis* infection (Verbeke, et al. 2006; Olive, et al. 2014; Carpenter, et al. 2017). Likewise, *C. trachomatis* recruits host myosin light chain kinase (MLCK) to inclusion microdomains for the phosphorylation of myosin

light chain 2 (MLC2) promoting the extrusion mechanism of host cell exit (Lutter, et al. 2013). The negative regulator of MLC2 phosphorylation, myosin phosphatase (MYPT1), is recruited by the chlamydial inclusion membrane protein, CT228 (Lutter, et al. 2013); thus, *Chlamydia* host cell exit is modulated by a pathogen-directed balance of host kinase (MLCK) and phosphatase (MYPT1) activities targeting MLC2 (Lutter, et al. 2013; Shaw, et al. 2018). Upstream regulation of these host signaling pathways that affect infectious progeny formation as well as host cell exit is largely unknown, although Protein Kinase C (PKC) has been implicated as a regulator of MYPT1 activity (Toth, et al. 2000).

PKC enzymes are classified according to the nature of their regulatory domains, calcium dependency and activators as either conventional (PKCα, PKCβ and PKC λ), novel (PKCδ, PKCθ, PKCε and PKCη) or atypical (PKCμ, PKC1/λ and PKCζ) (Johannes, et al. 1994; Wu-Zhang and Newton 2013). Phosphorylation of specific residues of PKC activate the enzyme to subsequently phosphorylate a variety of host proteins and signaling pathways (Keranen, et al. 1995; Nishizuka 2001). Activated PKC enzymes transduce various extracellular signals that lead to the generation of the lipid second messenger diacylglycerol (DAG) in order to regulate various cellular functions, such as growth and proliferation, migration, survival and apoptosis (Keranen, et al. 1995; Nishizuka 1995, 2001; Wu-Zhang and Newton 2013). Usurping PKC pathways may benefit chlamydial during its parasitic growth within the host cell as well as provide alternative exit modes for bacterial dissemination. Previous studies demonstrated the enrichment of both DAG, an activator of PKC, and GFP-tagged PKC variants proximal to the chlamydial inclusion (Tse, et al. 2005), suggesting a role for PKC in *C. trachomatis* infection.

Taken together, we hypothesized that activated/phosphorylated PKC would localize to microdomains of the chlamydial inclusion and affect bacterial growth. In this study we demonstrate recruitment of different isoforms of active PKCs to microdomains while PKC substrates localize throughout the periphery of the *C. trachomatis* inclusion. Moreover, we show that PKC substrates are differentially phosphorylated during infection. Inhibition of PKC led to a modest reduction of infectious progeny production suggesting the requirement of PKCs during *C. trachomatis* intracellular development.

2.2. Materials and Methods

2.2.1. *Chlamydia* strains and cell culture

HeLa cells were grown in RPMI 1640 supplemented with 5% fetal bovine serum (FBS) at 37ºC with 5% CO_2. *C. trachomatis* Serovar D, B/Jali20/OT, L2/434/Bu, *C. muridarum* mouse pneumonitis MoPN, *C. caviae* GPIC, *C. pneumoniae* AR-39 were propagated in HeLa 229 cells and purified by Renografin density gradient centrifugation as previously described (Caldwell, et al. 1981).

2.2.2. Antibodies

Anti-Src-pY419 (Clone 9A6, Cat# 05-677; Millipore Sigma, Burlington MA) was used to detect active Src-Family Kinases. Phospho-PKC antibody sampler kit (Cat# 9921, Cell Signaling Technology, Danvers MA) was used to detect phosphorylated PKC isoforms. Anti-PKC substrate (Cat# 2261; Cell Signaling Technology) and Anti-Akt substrate (Cat# 9614; Cell Signaling Technology, Danvers MA) were used to detect phosphorylated PKC and Akt substrates, respectively. Anti-phospho PKC pan (Cat# PA5-38428; ThermoFisher Scientific, Waltham MA) was used to detect phosphorylated

PKC isoforms. Anti-Hsp60 (Clone A57-B9 Cat# MA3023; ThermoFisher Scientific, Waltham MA) was used to detect *Chlamydia* by western blotting.. Anti-rabbit or anti-mouse DyLight 594 and DyLight 488 (Jackson ImmunoResearch, West Grove PA) was used as secondary antibodies for immunofluorescence. Anti-rabbit-HRP or anti-mouse HRP (Cell Signaling Technology, Danvers MA) was used for western blot analysis. Anti-EB rabbit polyclonal antibody (Cat# PA1-73069; ThermoFisher Scientific, Waltham MA) was used to stain EBs and anti-rabbit DyLight 594 was used as a secondary for progeny count.

2.2.3. Immunofluorescence microscopy

HeLa cells were cultured in 24 well plates (CellTreat Scientific, Pepperell MA) containing round cover slips and infected with *C. trachomatis* serovars L2 D, B/Jali20/OT, *C. muridarum*, *C. pneumoniae*, and *C. caviae* GPIC at MOI of approximately 0.5. HeLa cells infected with L2, *C. muridarum* and *C. caviae* were fixed at 18 hours post-infection while cells infected with Serovar D, B-Jali/20 and *C. pneumoniae* were fixed at 42 hours post infection. For the time course of infection experiments, HeLa cells were infected with an MOI of approximately 0.5 and fixed at 12, 24, 36 and 48 hours post-infection. All cells were fixed with methanol or 4% paraformaldehyde followed by permeabilization with Triton X-100, washed in phosphate buffered saline (PBS) and blocked with 1% bovine serum albumin (BSA). Cells were treated with primary antibodies against PKC isoenzyme, Akt substrate, Phospho (Ser) PKC substrate, Phospho-PKC-pan, anti-*Chlamydia* LPS or Src Family Kinases followed by wash in PBS and blocking with BSA. After the PBS washes, anti-mouse/rabbit secondary antibodies were added. Coverslips were mounted onto slides using Dako

Mounting Medium (Agilent Technologies, Santa Clara CA) and observed using a Leica DMI6000B (Leica, Buffalo Grove, IL).

2.2.4. PKC inhibition and Infectious progeny enumeration

HeLa cells in 24 well plates (CellTreat Scientific, Pepperell MA) were infected with *C. trachomatis* serovar L2 EBs at MOI of 1 and treated with inhibitor/control at4 hours post-infection. Staurosporine (Cat# S4400-.1MG; Sigma-Aldrich, St. Louis MO) and Go6983 (Cat# G1918-1MG; Sigma-Aldrich, St. Louis MO) were used at 0.5µM concentration to inhibit PKCs and DMSO was used as a vehicle control. The 0.5µM concentration of PKC inhibitors did not affect cell viability. Cells were incubated for 48 hours at 37ºC in the presence of 5% CO_2. After incubation cells were lysed with sterile water and serially diluted (10^{-1} to 10^{-6}) in Hank's Balanced Salt Solution (HBSS). Fresh HeLa cell monolayers in 24 well plates were infected with 200 µL of each dilution and incubated for 24 hours followed by methanol fixation and staining with anti-EB antibody and anti-rabbit DyLight 594. Inclusions were counted on 30 microscopic fields for each time point using a Leica DMI6000B microscope and total inclusion forming units (IFUs)/mL were calculated.

2.2.5. Western blotting

HeLa cells, in 24 well plates, were infected with *C. trachomatis* L2/434/Bu elementary bodies (EBs) at MOI of 1. Infected cells were grown in RPMI containing chloramphenicol (200µg/mL) or vehicle (Ethanol) 1-hour post infection (hpi). Infected cells were lyzed at different time points during infection (4, 12, 24, 36, 48 hpi). Mock infected HeLa cells were used as control. For time point 24, 36, and 48 hpi, cells were

treated with RPMI containing 150μM CPAF inhibitor (Clasto-lactacystin β-lactone, Cat# 426102; Millipore Sigma, Burlington MA) for 1 hour before lysis. Cells were washed with 1X phosphate buffered saline (PBS) before lysis. One hundred μL of 8M Urea supplemented with 325 units/mL Benzoase nuclease (Millipore Sigma, Burlington MA) and 1X protease inhibitor cocktail (ThermoFisher Scientific, Waltham MA) was added per well of 24 well plates and incubated on ice for 10 minutes. Lysate was collected and 100μL of 2X Laemmli buffer was added. Protein samples were separated by SDS-Polyacrylamide gel electrophoresis and transferred to 0.2 um nitrocellulose membrane (Bio-Rad, Hercules, CA). Membranes were blocked with 5% non-fat dry milk in 1X Tris-buffered saline containing 0.1% Tween-20 (TBST) for 1 hour at room temperature. After blocking, membranes were incubated with rabbit polyclonal antibodies against PKC substrates diluted in 5% BSA in 1X TBST at 4^{o}C overnight. Reacting proteins were detected using horseradish peroxidase conjugated anti-rabbit antibodies and observed by enhanced chemiluminescence using SignalFire ECL reagents (Cell Signaling Technology, Danvers, MA). Immunoblot images were acquired using Fluorchem E FE0622 system (ProteinSimple, San Jose, CA).

2.2.6. Statistical analysis

Statistical analysis was carried out using Prism 5.0. One-way ANOVA was performed with *post hoc* Tukey test for the comparison of infectious progeny in the presence and absence of PKC inhibitors.

2.3. Results

2.3.1. PKC is recruited to the *C. trachomatis* inclusion

Many different isoforms of PKC are produced in eukaryotic cells (Wu-Zhang and Newton 2013) hence, there are several candidates for recruitment to the *C. trachomatis* inclusion. To assess whether PKC is recruited to the inclusion during *C. trachomatis* L2 infection a general Phospho-PKC (pan) antibody that detects levels of multiple phosphorylated isoforms of PKC (PKCα, PKCβ, PKCδ, and PKCε) was utilized initially. This antibody detects the PKC isoforms phosphorylated at a C-terminal residue homologous to the threonine residue at position 497. Figure 2.1A shows that phospho PKC was recruited to the inclusion at small discrete punctate regions that resemble active Src kinase microdomain staining (Mital, et al. 2010; Mital and Hackstadt 2011a). Uninfected neighboring cells only contain diffuse staining of phospho PKC and clearly lack any discrete or punctate staining. The timing of phospho-PKC recruitment was monitored via a time course of infection at 12, 24, 36 and 48 hours post-infection (Figure 2.1B). At 12 hours post-infection, phospho-PKC is seen to be diffuse throughout the infected cells, similar to uninfected cells. However, by 24 hours post-infection phospho-PKC is seen recruited to the chlamydial inclusion in discrete microdomains which become more pronounced as infection progresses.

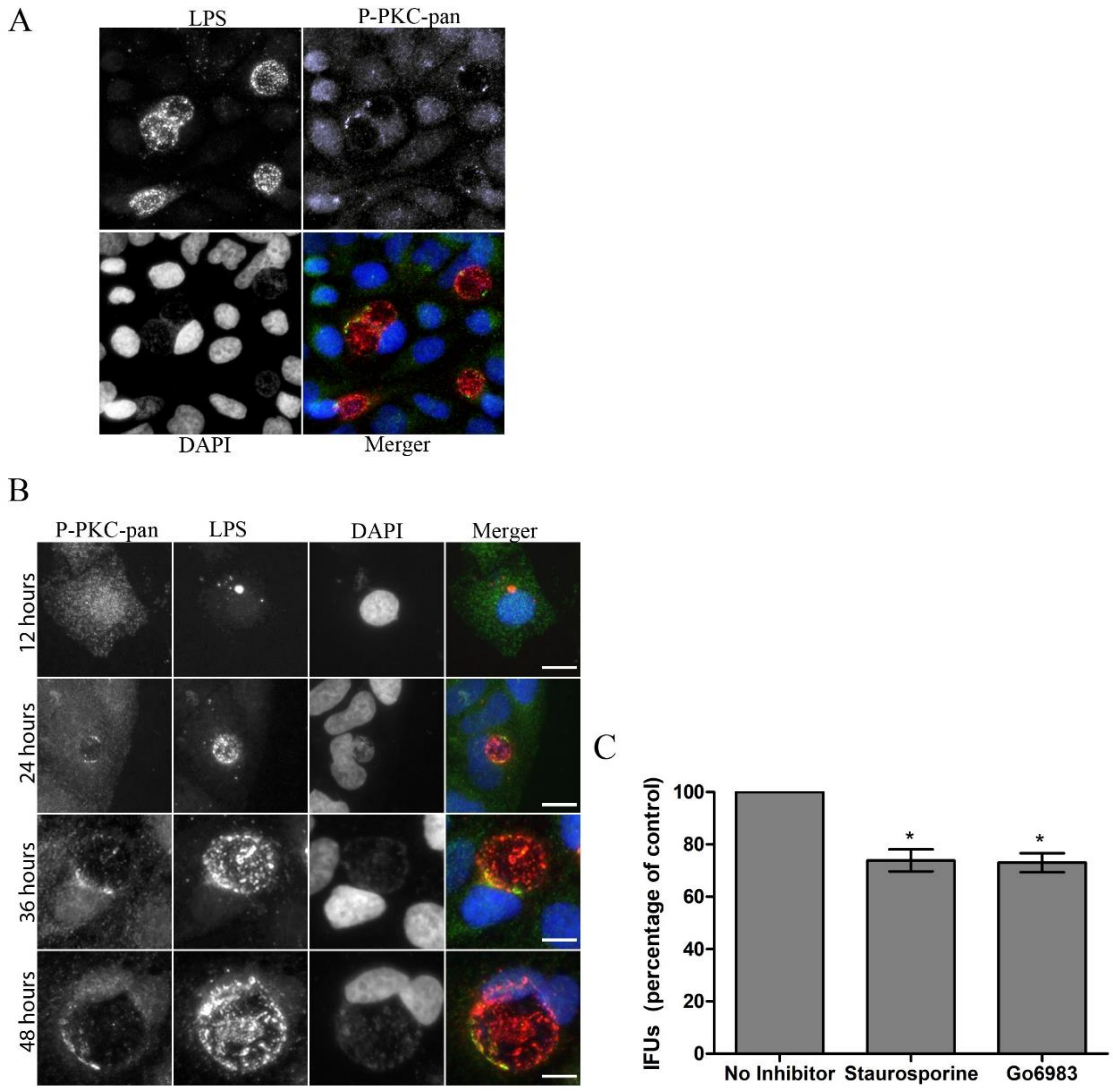

Figure 2.1. PKC is recruited to the chlamydial inclusion and PKC inhibitors reduce *C. trachomatis* IFUs. (A) HeLa cells were infected with *C. trachomatis* for 36 hours and prepared for immunofluorescence microscopy. Phospho-PKC-pan antibody was used to detect endogenous levels of phosphorylated PKCs recruited to the chlamydial inclusion. (B) Phosho-PKC pan recruitment was monitored over a time course of infection. Shown are 12, 24, 36 and 48 hours post-infection. (C) HeLa cells were infected with *C. trachomatis* L2 and treated with staurosporine (0.5 µM) or Go6893 (0.5 µM) with the inhibitors being present throughout infection. At 48 hours post-infection, the cells were

lysed to release *Chlamydia* and cell lysates were serially diluted and used to infect HeLa cell monolayers. Infection was allowed to proceed for 18 hours, cells were fixed with cold methanol, processed for microscopy and 30 fields of view were counted for each condition in triplicate. Error bars indicated standard deviation. Scale bar, 10 μm. * $p < 0.001$.

2.3.2. Pharmacological inhibition of PKC results in decreased recoverable IFUs

The presence of PKC in inclusion membrane microdomains suggests specific and active recruitment by *C. trachomatis* during infection. To determine whether PKC is important for chlamydial intracellular growth and survival we pharmacologically inhibited PKC enzymatic activity and assessed the possibility of growth defects. Two different PKC pharmacological inhibitors, staurosporine and Go 6893, were added at 4 hours post-infection and maintained in the cell culture supernatant for the duration of the infection. At 48 hours the cells were lysed, serially plated on fresh HeLa cells and infectious progeny enumerated. Treatment by both inhibitors, staurosporine and Go 6893, modestly reduced the recoverable infectious progeny by approximately 20% compared to the control (no inhibitor treatment) (Figure 2.1C; $p<0.001$) indicating the importance of host PKC for optimal chlamydial development.

2.3.3. Multiple phosphorylated isoforms of PKC are recruited to inclusion microdomains

Recruitment of different isoforms and phosphorylation states of PKC to the chlamydial inclusion were assessed by immunofluorescent microscopy. The endogenous form of PKCα, PKCδ and PKD/PKCμ were tested for colocalization with active Src

Kinases (Figure 2.2A and B). The antibodies employed detect total levels of PKC isoforms and are not specific to any phosphorylation. PKC enzymes are regulated by phosphorylation at specific sites, which determines their consequent enzymatic activity. To determine if the PKC isoforms recruited to the chlamydial microdomains were in their activated state, immunofluorescent microscopy was performed utilizing phosphospecific antibodies to different isoforms of PKC (Figure 2.2C). As can be clearly seen in Figure 2.2C, each phosphorylated PKC isoform also colocalized with active Src kinases in the microdomains.

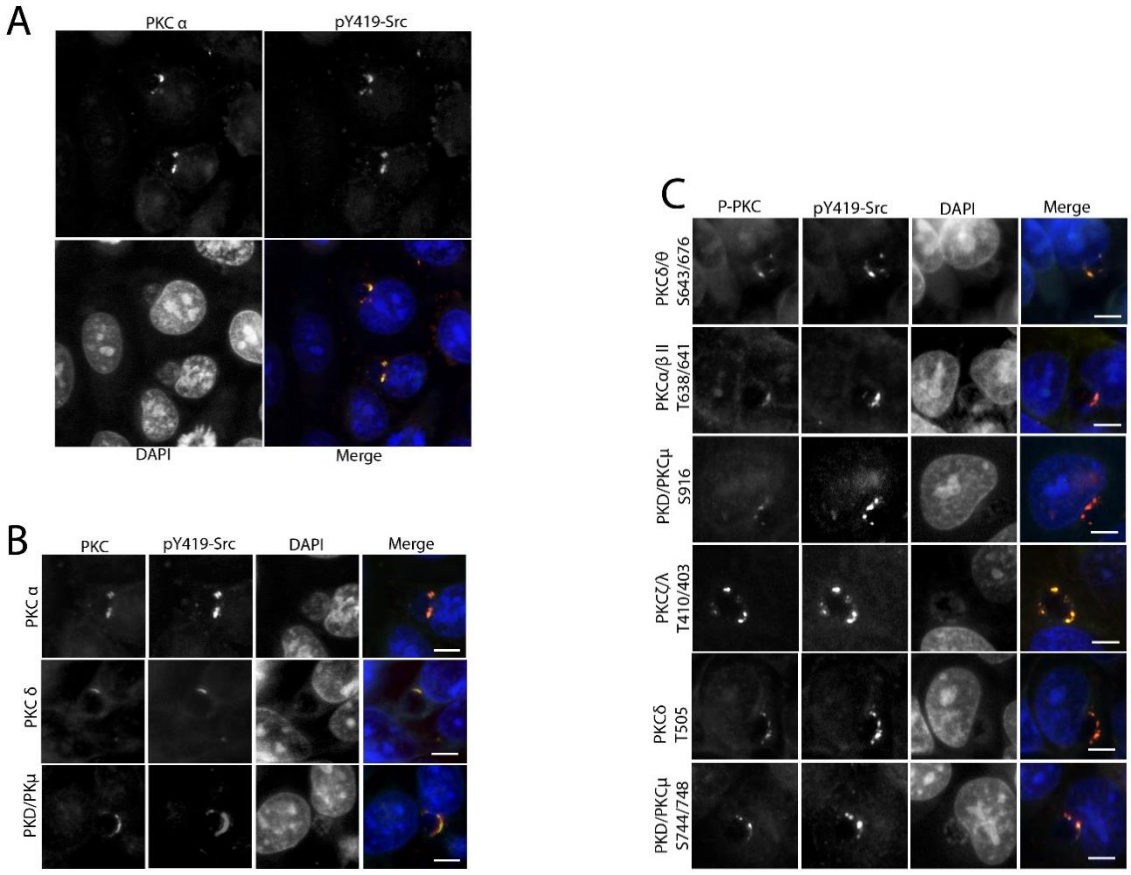

Figure 2.2. Multiple isoforms of PKC are recruited to the inclusion microdomains by *C. trachomatis*. HeLa cells were infected with *C. trachomatis* L2 for 18 hours, fixed and prepared for immunofluorescence microscopy. (A) Endogenous levels of PKCα

showing colocalization with active Src kinases (pY419-Src)**.** Multiple infected and uninfected cells are shown. (B) Endogenous levels (irrespective of phosphorylation state) of PKCα, PKDδ and PKD/PKCμ were assessed for colocalization with active Src kinases (pY419-Src). (C) Phosphospecific antibodies were used to detect the different phosphorylated isoforms of PKC also colocalizing with active Src Kinases (pY419-Src). Scale bar, 10 μm.

2.3.4. Phosphorylated PKC substrates are recruited throughout the periphery of the inclusion membrane

The phosphorylated PKC isoforms recruited to the inclusion microdomains correlated with the active state of the PKC enzymes since the antibodies used were specific to the phosphorylated sites and do not cross react with non-phosphorylated sites. PKC enzymes are Serine/Threonine kinases known to phosphorylate their substrates at specific residues. A commercial Phospho-Serine PKC antibody detects various proteins phosphorylated at serine residues that are flanked by an Arginine or Lysine at the -2 and +2 positions, respectively, with a hydrophobic residue at the +1 position. Positive staining with this phosphospecific PKC substrate antibody would suggest PKC phosphorylation of substrates. Immunofluorescent microscopy of *C. trachomatis* L2-infected HeLa cells revealed abundant staining of PKC phosphorylated substrates throughout the entire periphery of the inclusion (Figure 2.3A, B and C). An antibody against Akt specific substrates was used as a comparative control to demonstrate the specificity of PKC substrates recruited to the chlamydial inclusion (Figure 2.3B). Active Src kinases were seen to form microdomains that colocalized with the PKC substrates at the inclusion membrane (Figure 2.3C).

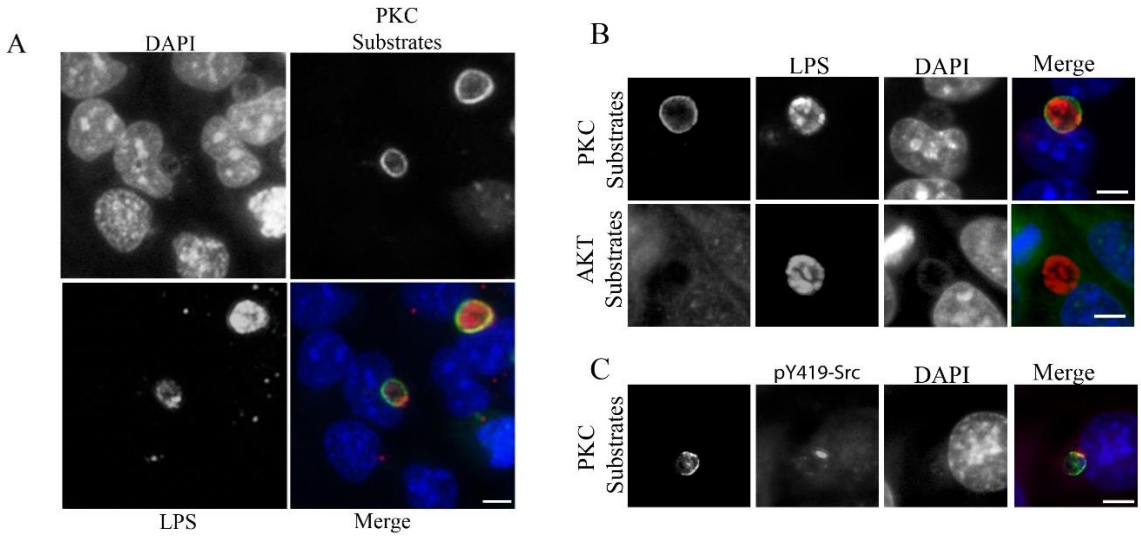

Figure 2.3. PKC phosphorylated substrates are recruited to the entire periphery of the *C. trachomatis* inclusion. HeLa cells were infected with *C. trachomatis* L2 at an MOI of 0.5 for 18 hours, fixed in cold fixative and processed for immunofluorescence microscopy. (A) Phospho (Ser)-PKC substrates are shown surrounding the chlamydial inclusion (*Chlamydia* detected with anti-*Chlamydia* LPS). Multiple infected and uninfected cells can be seen for comparison. (B) Phospho (Ser)-PKC substrates and Akt substrates were detected with phosphospecific antibodies for recruitment to the chlamydial inclusion (*Chlamydia* detected with anti-*Chlamydia* LPS). (C) Active Src kinases (pY49-Src) are shown colocalizing in discrete microdomain overlapping the Phospho-(Ser)-PKC. Scale bar, 10 µm.

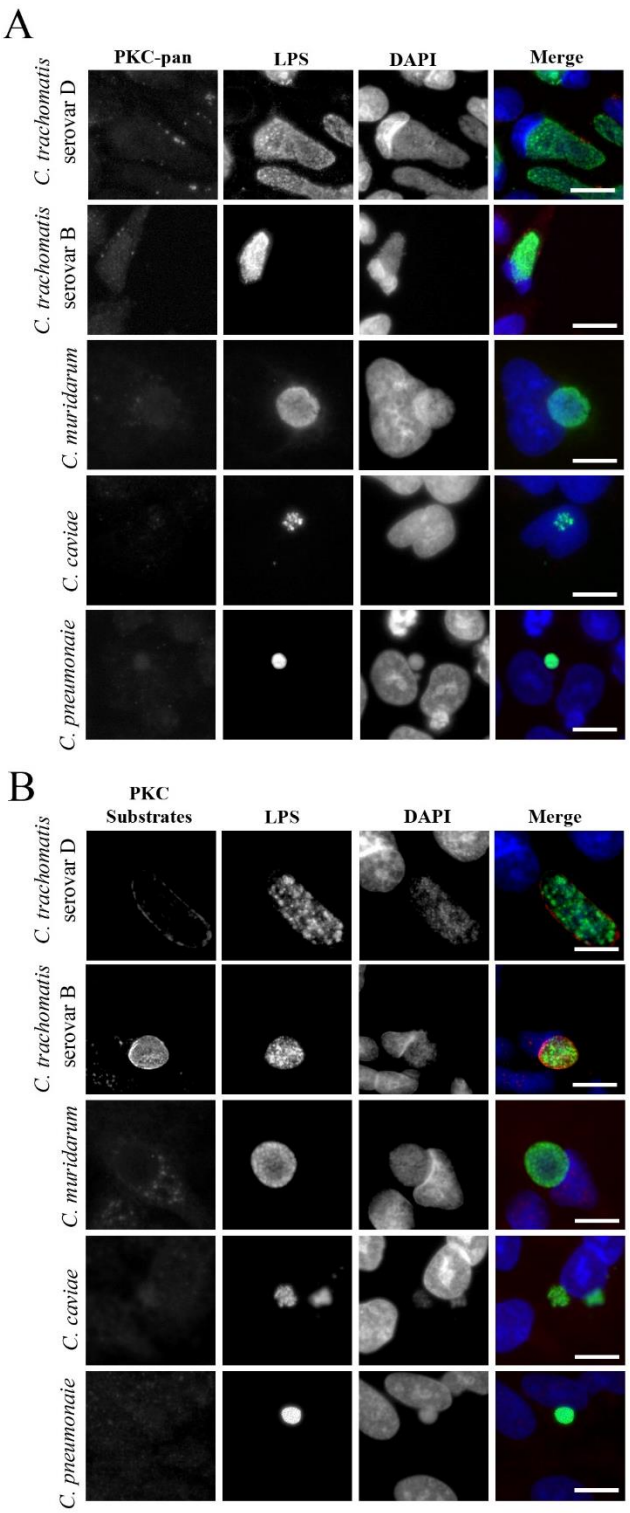

Figure 2.4. PKC and PKC substrate recruitment is limited to *C. trachomatis* serovars. HeLa cell monolayers were infected with *C. trachomatis* serovar D (42 hours),

C. trachomatis serovar B, (42 hours), *C. muridarum* (18 hours), *C. caviae* (18 hours) and *C. pneumoniae* (42 hours) at an approximate MOI of 0.5, fixed in cold methanol and processed for immunofluorescence microscopy. (A) Total phospho-PKC recruitment as detected by a phospho-PKC-pan antibody (arrows indicate discrete regions of phosho-PKC recruitment) and (B) recruitment of phosphorylated PKC substrates are shown. All *Chlamydia* species were detected with anti-*Chlamydia* LPS antibody. Scale bar, 10 µm.

2.3.5. PKC and PKC recruitment is limited to *C. trachomatis* serovars

The species specific recruitment of PKC and PKC substrates to the chlamydial inclusion during infection was examined using two different serovars of *C. trachomatis* (serovars B and D) as well as *C. muridarum*, *C. caviae* and *C. pneumoniae.* HeLa cells were infected with each species, fixed at designated times post-infection and probed with either the PKC pan antibody (to detect endogenous forms of phosphorylated PKC isoforms) or the Phospho-Serine PKC substrate antibody. Interestingly, only the *C. trachomatis* serovars B and D displayed recruitment of phosphorylated PKC and PKC substrates to the inclusion during infection (Figure 2.4). PKC was recruited to the inclusion in small discrete microdomain-like regions for serovar B and D (Figure 2.4A) in the same manner as what was observed for serovar L2 (Figure 2.1). Likewise, the PKC phosphorylated substrates were recruited to the entire periphery of chlamydial inclusions in *C. trachomatis* serovars B and D (Figure 2.4B), consistent with the recruitment observed in serovar L2 (Figure 2.3). *C. pneumoniae*, *C. muridarum*, and *C. caviae* were negative for recruitment of both phosphorylated PKC isoforms and PKC phosphorylated substrates.

2.3.6. Phosphorylation of PKC substrates are altered during *C. trachomatis* infection

PKC is an essential host protein known to regulate numerous downstream targets and signaling pathways. The various isoforms of PKC are all regulated by phosphorylation (Reyland 2009) and exhibit overlapping roles within the cell. Due to the complexity of PKC isoforms recruited to the *C. trachomatis* inclusion, total PKC activity was monitored by visualizing the phosphorylation of downstream substrates (Figure 2.5). HeLa cells were infected with *C. trachomatis* L2 with and without chloramphenicol treatment and whole cell lysates collected at 4, 12, 24, 36 and 48 hours post-infection (uninfected HeLa lysates served as a negative control) followed by immunoblot analysis using the Phospho (Ser) PKC substrate antibody to detect substrates phosphorylated at serine residues. Changes in the phosphorylation of PKC substrates were observed as early as 4 hours post-infection with multiple proteins increasing in phosphorylation status during the course of infection (Figure 2.5). This is especially evident at 24, 36 and 48 hours post-infection when the bacterial burden was the greatest within the cell. No increased Phospho (Ser) PKC substrate phosphorylation was observed in the chloramphenicol treated infected cells, suggesting that *Chlamydia* were actively manipulating PKC activity during infection. GAPDH was monitored as a control during infection to control for total protein content.

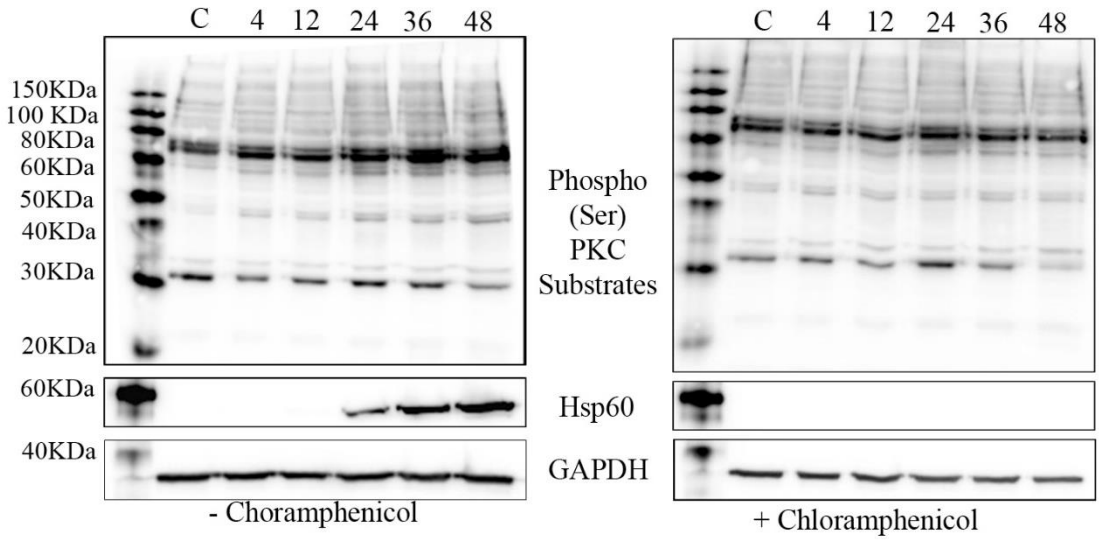

Figure 2.5. PKC substrates are differentially phosphorylated during *C. trachomatis* infection. *C. trachomatis* L2 infected HeLa cell lysates with and without chloramphenicol treatment were collected at 4, 12, 24, 36 and 48 hours post-infection and probed for Serine-phosphorylated PKC substrates. Uninfected HeLa lysates, C, serve as a control and total protein reference. GAPDH was used as a loading control and Hsp60 was used to detect *Chlamydia*. Molecular mass is shown in kilodaltons (kD).

2.4. Discussion

Recruitment of PKC to the inclusion microdomains is not surprising as other obligate intracellular pathogens, such as *Coxiella burnetti*, require PKC for its intracellular development (Hussain, et al. 2010) and PKC activates NF-κB signaling during *Rickettsia rickettsii* infections (Sahni, et al. 1999; Sahni and Rydkina 2009). In this study, all PKC isoforms, including PKC isoforms phosphorylated at specified residues, were recruited to the inclusion microdomains wherein multiple kinases reside: Src, Yes and Fyn (Mital, et al. 2010; Mital and Hackstadt 2011a) and MLCK (Lutter, et

al. 2013). The additional recruitment of multiple phosphospecific isoforms of PKC to the already kinase rich microdomains supports the notion that these regions are hubs for kinase activity on the inclusion membrane. Previous studies have demonstrated the recruitment of multiple isoforms of PKC to the vicinity of the inclusion, but the ectopic expression of fluorescently tagged PKC constructs reported in *Chlamydia*-infected cells did not elucidate the enzymatic activity or phosphorylation states nor were they shown to be localized to the inclusion microdomains (Tse, et al. 2005). A recent phosphoproteomic study by Zadora *et al.,* 2019 not only demonstrated that *C. trachomatis* affected multiple host signaling pathways including PKC signaling but that 25 chlamydial proteins, majority of which were inclusion membrane proteins, were phosphorylated at predicted PKC phosphorylation sites (Zadora, et al. 2019). This study strongly suggested that PKC, among other host kinases, regulate *C. trachomatis* proteins via phosphorylation.

The recruitment patterns for PKCs and phosphorylated PKC substrates were found to be quite different. The PKCs all colocalized at microdomains with active Src Kinases whereas the phosphorylated PKC substrates displayed substantial recruitment throughout the periphery of the inclusion. This distinction contradicts the concept that PKC is first recruited then acts to phosphorylate proteins in the vicinity of the microdomains. Rather, our data suggest that host proteins may be recruited after PKC phosphorylation. The significant recruitment of PKC substrates to the periphery of the inclusion also suggests that there may be multiple proteins recruited during the course of infection. The variation in recruitment pattern to either microdomains or inclusion periphery has been established with multiple host proteins and Chlamydial Incs.

Chlamydial Incs including CT850 (Mital, et al. 2010; Mital, et al. 2015), CT101 (Mital, et al. 2010; Nguyen, et al. 2018) and CT228 (Lutter, et al. 2013; Shaw, et al. 2018) all localize to microdomains whereas IncD (CT115) (Agaisse and Derre 2014a), IncG (CT118) (Scidmore and Hackstadt 2001) and IncA (CT119) (Scidmore-Carlson, et al. 1999) are expressed circumferentially around the periphery of the inclusion. The differential localization pattern of Incs on the inclusion membrane affords *C. trachomatis* the luxury of recruiting host proteins in an explicit manner depending on the demands of parasitism. As such, PKC substrates may be optimally positioned circumferentially whereas active PKC enzymes may need to reside within kinase rich regions for proper activation of signaling cascades through phosphorylation events. It is also likely that many chlamydial Incs are also phosphorylated by PKC during infection (Zadora, et al. 2019) contributing for the circumferential staining of PKC phosphorylated substrates around the chlamydial inclusion.

Species specific recruitment of PKC and phosphorylated PKC substrates to the inclusion proposes a distinctive role for *C. trachomatis* infection and putative requirements for species specific infection, which is unremarkable as recruitment of other kinases or host proteins during infection has also been reported as species specific. *C. trachomatis* serovars and *C. pneumoniae* recruit Src-family kinases to inclusion microdomains, however there is no evidence of kinase rich microdomains identified for *C. caviae* or *C. muridarum* (Mital and Hackstadt 2011a). Myosin phosphatase, which regulates the activity of MLC2, is recruited to the inclusion by *C. trachomatis* serovars and *C. muridarum,* but not *C. pneumoniae* or *C. caviae* (Lutter, et al. 2013). It is clear that the prerequisites for host kinases and phosphorylated host proteins vary between

chlamydial species and may be key to addressing questions in chlamydial biology, host tropism and pathogenesis.

Given the diversity of PKC recruitment to the *C. trachomatis* inclusion, two different PKC pharmacological inhibitors were used in this study: staurosporine which is a potent inhibitor of multiple PKC isoforms (PKCα, PKCγ and PKCη but less potent to PKCδ, PKCε and PKCζ) (Ward and O'Brian 1992) and Go 6893, a broad spectrum PKC inhibitor that targets all isoforms (PKCα, PKCβ, PKCγ, PKCδ, PKCζ and PKCμ) (Peterman, et al. 2004). Inhibitors were used at low concentrations (0.5 μM) to limit host cell death. Both inhibitors produced similar results with no significant differences between the two different inhibitors indicating that, despite their different PKC targets, both were able to target PKC isoforms relevant to *Chlamydia* infection. Pharmacological treatment of *Chlamydia*-infected cells exhibited a modest yet significant reduction in recoverable infectious progeny, suggesting that PKC may be an important host factor during chlamydial infection. In previous studies, it was demonstrated that *C. trachomatis* inhibited apoptosis induced by staurosporine (Xiao, et al. 2004) and that *Chlamydia*-infected HeLa cells are resistant to staurosporine induced apoptosis (Fan, et al. 1998; Dean and Powers 2001). This supports our observation that the viability of cells infected by *C. trachomatis* were not affected by staurosporine and the reduced infectious progeny is due to inhibition of PKC rather than host cell viability.

In summary, our findings show that PKC is a host cell kinase manipulated by *C. trachomatis* during infection with multiple phosphorylated isoforms being recruited to the inclusion membrane microdomains. PKC is an integral host protein involved in multiple host signaling pathways that regulate many proteins through phosphorylation events.

Given the central role PKC plays in host cell dynamics, it is not surprising to see recruitment of phospho-PKC kinases and PKC phosphorylated substrates to the periphery inclusion membrane. Future investigations to identify and characterize the recruited PKC phosphorylated substrates will provide significant insights into *Chlamydia* pathogenic mechanisms and may represent targets for future therapies designed to treat intracellular pathogens.

CHAPTER III

CHLAMYDIA TRACHOMATIS SUBVERTS PROTEIN KINASE A DURING INFECTION

3.1. Introduction

Chlamydia trachomatis infections represent a significant global public health problem. Trachoma, an ocular infection caused by *C. trachomatis* serovars A-C, is the leading cause of preventable infectious blindness worldwide (Resnikoff, et al. 2004; Burton and Mabey 2009). *C. trachomatis* serovars D-K and L1-L3 represent the most common bacterial sexually transmitted infections (STIs) in the US (CDC 2019). Although easily treatable, chlamydial STIs are often asymptomatic and prolonged infections can lead to serious sequelae such as infertility, ectopic pregnancy and pelvic inflammatory disease (Malhotra et al., 2013). *C. trachomatis* infections have also been associated as a co-factor for cervical cancer development (Koskela, et al. 2000; Zhu, et al. 2016).

C. trachomatis is a Gram-negative, obligate intracellular pathogen that replicates inside the host cell in a parasitophorous vacuole called an inclusion (Moulder 1991). It exhibits a unique biphasic developmental cycle alternating between two distinct forms; the elementary bodies (EBs) and the reticulate bodies (RBs) (Moulder 1991; Abdelrahman and Belland 2005).

EBs enter the host cell within a vacuole called an inclusion that is trafficked along microtubules to the microtubule organizing center (MTOC) while avoiding fusion with lysosomes (Carabeo, et al. 2002; Fields and Hackstadt 2002; Grieshaber, et al. 2003). Inside the inclusion EBs differentiate into RBs to undergo several rounds of replication and about mid-cycle RBs re-differentiate back into EBs. From within the inclusion *C. trachomatis* subverts several host cell processes to promote its intracellular development by secreting an arsenal of effector proteins (Bastidas, et al. 2013; Elwell, et al. 2016). EBs eventually exit the host cell either by lysis or extrusion to initiate new cycles of infections (Hybiske and Stephens 2007).

As the inclusion develops it is extensively modified by *Chlamydia*-encoded inclusion membrane proteins (Incs) and an assortment of recruited host proteins (Abdelrahman and Belland 2005; Bastidas, et al. 2013; Elwell, et al. 2016). Among the host proteins that localize at the inclusion membrane are several host kinases which regulate host cell processes that are targeted by *C. trachomatis*. Src family kinases (SFKs) such as Src, Fyn, and Yes localize to discrete sites on inclusion membrane called microdomains and are important for overall growth and development of *Chlamydia* (Mital, et al. 2010; Mital and Hackstadt 2011a). Fyn was also shown to play role in lipid acquisition form the host (Mital and Hackstadt 2011b). Myosin light chain kinase (MLCK) also localizes at inclusion microdomains along with other components of the myosin pathway (Lutter, et al. 2013; Shaw, et al. 2018). Myosin phosphatase regulatory subunit 1 (MYPT1) binds to the Inc CT228 and phosphorylated inactive form of MYPT is recruited at the microdomains where the pathogen regulates activities of the kinase and phosphatase on myosin light chain 2 (MLC2) to regulate extrusion (Lutter, et al. 2013;

Shaw, et al. 2018). Multiple isoforms of PKC also localize at inclusion microdomains (Sah, et al. 2019). PKC has been implicated in apoptosis resistance and a likely role in lipid acquisition (Tse, et al. 2005; Shivshankar, et al. 2008; Elwell and Engel 2012).

Several studies have shown that *C. trachomatis* activates mitogen activated protein kinase-extracellular signal regulated kinase/ERK (MEK/ERK) and phosphatidylinositol-3-kinase (PI3K) signaling. MEK/ERK activation during *C. trachomatis* infection regulates apoptosis resistance, bacterial replication, glycerolipids acquisition, cytokine induction and *Chlamydia* induced epithelial-to-mesenchymal transition (EMT) (Su, et al. 2004; Buchholz and Stephens 2007; Rajalingam, et al. 2008; Chen, et al. 2010; Gurumurthy, et al. 2010; Mehlitz, et al. 2010; Du, et al. 2011; Kim, et al. 2011; Chumduri, et al. 2013; Kun, et al. 2013; Du, et al. 2018; Zadora, et al. 2019). *Chlamydia* induced EMT has been implicated in immunopathology of chlamydial infection and is associated with cervical cancer development (Igietseme, et al. 2015). PI3K and its downstream kinase AKT/protein kinase B is important in regulating invasion, replication, apoptosis resistance, and sphingolipid acquisition during chlamydial infections (Verbeke, et al. 2006; Lane, et al. 2008; Rajalingam, et al. 2008; Siegl, et al. 2014; Subbarayal, et al. 2015; Carpenter, et al. 2017; Capmany, et al. 2019). *C. trachomatis* also activates 3-Phosphoinositide dependent protein kinase 1 (PDPK1), a component of PI3K pathway to prevent host cell apoptosis by reprograming host metabolism (Al-Zeer et al., 2017).

Protein kinase A (PKA) transduces signals that result in production of the second messenger cyclic adenosine monophosphate (cAMP) and regulates many host processes such as transcription, cell survival, and cytoskeletal organization (Pearce, et al. 2010).

PKA holoenzyme is a tetramer of catalytic and regulatory subunits (R_2C_2) and upon binding to cAMP the regulatory subunits release catalytic subunits that phosphorylate substrates (Skalhegg and Tasken 2000). There are two types of PKA holoenzymes, PKAI and PKAII based on the type of regulatory subunits (RI and RII) that also regulate their localization by binding to scaffolding proteins, A kinase anchoring proteins (AKAPs) (Skalhegg and Tasken 2000; Wong and Scott 2004). PKAI is located in the cytosol whereas PKAII is localized to subcellular structures via AKAPs (Meinkoth, et al. 1990; Skalhegg and Tasken 2000). PKA signaling is manipulated by several intracellular pathogens such as *Brucella suis*, *Mycobacterium tuberculosis*, and *Coxiella burnetii* for their intracellular survival (Gross, et al. 2003; Kalamidas, et al. 2006; MacDonald, et al. 2012; Macdonald, et al. 2014). A recent phosphoproteome study revealed several *C. trachomatis* proteins, including many inclusion membrane proteins, to be phosphorylated in *Chlamydia*-infected cells. PKA was identified as one of the potential host kinases responsible for these phosphorylation events suggesting that PKA may regulate *C. trachomatis* proteins (Zadora, et al. 2019). Taken together, these suggest that *C. trachomatis* may modulate or rely on PKA during infection.

In this study, we investigated PKA modulation during *C. trachomatis* infection. We showed that PKA catalytic and regulatory subunits localize in the vicinity of inclusion with a Golgi marker. Phosphorylated PKA substrates localize to the inclusion membrane specifically at mid to late stages of infection. Similarly, PKA substrates show higher phosphorylation towards mid to late stage of infection. Pharmacological inhibition of PKA leads to a reduction in extrusion events, implicating that PKA may play a role in

regulating host cell exit. Despite this, inhibition of PKA only slightly decreased the phosphorylation of MLC2 suggesting involvement of other host factors in extrusion.

3.2. Materials and Methods

3.2.1. *Chlamydia* Strains and Cell culture

HeLa cells were grown in RPMI 1640 supplemented with 5% fetal bovine serum (FBS) at 37ºC with 5% CO_2 and 95% humidified air. *C. trachomatis* L2/434/Bu was propagated in HeLa 229 cells and purified by Renografin density gradient centrifugation as previously described (Caldwell, et al. 1981).

3.2.2. Antibodies

Anti-phospho PKA substrate (Cat#9624 and #9621; Cell Signaling Technology) was used to detect phosphorylated PKA substrates. Anti-CREB (Cat#PA1-850; ThermoFisher Scientific) and Anti-phospho CREB (Cat#44-298G; ThermoFisher Scientific) was used to detect CREB and phospho-CREB (S133) respectively. Anti-GSK-3β (Cat#12456; Cell Signaling Technology) and anti-phospho-GSK-3β (Cat#5558; Cell Signaling Technology) was used to detect GSK-3β and phospho-GSK-3β (S9). PKA-Cα and PKA-RIIα was detected using anti-PKA-C alpha (Cat#PA5-17626; ThermoFisher Scientific) and anti-PKA-RII alpha (Cat#PA5-106470; ThermoFisher Scientific). Anti-MYL9 (Cat #PA5-17624; ThermoFisher Scientific) and anti-phospho MYL9 (PA5-17726; ThermoFisher Scientific) was used to detect MLC2 and phospho MLC2 (S19). Anti-Hsp60 (Clone A57-B9 Cat# MA3023; ThermoFisher Scientific), Anti-MOMP (Clone CL12-707.7 Cat#MA1-10665 ThermoFisher Scientific) and was used to detect *Chlamydia* while anti-GAPDH (Cat #25778, Santa Cruz Biotechnology) was used to

detect GAPDH. Anti-rabbit or anti-mouse DyLight 594 and DyLight 488 (Jackson ImmunoResearch) was used as secondary antibodies for immunofluorescence. Anti-rabbit-horseradish peroxidase (HRP) (Cat#7074) or anti-mouse-HRP (Cat# 7076; Cell Signaling Technology) was used for western blot analysis. Anti-MOMP-FITC polyclonal antibody (Cat#PA1-73073; ThermoFisher Scientific) was used to stain *Chlamydia* for infections forming units (IFU) count.

3.2.3. Immunofluorescence microscopy

HeLa cells were cultured in 24 well plates (CellTreat Scientific) containing round cover slips and infected with *C. trachomatis* L2 at multiplicity of infection (MOI) of approximately 0.5. Infected cells were fixed at indicated time points post-infection. All cells were fixed with methanol or 4% paraformaldehyde followed by permeabilization with Triton X-100, washed in phosphate buffered saline (PBS) and blocked with 1% bovine serum albumin (BSA). Cells were treated with primary antibodies against PKA-Cα, PKA-RIIα, phospho-PKA substrate, golgin-97, and *Chlamydia* LPS/MOMP followed by washing in PBS and blocking with 1% bovine serum albumin (BSA). After the PBS washes, anti-mouse/rabbit secondary antibodies were added along with DAPI. Coverslips were mounted onto slides using Dako Mounting Medium (Agilent Technologies) and observed using a Leica DMI6000B fluorescent microscope (Leica Microsystems). Images were acquired at 40X magnification and representative images were used for making panels.

3.2.4. Extrusions and Infectious progeny enumeration

HeLa cells in 24 well plates were infected with *C. trachomatis* serovar L2 EBs at MOI of 1 and treated with inhibitor/control at 2 hours post-infection. H89 (10µM) (Cat# S4400-.1MG; Sigma-Aldrich) and Rp-cAMPs (100µM and 250µM) (Cat# G1918-1MG; Sigma-Aldrich) were used to inhibit PKA and DMSO was used as a vehicle control. Inhibitor treatment was maintained throughout the infection cycle. Infected cells were incubated for 48 hours at 37ºC in the presence of 5% CO_2 and 95% humidified air. At 48 hours post infection, media from infected cells was saved and processed for extrusions counting while the cells were lysed with sterile water to be used for IFU enumeration.

For Extrusion enumeration, media from infected cells were gently spun at 1200 rpm for 20 minutes. Pellet was resuspended in media, mixed with Trypan Blue (Cat# 15250061 ThermoFisher Scientific), FM 4-64 (ThermoFisher Scientific) and stained with Nucblue Hoeschst live cell stain (Cat# R37605 Thermofisher Scientific). Stained samples were loaded onto a Hausser Bright-line hemocytometer and extrusions free of host cell nuclei was counted on a Leica DMI6000B fluorescent microscope.

For infection Forming Unit (IFU) enumeration, infected cell lysates were serially diluted (10^{-1} to 10^{-8}) in Hank's Balanced Salt Solution (HBSS). HeLa cell monolayers in 96 well plates were infected with 100 µL of each dilution and incubated for 24 hours followed by methanol fixation and staining with anti-MOMP-FITC (ThermoFisher Scientific) antibody. Inclusions were counted on 20 microscopic fields using a Leica DMI6000B microscope and total inclusion forming units IFU/mL were calculated.

3.2.5. Western blotting

HeLa cells, in 24 well plates, were infected with *C. trachomatis* L2 EBs at MOI of 1. Where indicated, L2 or mock infected cells were grown in RPMI containing chloramphenicol (200μg/mL) or vehicle (ethanol) added 1 hour post-infection H89 (10μM) or DMSO added 2 hours post-infection. Infected cells were lysed at different time points during infection. Cells were washed with PBS before lysis. For lysis, 100 μL of 8M Urea supplemented with 325 units/mL Benzoase nuclease (Cat# 70746 Millipore Sigma) and 1X protease and phosphatase inhibitor cocktail (Cat#78440 ThermoFisher Scientific) was added per well of 24 well plates and incubated on ice for 10 minutes. Lysate was collected and 100μL of 2X Laemmli buffer was added. Protein samples were separated by SDS-Polyacrylamide gel electrophoresis and transferred to 0.2 um nitrocellulose membrane (Cat# 1620112; Bio-Rad). Membranes were blocked with 5% non-fat dry milk/5% BSA in 1X Tris-buffered saline containing 0.1% Tween-20 (TBST) for 1 hour at room temperature. After blocking, membranes were incubated with primary antibodies diluted in 5% non-fat milk/5% BSA in 1X TBST at 4^{o}C overnight. Reacting proteins were detected using HRP conjugated anti-rabbit/mouse antibodies and observed by chemiluminescence using Supersignal west pico reagents (Cat#34577; ThermoFisher Scientific). Immunoblot images were acquired using Fluorchem E FE0622 system (ProteinSimple).

3.2.6. Statistical analysis

Statistical analysis was performed using Prism 5.0 (GraphPad Software). Unpaired *t*-test was used to compare extrusion counts between inhibitor treated cells and control.

3.3. Results

3.3.1. PKA localizes in the vicinity of the *C. trachomatis* inclusion

The localization of PKA subunits at the inclusion was tested by immunofluorescence in HeLa cells infected with *C. trachomatis*. PKA subunits are stained red, the *Chlamydia* are stained with MOMP (green) and the nucleus stained with DAPI (blue). PKA catalytic subunit α (PKA-Cα) are seen in the vicinity of the inclusion (Figure 3.1A). PKA-Cα showed two different localization patterns; one where it was around the inclusion and the other where it was adjacent to nucleus, reminiscent of Golgi staining. We then tested localization of the PKA regulatory subunit IIα (PKA-RIIα) that is known to localize at Golgi. PKA-RIIα was also found to localize around the inclusion exhibiting similar patterns as that of PKA-Cα. Given that *C. trachomatis* inclusions traffic to peri-Golgi region (Fields and Hackstadt 2002) and are known to cause Golgi fragmentation into mini stacks which then surround the inclusion (Heuer, et al. 2009), we hypothesized that PKA subunits around the inclusion may co-localize with Golgi. Accordingly, we tested whether PKA-Cα and PKA-RIIα co-localized with Golgi marker, golgin-97, around the inclusion. Both PKA-Cα and PKA-RIIα were found to co-localize with golgin-97 (stained green) (Figure 3.1B).

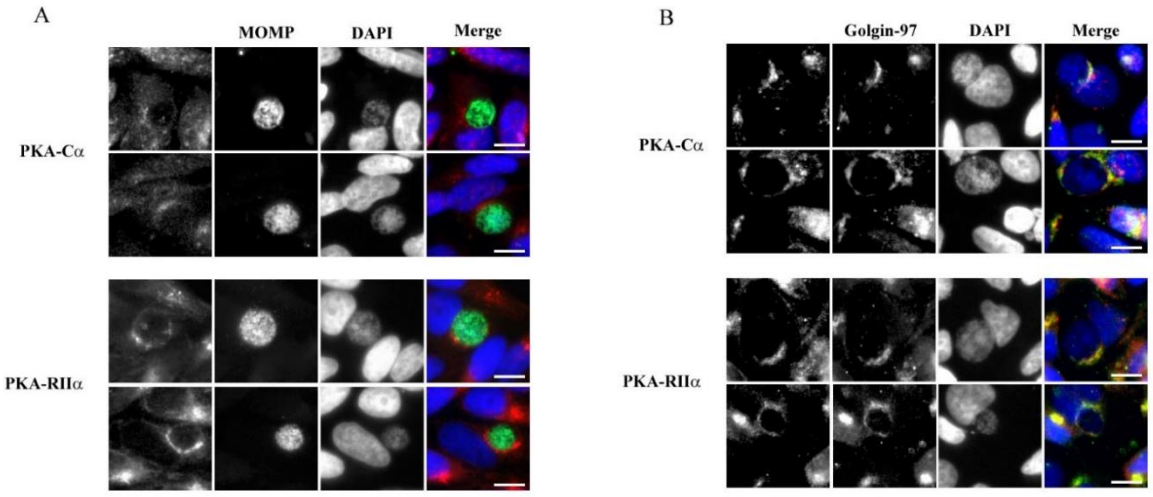

Figure 3.1. Localization of PKA subunits around the *C. trachomatis* inclusion. (A) HeLa cells were infected with *C. trachomatis* for 24 hours and processed for immunofluorescence. PKA-Cα and PKA-RIIα were stained red, *Chlamydia* was stained with MOMP (green) and nuclei were stained with DAPI (blue). (B) HeLa cells were infected with *C. trachomatis* for 24 hours and stained for PKA subunits (red) along with Golgi marker, golgin-97 (green). Scale bar, 10 μm.

3.3.2. Phosphorylated PKA substrates are recruited to the *C. trachomatis* inclusion

Immunofluorescence staining was used to examine whether phosphorylated PKA substrates localize around the inclusion. PKA substrate motif (RRXS/T) antibody was used to detect PKA serine/threonine phosphorylated substrates (red), *Chlamydia* were stained with MOMP (green) and nucleus was stained with DAPI (blue). Phosphorylated PKA substrates showed staining throughout the entire periphery of inclusion (Figure 3.2A). Further, to monitor the timing of phosphorylated PKA substrate recruitment, HeLa cells infected with *C. trachomatis* were processed for immunofluorescence at 18, 24, and 36 hours post-infection. At 18 hours post-infection phosphorylated PKA substrates were

recruited to the periphery of the inclusion which became more prominent at mid to late stages of infection (24 and 36hours post-infection) (Figure 3.2B).

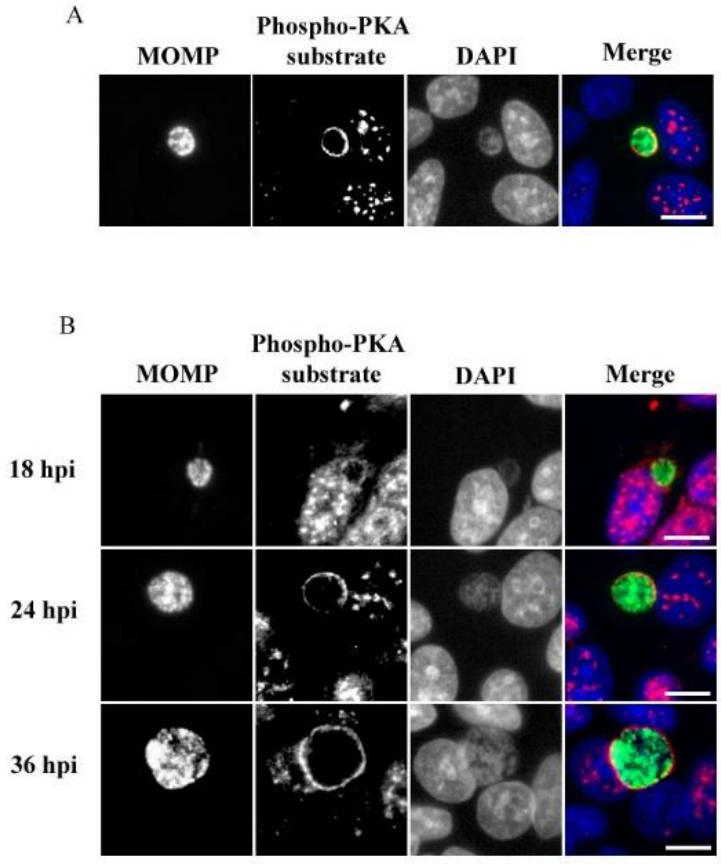

Figure 3.2. Phosphorylated PKA substrates are recruited to the entire periphery of the *C. trachomatis* inclusion. (A) HeLa cells were infected with *C. trachomatis* and processed for immunofluorescence at 24 hours post-infection. Phosphorylated PKA substrates were stained (red) using PKA substrate motif antibody, *Chlamydia* was stained with MOMP (green) and nuclei were stained with DAPI (blue). (B) Timing of phosphorylated PKA substrate recruitment was monitored at time points 18, 24 and 36 hours post-infection (hpi). Scale bar, 10 μm.

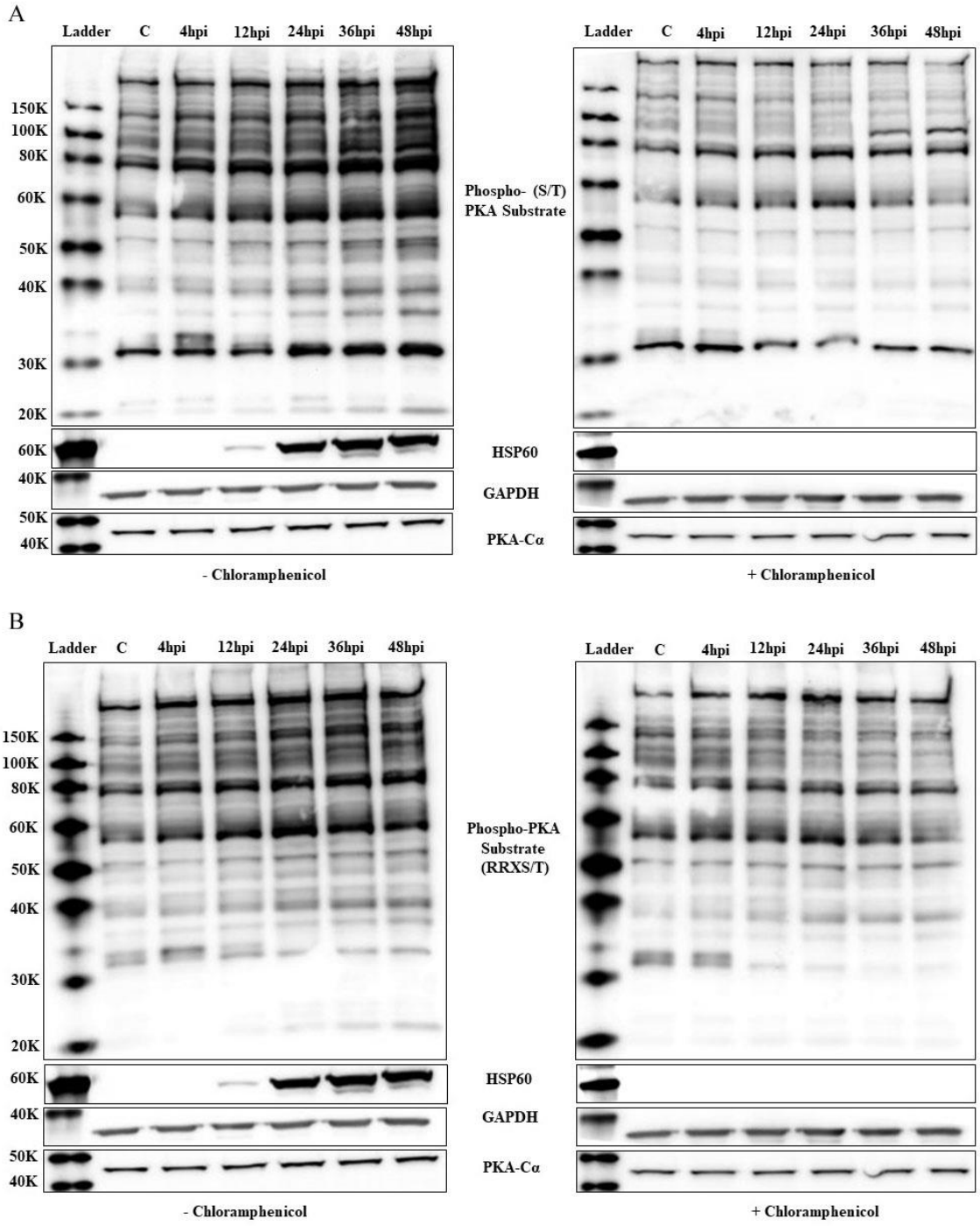

Figure 3.3. PKA substrate (Serine/Threonine) phosphorylation increases during *C. trachomatis* infection. Protein was collected from *C. trachomatis* infected cells (with or without chloramphenicol treatment) at 4, 12, 24, 36, and 48 hours post-infection and

probed for phosphorylated PKA substrates. Mock infected HeLa cells were used as control, (labeled C). GAPDH was used as loading control and *Chlamydia* was detected using HSP60. PKA-Cα was probed using anti-PKA-Cα. (A) Immunoblot for phosphorylated PKA substrates probed using PKA substrate motif (RXXS/T) antibody. (B) Immunoblot for phosphorylated PKA substrates probed using PKA substrate motif (RRXS/T) antibody.

3.3.3. PKA substrate phosphorylation increases during *C. trachomatis* infection

PKA substrate phosphorylation activity was detected using two separate motif antibodies that detect serine/threonine phosphorylated proteins. Whole cell lysate was collected from HeLa cells infected with *C. trachomatis* (with or without chloramphenicol treatment to inhibit bacterial protein synthesis) at indicated time points followed by immunoblotting to detect PKA phosphorylated substrates (Figure 3.3). GAPDH was used as a loading control while chlamydial HSP60 was used to indicate presence/absence of *C. trachomatis* in the samples. Immunoblot analysis using PKA substrate motif (RXXS/T) antibody showed an increase in PKA substrate phosphorylation especially mid to late in the infection cycle (Figure 3.3A). The increase in PKA substrate phosphorylation was not seen in samples treated with chloramphenicol indicating active involvement of *C. trachomatis*. Similar results were obtained with immunoblot analysis using another PKA substrate motif (RRXS/T) antibody (Figure 3.3B). The total PKA-Cα level was similar across all conditions. To further examine PKA activity during *C. trachomatis* infection, phosphorylation levels of PKA substrates cAMP response element binding protein (CREB) and glycogen synthase kinase 3β (GSK-3β) were analyzed by immunoblotting (Figure 3.4). While phosphorylated CREB (S133) showed an increase in phosphorylation

at mid to late time points, there was also an increase in total CREB in *C. trachomatis* infected cells. A similar trend was also seen in chloramphenicol treated cells (Figure 3.4A). Phosphorylation of GSK-3β (S9) showed marked increase in *C. trachomatis* infected samples especially towards mid to late time points compared to chloramphenicol treated samples (Figure 3.4B). The total GSK-3β remained uniform across all the time points in both conditions. The trend of GSK-3β phosphorylation similar to that seen with the overall PKA substrates in Figure 3.3.

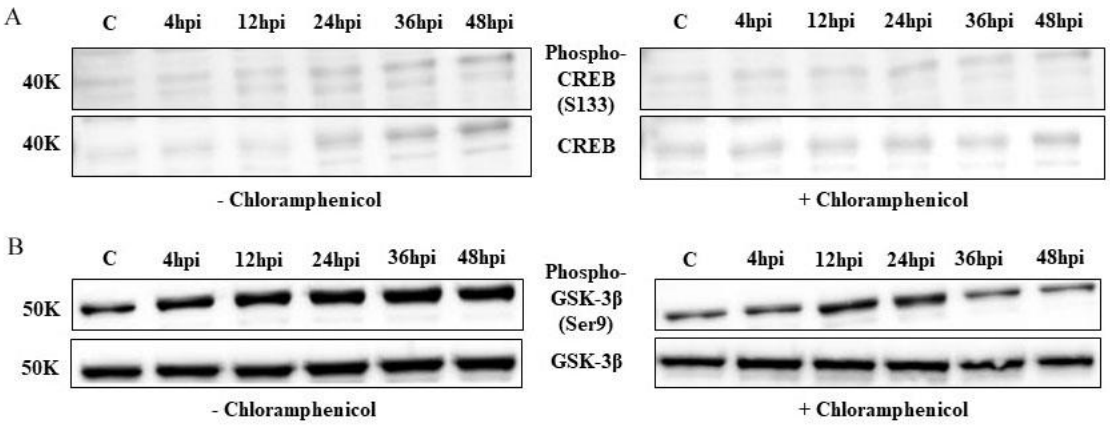

Figure 3.4. Phosphorylation of PKA substrates, GSK-3β and CREB during *C. trachomatis* infection. Protein was collected from *C. trachomatis* infected HeLa cells treated or untreated with chloramphenicol and probed for: (A) total CREB and phosphorylated CREB (S133), (B) total GSK-3β and phosphorylated GSK-3β (S9).

3.3.4. Pharmacological inhibition of PKA results in decreased extrusion

Given the abundance of phosphorylated PKA substrates recruited to *C. trachomatis* inclusion, we hypothesized PKA may be important for *C. trachomatis* development. PKA pharmacological inhibitors H89 and Rp-cAMPS were used to assess

the effect of PKA inhibition on *C. trachomatis* growth and exit. Rp-cAMPS being a more specific inhibitor than H89, two different concentrations of Rp-cAMPS, 100 μM and 250 μM, were used. Inhibitors were added 2 hours post-infection and maintained throughout infection cycle. Infected cells were subjected to progeny count and extrusion count analysis as described in the methods. Extrusions were almost completely inhibited by H89 (10 μM) treatment (Figure 5A; *P* value<0.0001). Rp-cAMPS at 100 μM concentrations resulted in a modest decrease in recoverable extrusions compared to the control (Figure 3.5A; *P* value=0.0031). At 250 μM concentration Rp-cAMPS showed a further decrease in extrusion production (Figure 5A; *P* value=0.0005). H89 (10μM) treatment resulted in slight decrease in IFU counts while Rp-cAMPs did not show any difference in IFUs compared to the control (DMSO treated cells) (Figure 3.5B).

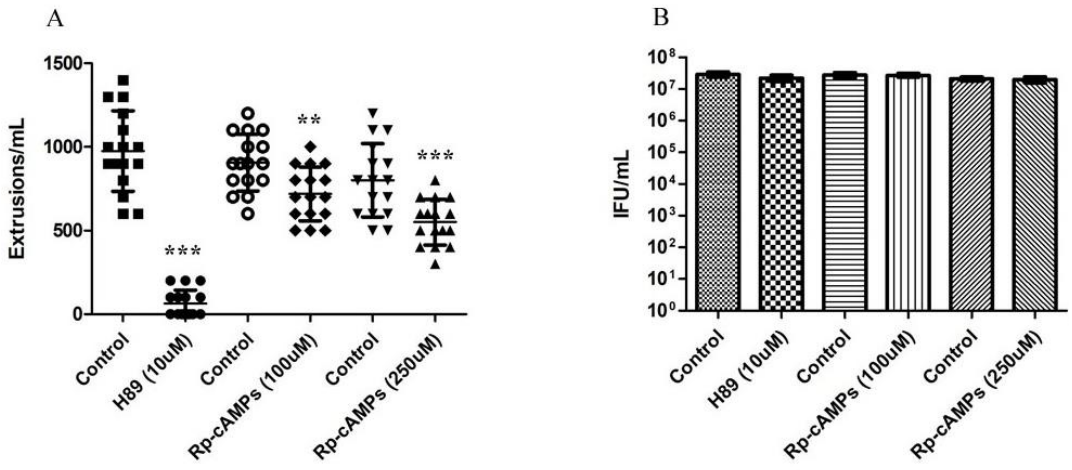

Figure 3.5. Effect of pharmacological inhibition of PKA on IFUs and extrusion production. (A) HeLa cells infected with *C. trachomatis* were treated with H89 (10 μM) or Rp-cAMPS (100 μM or 250 μM) or DMSO (control) 2 hours post-infection and maintained throughout infection. Extrusions from the infected cells were enumerated at 48 hours post-infection (H89 vs Control ***p<0.0001; Rp-cAMPS 100 μM **p=0.0031;

Rp-cAMPs 250 μM ***p=0.0005). (B) IFUs were enumerated from the infected cells by plating dilutions of lysed infected cells onto fresh HeLa cells Infection was allowed to proceed for 24 hours followed by processing for microscopy and 20 fields of view were counted for each condition in triplicate. Error bars indicate standard error of mean.

Extrusion begins late in the infection cycle peaking at about 48 hours followed by a decline (Lutter, et al. 2013). To determine whether H89 was inhibiting or delaying extrusions produced by *C. trachomatis* infected cells, extrusion enumeration was done at 42, 48, and 54 hours post-infection. Extrusion counts remained consistently low across all the time points while the control showed extrusion peaking at 48 hours post-infection as expected (Figure 3.6A). The corresponding IFU counts showed a slight decrease in H89 treated cells compared to the control (Figure 3.6B).

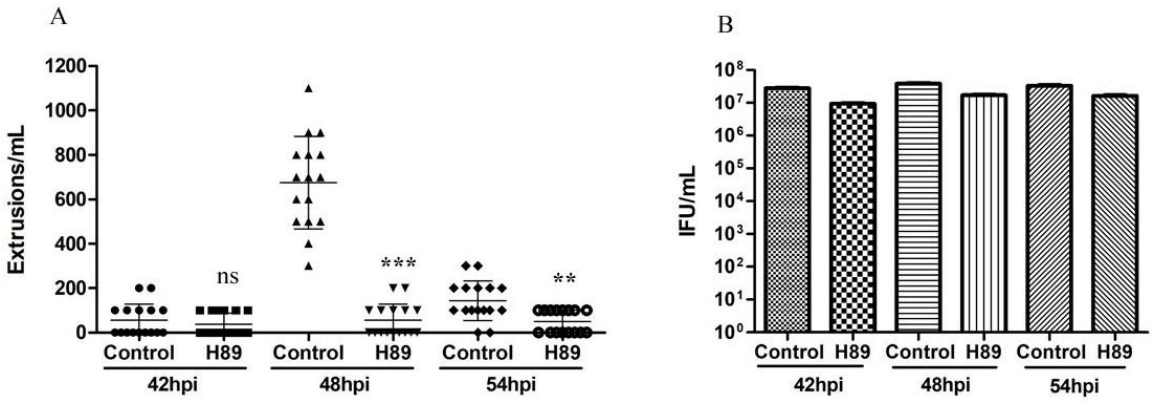

Figure 3.6. Time course of extrusion production in H89 treated *Chlamydia*-infected cells. (A) Extrusion enumeration from H89 or DMSO (control) treated HeLa cells at 42, 48, and 54 hours post-infection (ns- not significant; **p=0.001; ***p<0.0001). (B) IFU enumeration from infected cells at 42, 48 and, 54 hours post-infection time points. For

each condition/time point, 20 fields of view were counted in triplicate. Error bars indicate standard error of mean.

The phosphorylation level of MLC2 is modulated by *C. trachomatis* to regulate extrusion (Lutter, et al. 2013). Phosphorylated MLC2 favors *C. trachomatis* extrusion production by activating the myosin motor complex. Given the drastic effect of H89 on extrusion, MLC2 phosphorylation levels in *C. trachomatis* infected cells treated with H89 or DMSO were analyzed by immunoblotting. Mock infected cells were used as a control. In *C. trachomatis* infected cells, H89 treatment resulted in only a slight decrease in levels of phosphorylated MLC2 compared to DMSO treated cells while no obvious change in total MLC2 level was seen (Figure 3.7). In infected cells, the decrease was more evident at 36 and 42 hours post-infection than at 48 hours post-infection time point. The reduction in MLC2 phosphorylation was also seen in H89 treated mock infected cells compared to DMSO treatment.

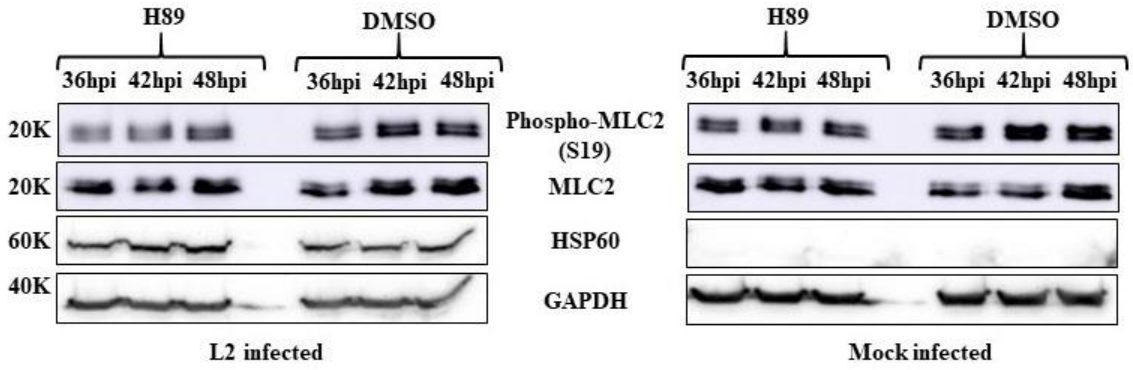

Figure 3.7. MLC2 phosphorylation levels in *C. trachomatis* infected cells treated with H89. Protein was collected from *C. trachomatis*/mock infected cells grown in presence of H89 (10 μM) or DMSO at 36, 42, and 48 hours post-infection and probed for

MLC2 and phosphorylated MLC2 (S19). Mock infected HeLa cells were used as a control. GAPDH was used as loading control and *Chlamydia* was detected using HSP60.

3.4. Discussion

C. trachomatis usurps various host signaling networks to promote its intracellular development. A large scale Inc-human interactome study and proteome analysis of isolated *C. trachomatis* inclusions revealed association of host kinases with Incs and the inclusion (Aeberhard, et al. 2015; Mirrashidi, et al. 2015). These studies highly suggest that *C. trachomatis* may rely on host kinases and signaling pathways during the infection process. Within an additional study, multiple host kinases including PKA, Protein Kinase C, Casein Kinase 2, and GSK-3β among others, have been implicated in host kinase phosphorylation of chlamydial proteins (Zadora, et al. 2019). Most notably, PKA was one of the major host kinases predicted to phosphorylate the greatest number of *C. trachomatis* proteins including many Incs (Zadora, et al. 2019). In this study we aimed to characterize PKA modulation by *C. trachomatis* during infection.

Given that PKA is predicted to phosphorylates Incs during *C. trachomatis* infection (Zadora, et al. 2019), this highly suggested that PKA may likely localize at or near inclusion. This, however, was somewhat expected since the *C. trachomatis* inclusion is located in the peri-Golgi region where a diverse set of signaling proteins are known to localize in host cells (Fields and Hackstadt 2002; Mayinger 2011). Pertinent to this study, components of PKA signaling, specifically PKAII, are known to localize at the Golgi via their association with AKAPs (Skalhegg and Tasken 2000; Tasken and Aandahl 2004). PKA activity itself has been shown to be involved in Golgi biogenesis and stability

(Bejarano, et al. 2006; Mavillard, et al. 2010). Therefore, the localization of catalytic and regulatory subunits of PKAII in *C. trachomatis* infected cells was tested by immunofluorescence. Both PKA-Cα and PKA-RIIα subunits were found to co-localize with the Golgi marker, golgin-97, around the *C. trachomatis* inclusion. In some cells, PKA-Cα and PKA-RIIα co-localized with golgin-97 at peri-nuclear region and in others, they seemed to surround the inclusion which is reminiscent of *C. trachomatis* induced Golgi fragmentation. *C. trachomatis* is known to usurp Golgi function and cause Golgi fragmentation into mini-stacks surrounding the inclusion (Heuer, et al. 2009). Although, initially suggested to be important for lipid acquisition, *C. trachomatis* induced Golgi fragmentation is dispensable for acquisition of lipids from Golgi (Heuer, et al. 2009; Gurumurthy, et al. 2014). The role of *C. trachomatis* induced Golgi fragmentation thus remains unsolved. However, it may serve as platform for subversion of host signaling pathways that localize at Golgi, including PKA signaling. Further, phosphorylated PKA substrates were shown to be recruited at inclusion around mid to late time points during infections. This indicated that localization of inclusion near Golgi may serve to localize PKA signaling components around the inclusion. The recruitment of phosphorylated PKA substrates is similar to that of PKC substrates that we have reported previously (Sah, et al. 2019). PKC, like PKA, is also implicated in phosphorylation of chlamydial Incs (Zadora, et al. 2019).

Immunoblot analysis of protein samples from *C. trachomatis* infected cells using two different phospho-PKA substrate motif antibodies revealed an overall increased level of phosphorylation of PKA substrates. The increase was marked especially mid to late time points in the infection. When bacterial protein synthesis was inhibited using

chloramphenicol, the increase in phosphorylation was abrogated. Phosphorylation levels of GSK-3β, a PKA substrate, also showed similar trends. A recent study showed that *C. trachomatis* causes an overall decreased PKA phosphorylation activity in the nuclear fraction (Zadora, et al. 2019).The same study also implicated PKA as one of the host kinases that phosphorylates many chlamydial proteins including Incs (Zadora, et al. 2019). In our study, we observed phosphorylated PKA substrates being recruiting at the inclusion where Incs localize. It is likely that the phosphorylated PKA substrates seen at the inclusion not only represent host proteins but also *C. trachomatis* proteins. To maintain specificity in phosphorylation, PKA activity is spatially controlled in the host cell via their association with AKAPs (Tasken and Aandahl 2004; Mayinger 2011). Further, it has been observed that following activation of Golgi associated PKA, the catalytic subunits localize and phosphorylate proteins nearby proteins instead of diffusing to nucleus (Mavillard, et al. 2010). Thus, *C. trachomatis* may induce only localized activation of PKA around the inclusion where host and *C. trachomatis* proteins may be phosphorylated.

Pharmacological inhibitors of PKA, H89 and Rp-cAMPS, were employed to assess the effect of PKA inhibition on *C. trachomatis* growth and exit. H89 is a broad range inhibitor while Rp-cAMPS is a more specific PKA inhibitor (Lochner and Moolman 2006). In our study, PKA inhibition with H89 resulted in a slight decrease in IFUs while no effect on IFUs was seen with Rp-cAMPS. A previous study reported cAMP, which is a regulator of PKA activity, is inhibitory to *C. trachomatis* development while cAMP analogs or breakdown products did not show this inhibitory effect (Kaul and Wenman 1986). A subsequent study showed the inhibitory effect of accumulation of

cAMP on *C. trachomatis* development is independent of PKA activity (Pettengill, et al. 2009). H89 treatment of *C. trachomatis* infected cells resulted in a drastic reduction in extrusion. Reduction in extrusion in Rp-cAMPS treated cells was seen but to a lesser extent than that of H89. Rp-cAMPS also showed a dose dependent reduction in extrusion production. Taken together, our observations suggest a possible role for PKA in extrusion production. The discrepancies in extrusion as well as IFU counts seen between H89 and Rp-cAMPS treatment may be explained by H89 targeting other host kinases in addition to PKA. In addition to PKA, H89 can inhibit other host kinases such as mitogen- and stress-activated protein kinase 1 (MSK1), ribosomal protein S6 kinase 1 (S6K1), and Rho-associated coiled-coil containing protein kinase 2 (ROCK2) among other host kinases (Lochner and Moolman 2006). This indicates involvement of kinases targeted by H89 in *C. trachomatis* development and extrusion formation. This is not surprising as a previous study by the Hybiske lab has shown that multiple signaling pathways are important for extrusion (Hybiske and Stephens 2007; Zuck and Hybiske 2019). Time course analysis of extrusion production showed that H89 treatment resulted in inhibition of extrusion events after 48 hours post-infection rather than delaying extrusion. *C. trachomatis* recruits the elements of Myosin phosphatase pathway to regulate extrusion. The recruitment of MYPT1, a component of myosin phosphatase, (by Inc CT228) and MLCK at the inclusion by *C. trachomatis* determines phosphorylation level of MLC2 which in turn regulates extrusion (Lutter, et al. 2013; Shaw, et al. 2018). Thus, in the event of extrusion production coming to a halt, the phosphorylation levels of MLC2 is expected to reduce substantially. Immunoblot analysis of H89 treated *C. trachomatis* infected cells showed only a slight decrease in MLC2 phosphorylation levels, especially

at 48 hours post-infection time point when extrusion production peaks. This indicated that PKA or other host kinases targeted by H89 may involve a mechanism other than myosin phosphatase pathway in extrusion formation.

CHAPTER IV

INTERACTIONS OF *CHLAMYDIA TRACHOMATIS* INCLUSION MEMBRANE PROTEIN CT226

4.1. Introduction

Chlamydia trachomatis is a Gram-negative intracellular pathogen that causes widespread sexually transmitted infections (STIs) and ocular infections (Belland, et al. 2004). *C. trachomatis* is the most frequently reported bacterial STI agent in the US with chronic infections leading to sequelae such as pelvic inflammatory disease (PID), ectopic pregnancy, and infertility (Malhotra, et al. 2013; CDC 2019). *C. trachomatis* has also been associated as risk factor for development of cervical cancer (Koskela, et al. 2000; Zhu, et al. 2016). The ocular infection caused by *C. trachomatis*, trachoma, is the leading cause of preventable infectious blindness in the developing countries (Resnikoff, et al. 2004; Burton and Mabey 2009). *C. trachomatis* has a unique biphasic developmental cycle that consists of alternation between the infectious elementary bodies (EBs) and the non-infectious reticulate bodies (RBs) (Moulder 1991; Abdelrahman and Belland 2005). Inside the host cell *C. trachomatis* reside within a parasitophorous vacuole called the inclusion from where it is able to subvert host cell processes to promote its intracellular survival (Abdelrahman and Belland 2005; Elwell, et al. 2016).

C. trachomatis employs a type 3 secretion system (T3SS) to secrete and localize an arsenal of effectors into host cytosol or chlamydial inclusion membrane (Fields, et al. 2003; Mueller, et al. 2014). These virulence effectors represent about 10% of the highly reduced *C. trachomatis* genome indicating their importance for chlamydial development (Betts-Hampikian and Fields 2010). Inclusion membrane proteins (Incs) are a specialized group of T3SS effectors that localize at inclusion membrane and are exposed to host cytosol where they can interact with host proteins (Bannantine, et al. 2000; Rockey, et al. 2002; Dehoux, et al. 2011; Lutter, et al. 2012). Incs share little to no similarity with other proteins, however, they do share a hydrophobic transmembrane domain (often bilobed). Over 50 Incs have been predicted in *C. trachomatis* of which 36 has been verified as bonafide Incs (Dehoux, et al. 2011; Lutter, et al. 2012; Bugalhao and Mota 2019). Incs are suggested to be key players in host-*Chlamydia* interactions and maintaining the stability of inclusion (Mital, et al. 2013; Weber, et al. 2017; Bugalhao and Mota 2019). Further, Incs are expressed at different times during *C. trachomatis* intracellular development indicating a stage specific role for Incs (Shaw, et al. 2000). Host interactions of several Incs have been characterized with roles in different aspects of chlamydial development (Scidmore and Hackstadt 2001; Rzomp, et al. 2006; Delevoye, et al. 2008; Derre, et al. 2011; Lutter, et al. 2013; Dumoux, Menny, et al. 2015; Mirrashidi, et al. 2015; Mital, et al. 2015; Stanhope, et al. 2017; Almeida, et al. 2018; Nguyen, et al. 2018). Further, putative interacting partners of several Incs have been identified in an Inc-host interactome study (Mirrashidi, et al. 2015). Several of these putative Inc-host interactions remains to be characterized.

Four host proteins, protein flightless I homolog (FLII), leucine-rich repeat flightless-interacting protein 1 (LRRFIP1), LRRFIP2, and tropomodulin-3 (TMOD3) were identified as putative binding partners of Inc CT226 in an Inc-host interactome study (Mirrashidi, et al. 2015). Further, FLII, LRRFIP1, and TMOD3 have been shown to localize at or interact with the inclusion membrane (Aeberhard, et al. 2015; Dickinson, et al. 2019; Olson, et al. 2019). Subsequently, another proximity labelling based proteomics study also identified LRRFIP1 as a binding partner of CT226 (Olson, et al. 2019). Interestingly, of the four putative binding partners of CT226, FLII is known to interact with LRRFIP1 and LRRFIP2 as well (Dai, et al. 2009). FLII is important for various cellular processes including actin remodeling and regulation of inflammatory response (Wang, et al. 2006; Dai, et al. 2009; Mohammad, et al. 2012; Kopecki, et al. 2016). FLII negatively regulates toll-like receptor (TLR) pathway by interacting with MyD88 (Wang, et al. 2006). FLII also interacts with other MyD88 binding partners including LRRFIP1 and LRRFIP2 during regulation of TLR pathway (Dai, et al. 2009). FLII is also known to regulate pro-inflammatory caspases (caspase-1 and caspase-11) (Li, et al. 2008). LRRFIP2 negatively regulates NLRP3 inflammasome activation via FLII mediated inhibition of caspase-1 (Jin, et al. 2013). LRRFIP1 has been implicated in regulation of a rapid type I interferon response (Bagashev, et al. 2010). On the other hand, TMOD3 is an actin capping (pointed end) protein that regulates several dynamic actin-based cellular processes (Parreno and Fowler 2018). These host proteins and their potential interaction with CT226 thus may represent a way for *C. trachomatis* to manipulate host cytoskeletal and immune response.

In this study, we investigated interactions of CT226 and its role in recruitment of the putative binding host proteins. Co-immunoprecipitation indicated CT226 interacts with FLII, LRRFIP1 and TMOD3. Using a mutant strain L2 ΔCT226 generated by fluorescence reported allelic exchange mutagenesis, we found FLII recruitment is completely abrogated in absence of CT226. Further, recruitment of FLII and TMOD3 is conserved among *Chlamydia* species containing CT226 homolog and siRNA knockdown of TMOD3 resulted in only a modest decrease in infectious progeny production.

4.2. Materials and methods

4.2.1. *Chlamydia* strains and cell culture

HeLa and McCoy cells were grown in RPMI 1640 containing 5% fetal bovine serum (FBS) at 37^0C in presence of 5% CO_2/95% humidified air. *C. trachomatis* L2/434/Bu, *C. trachomatis* D/UW3/Cx, *C. trachomatis* B/Jali20, *C. muridarum* MoPn, *C. pneumoniae* AR-39, and *C. caviae* GPIC were grown in HeLa cells. Crude and density gradient purified EBs preparation was done as described previously (Caldwell, et al. 1981). McCoy cells were used for transformation of *C. trachomatis* L2/434/Bu.

4.2.2. Antibodies

Anti-eGFP (Cat#CAB4211; ThermoFisher Scientific) was used to detect eGFP and CT226-eGFP fusion protein. Gal4-BD fusion of CT226 (C-terminal) and Myc-TMOD3 was detected using anti-Myc antibody (a kind gift from Dr. Tom Oomens, Oklahoma State University College of Veterinary Medicine). Gal4-AD fusion of TMOD3 was detected using anti-Gal4-AD (Cat#630402; TakaraBio). GAPDH was detected using anti-GAPDH (Cat#25778; Santa Cruz Biotechnology) antibody. FLII, LRRFIP1,

LRRFIP2, and TMOD3 were detected using anti-FLII (Cat#PA5-21735; ThermoFisher Scientific), anti-LRRFIP1 (Cat#PA5-21114; ThermoFisher Scientific), anti-LRRFIP2 (Cat#PA5-21115; ThermoFisher Scientific) and anti-TMOD3 (Cat#PA5-51645; ThermoFisher Scientific) respectively. *Chlamydia* strains were detected using anti-*Chlamydia* LPS antibody. *C. trachomatis* L2 was detected using anti-MOMP-FITC (Cat#PA1-73073; ThermoFisher Scientific) for infectious progeny enumeration. Secondary antibodies anti-rabbit or anti-mouse DyLight 594 and DyLight 488 (Jackson ImmunoResearch) were used for immunofluorescence. Anti-rabbit-horseradish peroxidase (HRP) (Cat#7074; Cell Signaling Technology) and anti-mouse-HRP (Cat#7076; Cell Signaling Technology) were used for western blot analysis.

4.2.3. *In silico* analysis of CT226

Sequences of *C. trachomatis* L2 CT226 and its homolog in *C. muridarum* TC0497 were obtained from National Center for Biotechnology Information (NCBI) database. Sequence alignment was done using MUSCLE (Madeira, et al. 2019). Transmembrane domain was predicted using TMHMM 2.0 and Phobius (Krogh, et al. 2001; Kall, et al. 2004). The location of predicted leucine zipper within coiled coil domain of C-terminal region of CT226 (Dehoux, et al. 2011) was determined using 2ZIP (Bornberg-Bauer, et al. 1998).

4.2.4. Cloning and DNA assembly

Primers used for amplification by polymerase chain reaction (PCR) are listed in Table 1. Cloning was performed in *Escherichia coli* DH5α/DH10β. Full length *CT226* and *CT226* C-terminus were PCR amplified from L2/434/Bu genomic DNA and cloned

into the XhoI/PstI sites of pEGFPN1 and EcoRI/SalI sites of pGBKT7, respectively. *TMOD3* was amplified from human *TMOD3* cDNA clone expression plasmid pCMV3-Myc-TMOD3 (Cat# HG15491-NM; Sino Biologicals) and cloned into the NdeI/EcoRI sites of pGADT7-AD. The construction of CT226 deletion plasmid, pSuMc-LF-*aadA-gfp*-RF was done as described previously (Wolf, et al. 2019). Briefly, two sequential assembly reactions were done to clone 3kb regions flanking left and right of *CT226* gene into pSuMc-*aadA-gfp* (a kind gift from Dr. Ken Fields, University of Kentucky College of Medicine) using NEBuilder HiFi DNA assembly master mix (Cat# E2621; NEB). After cloning, the pSuMc-LF- *aadA-gfp*-RF construct was transformed into methylation deficient *E. coli* K12-ER2925 to obtain non-methylated construct. All the plasmid constructs were verified by sequencing.

4.2.5. Generation of CT226 mutant by fluorescence reported allelic exchange mutagenesis (FRAEM)

Transformation of *C. trachomatis* with CT226 deletion plasmid, pSuMc-LF-*aadA-gfp*-RF (prepared from *E. coli* K12-ER2925) was performed as previously described (Wolf, et al. 2019). *C. trachomatis* L2 EBs (crude preparation) were transformed with unmethylated pSuMc-LF- *aadA-gfp*-RF DNA using $CaCl_2$ buffer (10mM Tris pH 7.4; 50mM CaCl2). Cells infected with transformed L2 EBs were passaged in presence of RPMI containing 500 μg/mL spectinomycin, 1 μg/mL cycloheximide and 50 ng/mL anhydrotetracycline (ATc) until red and green fluorescing inclusions developed. Following passage 4 (when red and green fluorescent inclusions were seen), cells were passaged in presence of RPMI containing 500 μg/mL spectinomycin and 1 μg/mL cycloheximide but without ATc until only green fluorescent

inclusions developed. Green fluorescent inclusions (representing the CT226 mutant) were expanded and a crude preparation of EBs was performed. Clonal population of CT226 mutant was isolated using limiting dilution method which was then expanded and purified by the density gradient method. Deletion of *CT226* was verified by PCR and whole genome sequencing.

Table 4.1. Primers used for PCR

Primer	**Sequence**
pEGPN1CT226FXhoI	AAACTCGAGTTGCGAAATAGAGGCG
pEGPN1CT226RPstI	AAACTGCAGTCTCAGACTTTCTTCC
pGBKT7CT226(C-term)EcoRIF	TTTGAATTCATGTATGGGTTTTCTTTAAAACC
pGBKT7CT226(C-term)SalIR	TTTGTCGACTTATCTCAGACTTTCTTCCAATACAC
pGADT7TMOD3NdeIF	TTTCATATGATGGCACTGCCATTCCG
pGADT7TMOD3EcoRIR	TTTGAATTCTTACTGGTGATCTCCTTC
CT226-LF-F	TCCGTCACTGCAGGTACCGGGAGAATAGAGTATTGAAAG
CT226-LF-R	GGAGGCATGATGATGAATGGAAAAGGCCGACATGCTACAG
CT226-RF-F	CTATACAAGTAAGACCTGCATTATTAATGGTTTCCAAGTAG
CT226-RF-R	ACGGGGTCTGACGCCCTGCATAAATACTTTAAATACAACTG
CT225R	AAAAGGTACCATCCCACCCATG
CT227F	TTTCTCGAGATGTCTTATCTTTTTTGTTCC

4.2.6. Co-immunoprecipitation

HeLa cells were transfected with pEGFPN1 and pEGFPN1-CT226 using Lipofectamine 3000 (Cat# L3000; ThermoFisher Scientific) as per manufacturer's instructions. Geneticin (Cat# 10131; Gibco) selection (300 µg/mL) was used in order to generate stably expressing HeLa-eGFP and HeLa-CT226-eGFP cells. For TMOD3 co-

immunoprecipitations, pCMV3-Myc-TMOD3 and the negative control vector (NCV) pCMV3-Myc were transfected (transiently) into HeLa-eGFP and HeLa-CT226-eGFP. GFPtrap and Myctrap kits (Cat# gta-20; yta-20; Chromotek) were used to perform co-immunoprecipitations as per manufacturer's instructions. Briefly, protein was collected from the cells using lysis buffer and mixed with GFPtrap/MycTrap beads. Beads were incubated at 4^0C for 2 hours with constant tumbling end-over-end. Following protein binding, beads were washed and eluted in Laemmli buffer followed by boiling at 95^0C for 10 minutes. Proteins in eluate were detected by western blotting.

4.2.7. Immunofluorescence microscopy

HeLa cells in 24 well plates (CellTreat Scientific) containing round cover slips and infected with *C. trachomatis* L2/434/Bu (WT and ΔCT226 mutant), *C. trachomatis* B/Jali20, *C. trachomatis* D/UW3/Cx, *C. muridarum* MoPn, *C. pneumoniae* AR-39 and *C. caviae* GPIC at multiplicity of infection (MOI) of approximately 0.5. Cells infected with serovars L2 and *C. caviae* were methanol fixed at 24 hours post-infection. Cells infected with serovars D, B and *C. muridarum* were fixed at 30 hours post-infection while cells infected with *C. pneumoniae* were fixed at 60 hours post-infection. For time course experiments with L2, cells were fixed at 18, 24, and 36 hours post-infection. Following fixation, cells were washed in phosphate buffered saline (PBS) and blocked with 1% bovine serum albumin (BSA). Cells were treated with primary antibodies against TMOD3, FLII, LRRFIP1, LRRFIP2, 14-3-3β, and *Chlamydia* LPS followed by PBS wash and blocking with 1% bovine serum albumin (BSA). Cells were washed with PBS and treated with anti-mouse/rabbit secondary antibodies along with DAPI. After staining, coverslips were mounted onto slides using Dako Mounting Medium (Agilent

Technologies, Santa Clara CA) and observed using a Leica DMI6000B fluorescent microscope (Leica Microsystems). Images were acquired at 40X magnification and representative images were used for making panels.

4.2.8. Yeast 2 hybrid experiments

Yeast strains *Saccharomyces cerevisiae* AH109 and Y187 were used for yeast 2 hybrid experiments. Plasmids pGBKT7, pGBKT7-Lam, pGBKT7-53, pGADT7-AD, pGADT7-T were obtained from Clonetech. pGBKT7-CT226 (C-term) (bait) and pGADT7-TMOD3 (prey) were constructed as described above. Bait and prey plasmids were transformed into AH109 and Y187 strains respectively using Frozen-EZ yeast transformation kit (Cat# T2001; Zymo Research). AH109 transformants were selected on synthetic dropout (SD) media without tryptophan (SD-T) while Y187 transformants were selected on SD media without leucine (SD-L). Bait and prey expression was verified by extracting protein from transformants using urea/SDS lysis method followed by western blotting. AH109 pGBKT7-CT226 (C-term) was mated with Y187 pGADT7-TMOD3. AH109 pGBKT7-Lam and AH109 pGBKT7-53 mated with Y187 pGADT7-T were used as positive and negative control respectively. Mated culture were selected on SD media without tryptophan, leucine (SD-TL). Testing for interaction was done on SD-TL and SD media without leucine, tryptophan, histidine (SD-TLH) containing X-α-Gal.

4.2.9. siRNA transfection and Infectious progeny enumeration

HeLa cells in 24 well plates (50% confluency) were transfected with Scramble or TMOD3 Targetplus Smartpool siRNA (Dharmacon) as per manufacturer's instruction. After 48 hours of transfection, cells were infected with *C. trachomatis* serovar L2 at MOI

of 1. At 48 hours post-infection, cells were washed with PBS and protein was collected by adding 100 µL of 2x Laemmli buffer to cells. Knockdown efficiency was assessed by western blotting. For infectious progeny enumeration, infected cells were lysed with sterile water and serially diluted (10^{-1} to 10^{-8}) in Hank's Balanced Salt Solution (HBSS). HeLa cell monolayers in 96 well plates were infected with 100 µL of each dilution and incubated for 24 hours followed by methanol fixation and staining with anti-MOMP-FITC antibody. Inclusions were counted on 15 microscopic fields using a Leica DMI6000B microscope and total inclusion forming units IFU/mL were calculated.

4.2.10. Western blotting

SDS-Polyacrylamide gel electrophoresis was used to separate protein samples and transferred to 0.2 um nitrocellulose membrane (Cat# 1620112 Bio-Rad). Membranes were blocked with 5% non-fat dry milk in 1X Tris-buffered saline containing 0.1% Tween-20 (TBST) for 1 hour at room temperature. After blocking, membranes were incubated with primary antibodies against TMOD3 and GAPDH diluted in 5% non-fat milk in 1X TBST at 4^{o}C overnight. Membranes were washed with TBST and HRP conjugated anti-rabbit antibody was added for 1 hour at room temperature. Reactions were developed using chemiluminescence using Supersignal west pico reagents (Cat#34577; Thermofisher Scientific). Immunoblot images were acquired using Fluorchem E FE0622 system (ProteinSimple).

4.3. Results

4.3.1. The putative leucine zipper in the coiled-coil region of CT226 is conserved in its homolog TC0497

The N-terminus of CT226 contains two transmembrane domains (predicted using TMHMM 2.0 and Phobius) spanning residues 40-62 and 72-94. The C-terminus of CT226 is predicted to contain a leucine zipper (LZ) within coiled coil region (Dehoux, et al. 2011). Using 2ZIP, the LZ was located within coiled coil region of CT226 spanning residues 120-168 (Figure 4.1A). A homolog of *C. trachomatis* CT226, TC0497 was found in the closely related *C. muridarum*. Multiple sequence alignment of CT226 and TC0497 revealed conservation of all four leucine residues of the LZ.

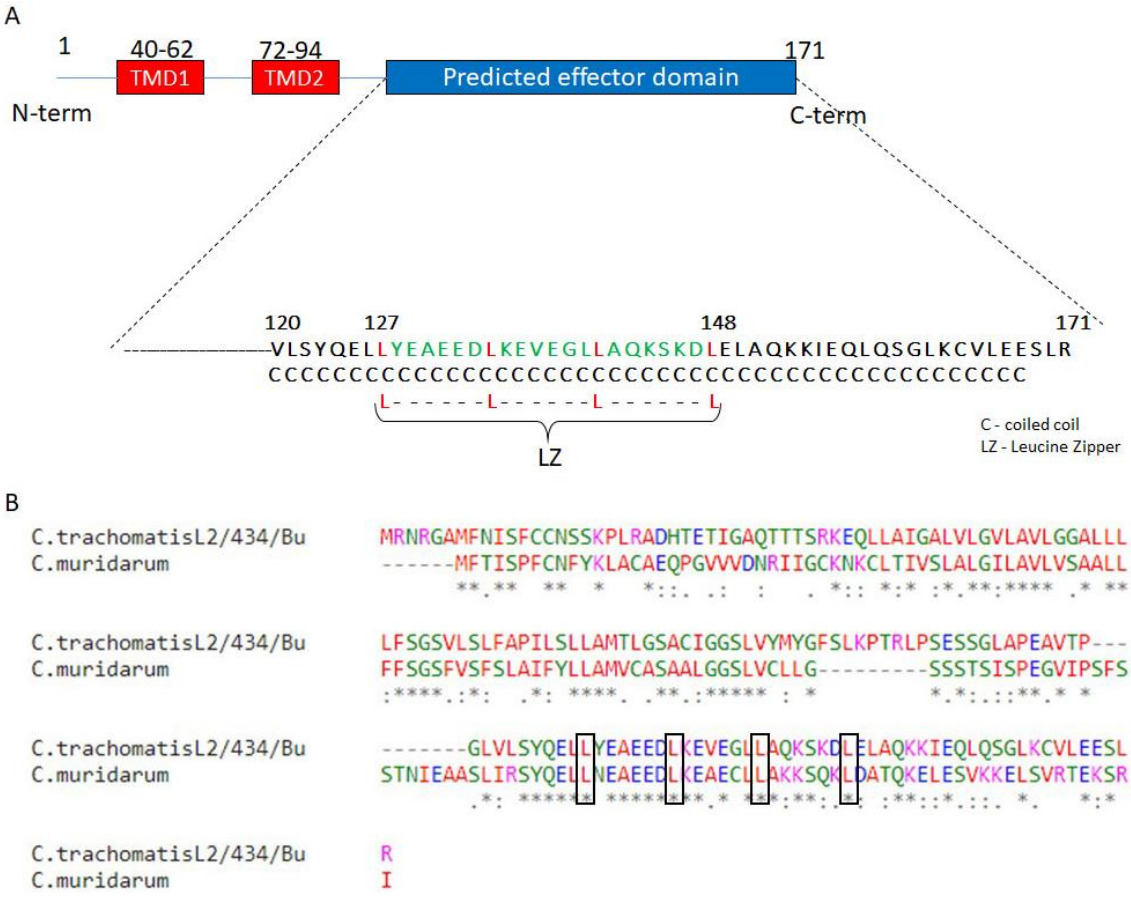

Figure 4.1. *In silico* analysis of CT226 and sequence alignment of CT226 and TC0497. (A) Two transmembrane domains in the N-terminal and LZ within coiled coil region of C-terminal are predicted in CT226. (B) Sequence alignment of CT226 (*C.*

trachomatis L2/434/Bu) and its homolog TC0497 (*C. muridarum*) revealed that leucine residues of the LZ are conserved.

4.3.2. Ectopically expressed CT226-eGFP fusion protein localizes in perinuclear region in HeLa cells

HeLa cells expressing CT226-eGFP fusion protein (HeLa-CT226-eGFP) or eGFP (HeLa-eGFP) were generated by transfection and selection with geneticin. Localization of ectopically expressed CT226-eGFP was analyzed by live fluorescence and immunofluorescence microscopy following methanol fixation. Both live and fixed cell microscopy showed a preferential perinuclear localization of CT226-eGFP in HeLa cells while eGFP remained diffuse throughout cytosol and nucleus (Figure 4.2).

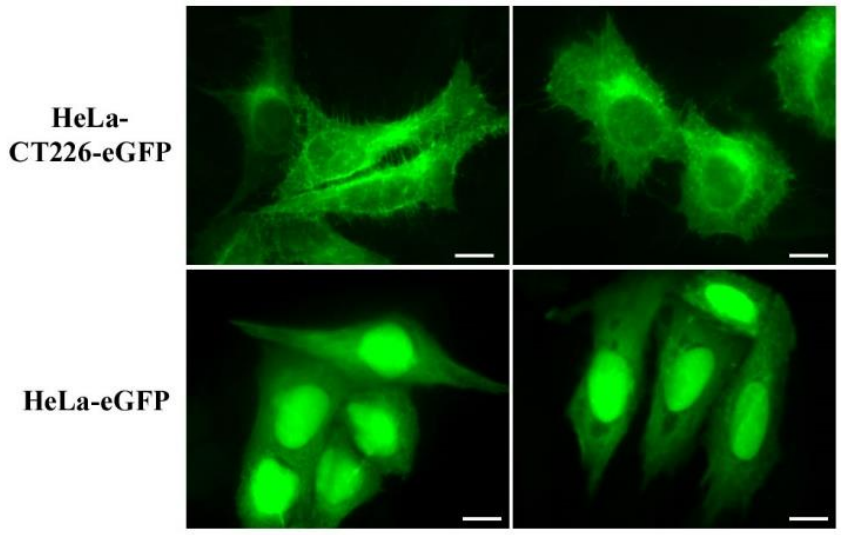

Figure 4.2. Localization of CT226-eGFP and eGFP in HeLa cells. Representative immunofluorescence microscopy images of HeLa-CT226-eGFP and HeLa-eGFP shows different localization pattern of CT226-eGFP and GFP. CT226-eGFP remains mostly in perinuclear region while eGFP is diffuse in cytosol and nucleus. Scale bar, 10 µm.

4.3.3. FLII, LRRFIP1, and TMOD3 co-immunoprecipitates with ectopically expressed CT226-eGFP fusion protein

HeLa-CT226-eGFP cells were used for co-immunoprecipitation experiments because an antibody against CT226 was unavailable. Protein was extracted from HeLa-CT226-eGFP and HeLa-eGFP cells followed by eGFP precipitation using GFPTrap beads. Eluates from GFPTrap co-immunoprecipitation were analyzed by western blotting for presence of putative binding partners of CT226. FLII, LRRFIP1, and TMOD3 co-precipitated with CT226-eGFP but not with the eGFP control (Figure 4.3). LRRFIP2 was not detected in the co-immunoprecipitation.

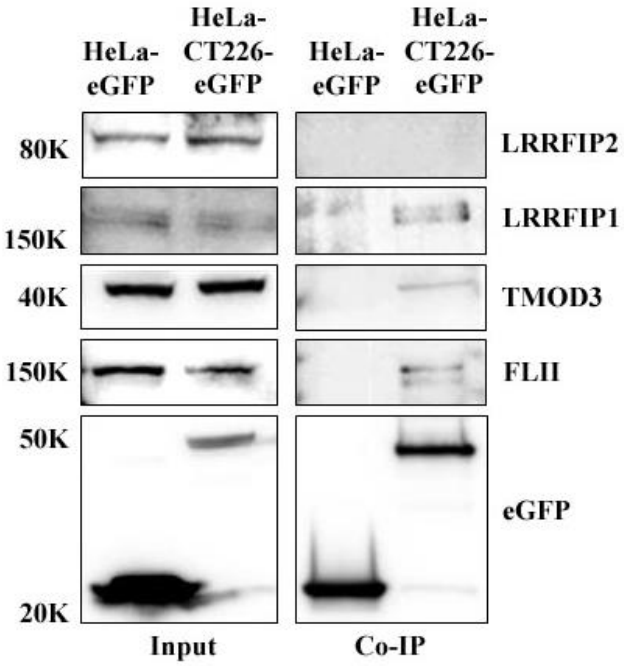

Figure 4.3. Co-immunoprecipitation of putative CT226 binding partners. CT226-eGFP/eGFP was expressed in HeLa cells and eGFP (or fusion protein) was precipitated using GFPTrap beads. Proteins were detected in Input and co-immunoprecipitation (Co-IP) samples by western blotting.

CT226 interaction with TMOD3 was further analyzed by expressing Myc-TMOD3 in HeLa-CT226-eGFP cells. Co-immunoprecipitations were performed using GFPTrap as well as Myctrap beads. CT226-eGFP pulled Myc-TMOD3 in GFPtrap co-immunoprecipitation and Myc-TMOD3 pulled CT226-eGFP in MycTrap co-immunoprecipitation (Figure 4.4).

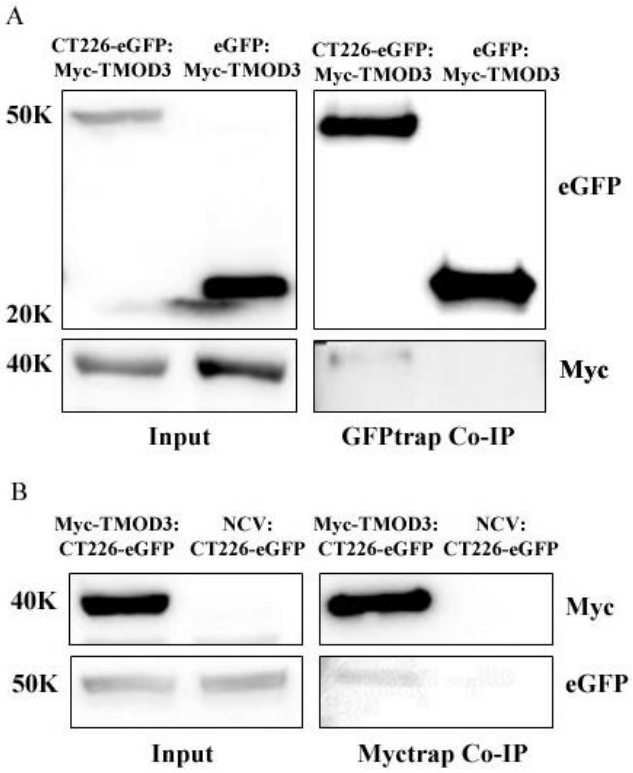

Figure 4.4. Co-immunoprecipitation of CT226-eGFP and Myc-TMOD3. (A) Myc-TMOD3 was expressed in HeLa-CT226-eGFP and HeLa-eGFP. GFPTrap beads were used to precipitate eGFP/CT226-eGFP. Proteins in input and Co-IP samples were detected by western blotting. (B) Myc-TMOD3/NCV (with just Myc tag) was expressed in HeLa-CT226-eGFP and MycTrap were used to precipitate Myc/Myc-TMOD3. Proteins in input and Co-IP samples were detected by western blotting.

4.3.4. Yeast 2 hybrid analysis of CT226 and TMOD3 interaction

The interaction of CT226 with TMOD3 was further analyzed by yeast 2 hybrid experiments. The C-terminal of CT226 (residues 93-171) (bait) was cloned into pGBKT7 and transformed into *S. cerevisiae* AH109. TMOD3 cDNA (Prey) was cloned into pGADT7-AD and transformed into *S. cerevisiae* Y187. AH109 and Y187 containing bait and prey plasmids were mated. AH109 pGBKT7-Lam and pGBKT7-53 cultures were mated with Y187 pGADT7-T as positive and negative controls respectively. Interaction was screened for by plating mated cultures on SD-TL and SD-TLH plates containing X-α-Gal. The appearance of blue colonies on X- α-Gal containing plates indicated interaction between bait and prey. pGBKT7-CT226 and pGADT7-TMOD3 mated culture showed blue colonies only on SD-TL plates after a week of incubation and failed to grow on SD-TLH plates (Figure 4.5A). Growth of Y187 expressing TMOD3-AD fusion was slower compared to Y187 expressing control plasmids pGADT7-AD and pGADT7-T indicating a possible negative effect of TMOD3 expression on its growth (Figure 4.5B). Western blot analysis of expression of bait and prey fusion proteins showed expression of prey fusion protein was much less than bait (Figure 4.5C).

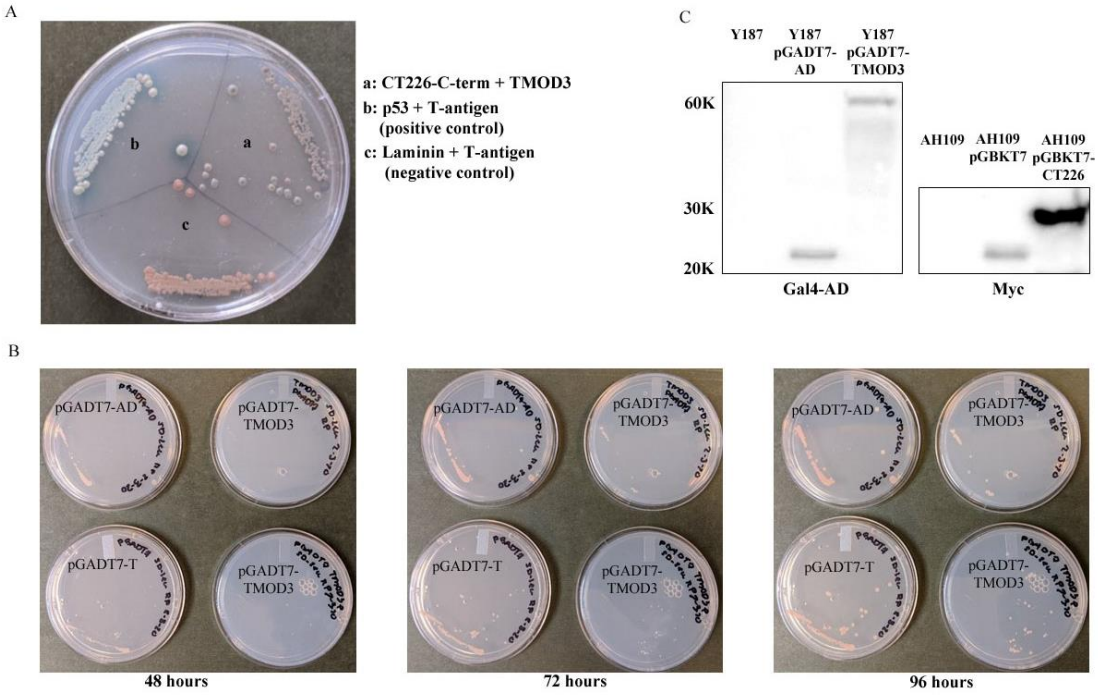

Figure 4.5. Yeast 2 hybrid analysis of CT226 and TMOD3 interaction. (A) Cultures of pGBKT7-CT226 (C-term) mated with pGADT7-TMOD3, pGBKT7-53 mated with pGADT7-T, and pGBKT7-Lam mated with pGADT7-T on SD-TL (containing X-α-Gal) plate. pGBKT7-CT226 (C-term) mated with pGADT7-TMOD3 shows blue (weakly) colonies. (B) Growth comparison of Y187 pGADT7-AD, Y187 pGADT7-T and two different Y187 pGADT7-TMOD3 strains on SD-L plates showing slow growth of Y187 pGADT7-TMOD3 strains. (C) Bait and prey fusion protein expression was analyzed by western blotting using anti-Myc and anti-Gal4BD respectively. Bait was expressed abundantly while prey expression was low.

4.3.5. TMOD3 localizes around the *C. trachomatis* L2 inclusion

Localization of TMOD3 in *C. trachomatis* L2 infected cells was analyzed by immunofluorescence. In addition to enrichment of TMOD3 around the inclusion,

localization at discrete sites on the inclusion membrane was observed as well (Figure 4.6A). Localization at the inclusion membrane was verified by co-localization with 14-3-3β, a host protein known to localize all around the inclusion membrane. Time course analysis of TMOD3 recruitment revealed TMOD3 is recruited beginning at 18 hours post-infection up to 36 hours post-infection (Figure 4.6B).

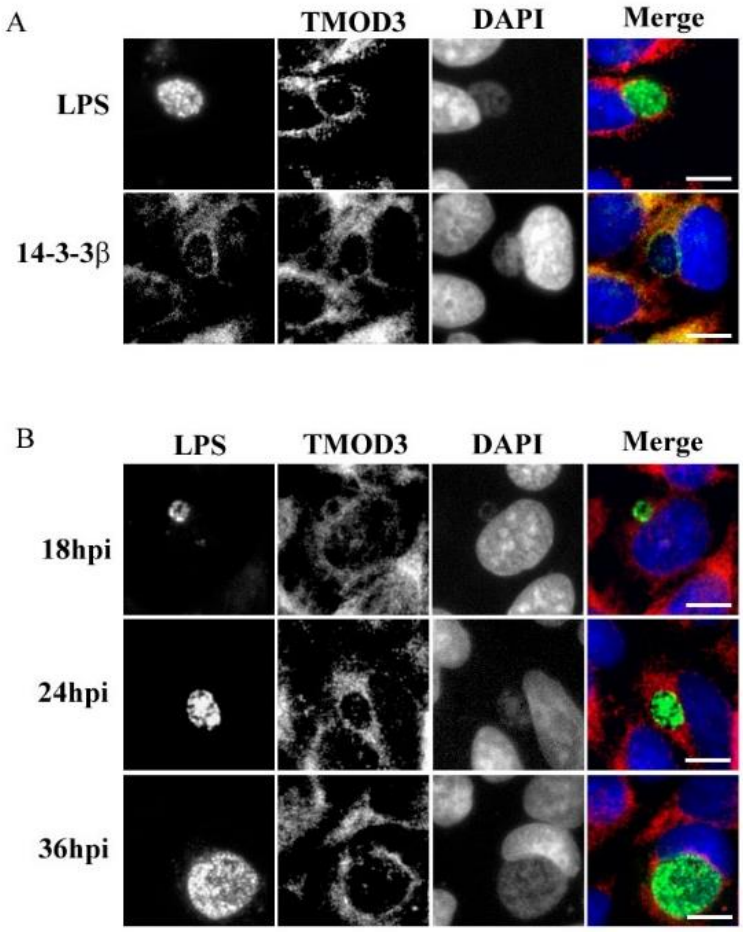

Figure 4.6. TMOD3 localization at the *C. trachomatis* L2 inclusion. (A) TMOD3 was recruited to inclusion and was also enriched around the inclusion. TMOD3 co-localized with 14-3-3β on the inclusion membrane. *C. trachomatis* was stained with anti-*Chlamydia* LPS (green), TMOD3 was stained with anti-TMOD3 (red) and nuclei was

stained with DAPI (blue) (B) Time course analysis of TMOD3 recruitment at 18, 24, and 36 hours post-infection (hpi). Scale bar, 10 µm.

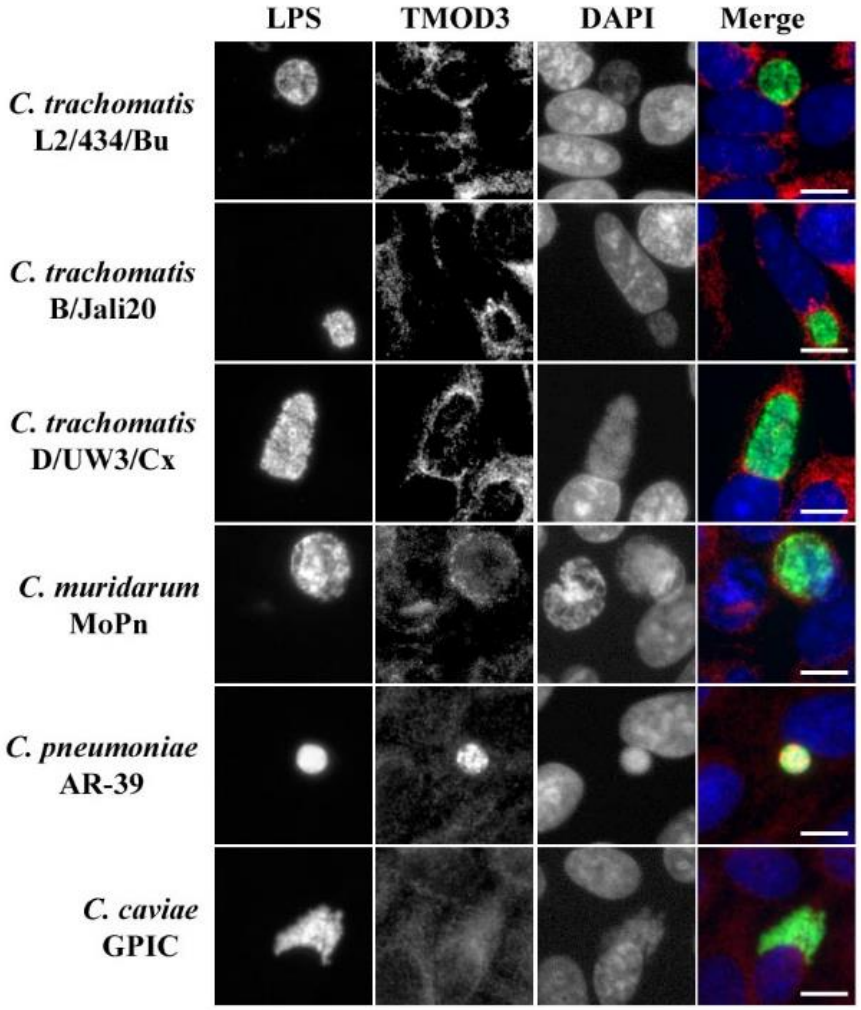

Figure 4.7. TMOD3 recruitment in *C. trachomatis* serovars and other *Chlamydia* species. *Chlamydia* are stained with anti-*Chlamydia* LPS (green), TMOD3 is stained with anti-TMOD3 (red), and nuclei is stained with DAPI (blue). Scale bar, 10 µm.

4.3.6. TMOD3 recruitment is conserved among *C. trachomatis* serovars and *C. muridarum*

CT226 is conserved among all *C. trachomatis* serovars and *C. muridarum* contains a homolog. Hence, TMOD3 recruitment in *C. trachomatis* serovars and other *Chlamydia* species was investigated next. HeLa cells were infected with *C. trachomatis* serovars B/Jali20, D/UW3/Cx, *C. muridarum* MoPn, *C. pneumoniae* AR-39 and *C. caviae* GPIC. TMOD3 recruitment was analyzed by immunofluorescence microscopy. All the serovars of *C. trachomatis* tested, as well as *C. muridarum,* showed recruitment of TMOD3 at the inclusion (Figure 4.7) while *C. caviae* did not recruit TMOD3. *C. pneumoniae* showed intra-inclusion staining with TMOD3 making it difficult to discern if TMOD3 recruitment was actually occurring.

4.3.7. TMOD3 siRNA knockdown results in a slight decrease in IFU production

The functional importance of TMOD3 recruitment by *C. trachomatis* L2 was investigated by siRNA knockdown of TMOD3. HeLa cells treated with TMOD3 specific siRNA or non-targeting scramble siRNA were infected with *C. trachomatis* L2 at 48 hours post transfection. After 48 hours post-infection, infected cells were processed for infectious progeny enumeration. Knockdown of TMOD3 resulted in only a slight decrease in infectious progeny production (Src siRNA: 7146000 ± 255700 IFU/mL; TMOD3 siRNA: 4979000 ± 262000 IFU/mL) (Figure 4.8A). TMOD3 knockdown was verified by western blotting (Figure 4.8B) showing a partial reduction in TMOD3 protein levels.

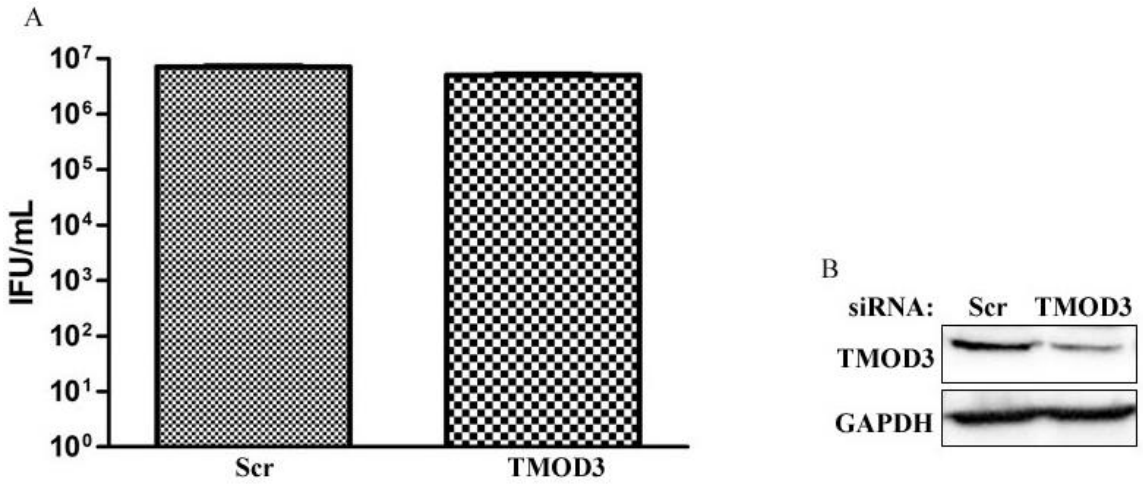

Figure 4.8. Effect of TMOD3 siRNA knockdown on *C. trachomatis* IFU production. (A) HeLa cells were transfected with scramble (Scr) or TMOD3 specific siRNA for 48 hours followed by infection with *C. trachomatis* L2. Infectious progeny enumeration was performed 48 hours post-infection. For each condition, 15 fields of view were counted in duplicate. Error bars indicate standard error of mean (B) TMOD3 knockdown efficiency was analyzed by western blotting with GAPDH as the control.

4.3.8. Generation of *C. trachomatis* L2 ΔCT226

A *C. trachomatis* L2 mutant strain lacking *CT226* was generated using FRAEM. *CT226* deletion plasmid, pSuMc-LF-*aadA*-*gfp*-RF was generated and transformed into *C. trachomatis* L2 EBs as described in the methods (Figure 4.9A). Transformants undergoing allelic exchange were selected using spectinomycin and monitored by live fluorescence microscopy for only green fluorescence. Deletion of *CT226* was verified by PCR amplification of *CT226* and *CT227-CT225* amplicon (Figure 4.9B) using primers listed in Table 1. Amplification of *CT226* using specific primers showed a ~500bp amplicon for the L2 wild type (WT) but no amplicon for the mutant strain, as expected

(Figure 4.9C). Similarly, amplification of the *CT227-CT225* region resulted in an expected ~1.5kbp amplicon for L2 WT while the mutant strain showed a shift up in amplicon size (~3kbp amplicon) owing to *CT226* replacement with *aadA-gfp* cassette (Figure 4.9D). Deletion of *CT226* was further verified by whole genome sequencing (data not shown here).

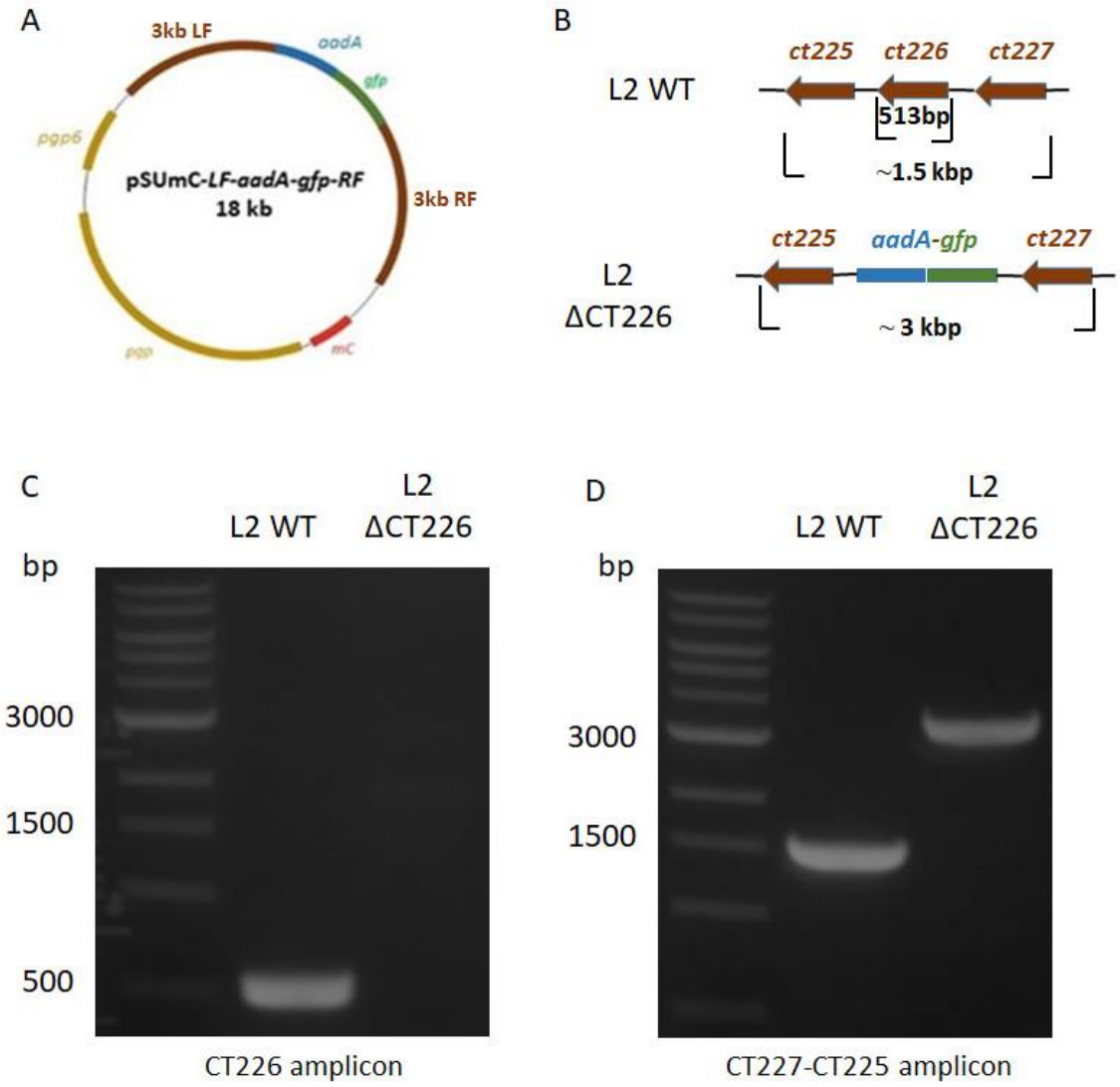

Figure 4.9. Generation and PCR verification of L2 ΔCT226. (A) Deletion plasmid, pSuMc-LF- *aadA-gfp*-RF containing 3kb regions on the left flank (LF) and right flank

(RF) of *CT226* (Figure adapted from Wolf, et al. 2019). (B) Expected size of *CT227-CT225* region in L2 WT and L2 ΔCT226 mutant. (C) PCR amplification of *CT226* from L2 WT and L2 ΔCT226 mutant genomic DNA showing no amplification in L2 ΔCT226 mutant. (D) PCR amplification of *CT227-CT225* from L2 WT and L2 ΔCT226 genomic DNA showing an expected shift up in amplicon size (~3kbp) in L2 ΔCT226.

4.3.9. Recruitment of FLII, LRRFIP1, LRRFIP2, and TMOD3 in L2 wild type and ΔCT226 strains

Next, the recruitment of FLII, LRRFIP1, LRRFIP2, and TMOD3 was compared between *C. trachomatis* L2 WT and the ΔCT226 mutant. HeLa cells infected with L2 WT and ΔCT226 mutant were analyzed by immunofluorescence microscopy. All four putative CT226 binding partners FLII, LRRFIP1, LRRFIP2, and TMOD3 were found to be recruited inclusion of L2 WT strain, as expected. We observed a complete loss of recruitment of FLII at the L2 ΔCT226 inclusion while LRRFIP1 showed a potential decrease in recruitment, although this is difficult to discern as the recruitment pattern also appears altered and more diffuse compared to recruitment in the WT. This was in stark contrast to what was observed with LRRFIP2; the recruitment of which was similar to that of L2 WT. Interestingly, TMOD3 recruitment showed a similar recruitment pattern to LRRFIP1. The recruitment in the CT226 mutant appeared to be altered and more diffuse than in the WT strain.

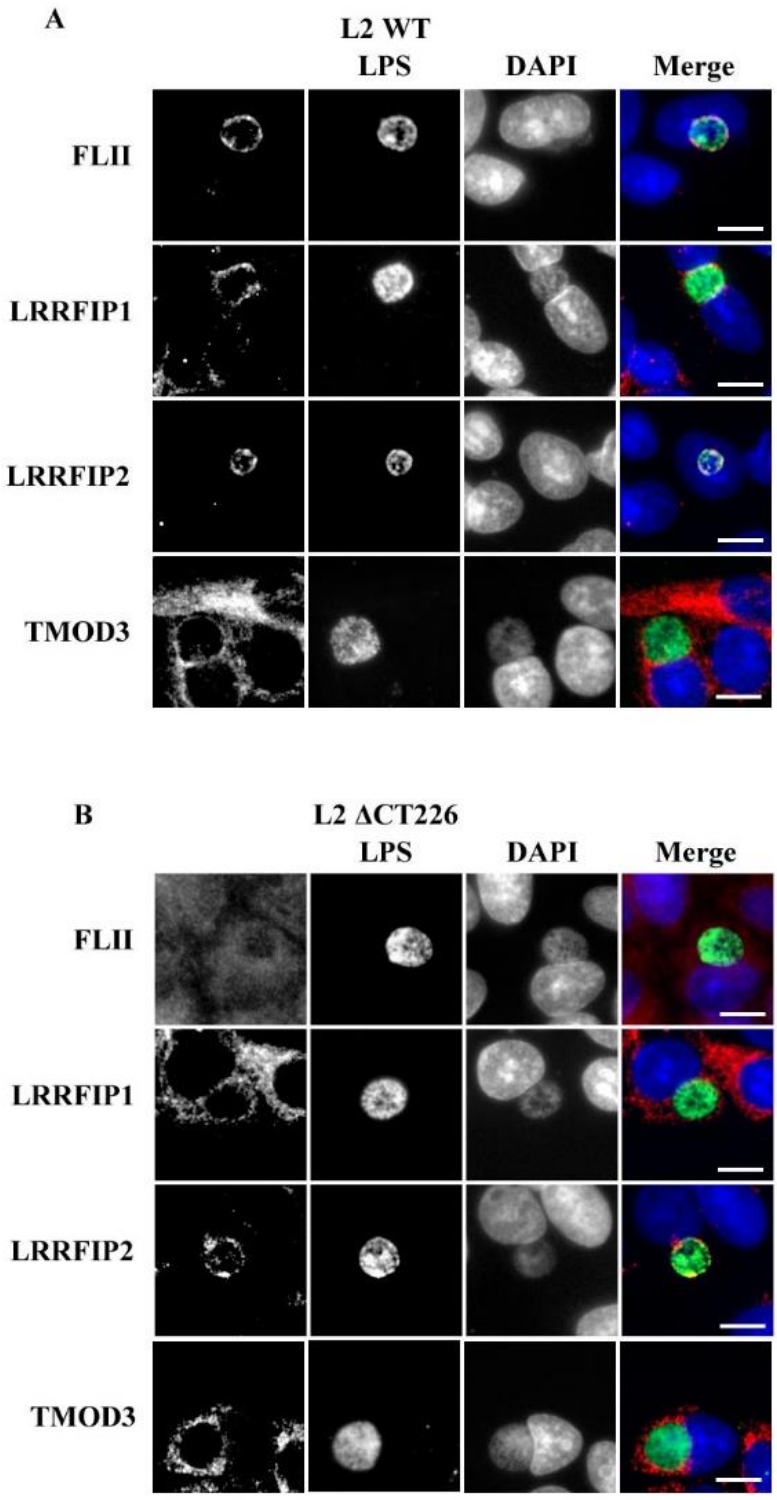

Figure 4.10. Recruitment of FLII, LRRFIP1, LRRFIP2, and TMOD3 in *C. trachomatis* L2 WT (A) and L2 ΔCT226 (B). *C. trachomatis* was stained with anti-

Chlamydia LPS (green) while FLII, LRRFIP1, LRRFIP2, and TMOD3 were stained with anti-FLII, anti-LRRFIP1, anti-LRRFIP2, and anti-TMOD3 (red). Nuclei was stained with DAPI (blue). Scale bar, 10 μm.

4.3.10. FLII recruitment is conserved among *C. trachomatis* serovars and *C. muridarum*

All *C. trachomatis* serovars encode CT226 and *C. muridarum* also contains a homolog of CT226. However, other species of *Chlamydia* lack a homolog of CT226. Hence, FLII recruitment among *C. trachomatis* serovars, *C. muridarum*, *C. caviae*, and *C. pneumoniae* was analyzed by immunofluorescence. As expected, FLII was found to be recruited to inclusion of *C. trachomatis* serovars and *C. muridarum*. No recruitment was observed at the *C. pneumoniae* or *C. caviae* inclusion which is consistent with the lack of CT226 in these species.

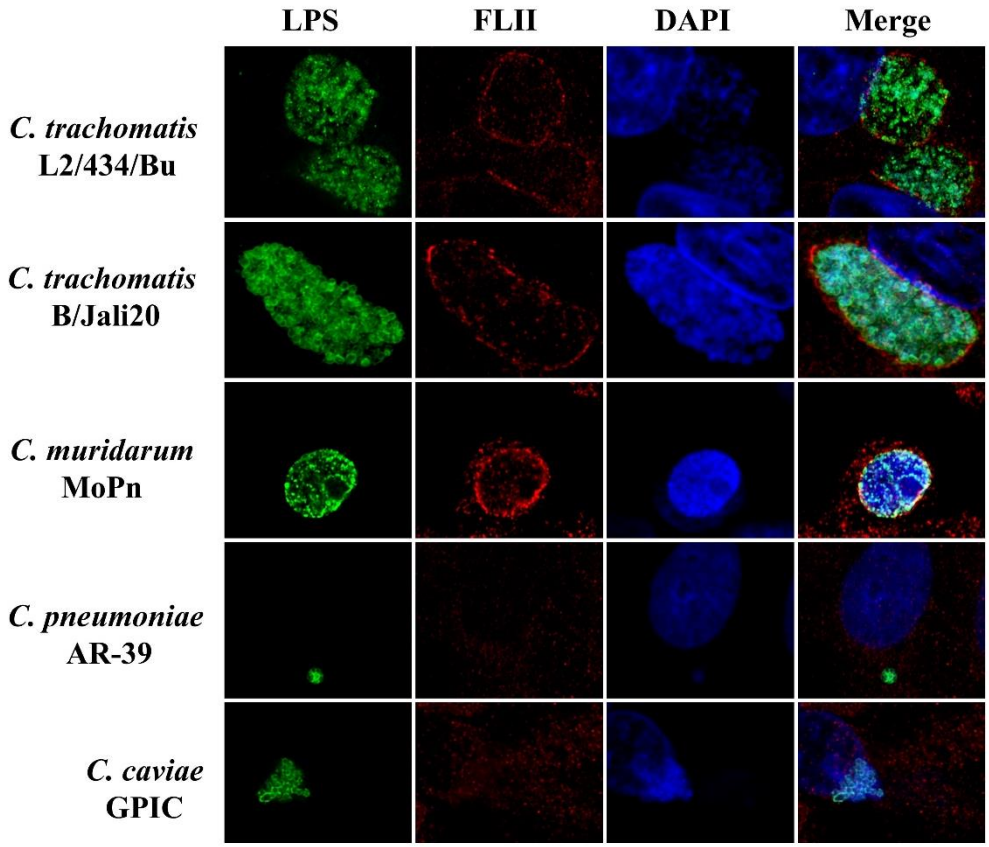

Figure 4.11. FLII recruitment in *C. trachomatis* serovars and other *Chlamydia* species. *Chlamydia* were stained with anti-*Chlamydi* LPS (green), FLII was stained with anti-FLII (red) and nuclei was stained with DAPI (blue).

4.4. Discussion

C. trachomatis replicates in a parasitophorous vacuole called the inclusion, in the host cell (Abdelrahman and Belland 2005). The inclusion membrane represents a key site for host-pathogen interactions and is rapidly modified by localization of T3SS effectors, Incs along with recruitment of a range of host proteins (Elwell, et al. 2016). Incs mediate interactions with host proteins as well as play a role in maintaining inclusion integrity (Bugalhao and Mota 2019). Although several Inc-host interactions have been studied,

many still remain uncharacterized. Four putative host binding proteins FLII, LRRFIP1, LRRFIP2, and TMOD3 for CT226 were identified in a large scale Inc-host interactome study (Mirrashidi, et al. 2015). Subsequent proteomic studies have shown localization of FLII, LRRFIP1, and TMOD3 at *C. trachomatis* inclusion as well as interaction of CT226 with LRRFIP1 (Aeberhard, et al. 2015; Dickinson, et al. 2019; Olson, et al. 2019). In this study, we utilized a L2 ΔCT226 mutant strain to further characterize the interactions of CT226.

CT226, a non-core Inc, has been predicted to have a bi-lobed transmembrane domain in the N-terminal and a coiled-coil region with a leucine zipper in the C-terminal of the protein (Dehoux, et al. 2011; Lutter, et al. 2012). This indicates that the putative effector domain of CT226 is located in the C-terminus and likely mediates the interactions with host proteins. Further, CT226 in different *C. trachomatis* serovars has been predicted to have truncations in N-terminus (Weber, et al. 2015). TC0497, a homolog of CT226 present in *C. muridarum* also contains the conserved coiled-coil region and the leucine zipper further indicating that the C-terminus likely plays role in interactions with host.

To verify whether CT226 interacts with FLII, LRRFIP1, LRRFIP2, and TMOD3, CT226 was expressed as an eGFP fusion (CT226-eGFP) in HeLa cells followed by co-immunoprecipitation. CT226 was tagged owing to the lack of antibody availability. Our co-immunoprecipitation data indicated that CT226 interacts with FLII, LRRFIP1 and TMOD3 while LRRFIP2 was not detected in the CT226-eGFP co-immunoprecipitation. A recent proximity labelling based study also found LRRFIP1 as interacting partner of CT226 (Olson, et al. 2019). Although FLII has been shown to be recruited to the

inclusion, no other study has reported its interaction with CT226 since it initial identification as putative binding partner of CT226 (Aeberhard, et al. 2015; Mirrashidi, et al. 2015; Olson, et al. 2019). Our data indicates that CT226 interacts with FLII in addition to LRRFIP1 and TMOD3 when ectopically expressed in HeLa cells. However, it remains unclear which of these proteins primarily bind to CT226, given that FLII interacts with LRRFIP1 and LRRFIP2 as well (Dai, et al. 2009).

Interaction of host proteins with an Inc implies their localization at the inclusion membrane. Immunofluorescence was used to test whether FLII, LRRFIP1, LRRFIP2, and TMOD3 localize at the inclusion. Interestingly, all the four host proteins were found to localize at the inclusion membrane with TMOD3 also showing an enrichment around the inclusion (discussed separately below). To further investigate the binding partner/s of CT226, we generated a *C. trachomatis* L2 ΔCT226 mutant. We then compared the recruitment of FLII, LRRFIP1, and LRRFIP2 in L2 WT and L2 ΔCT226. Loss of recruitment was observed for FLII further indicating FLII recruitment at inclusion requires CT226. Further, FLII recruitment was found to be conserved among *C. trachomatis* serovars and *C. muridarum*. Both of these *Chlamydia* species encode for CT226 or a homolog. LRRFIP2 recruitment was seen in both L2 WT and L2 ΔCT226 indicating its recruitment is independent of CT226. LRRFIP1, however, had an altered recruitment in L2 ΔCT226 exhibiting a more diffuse recruitment compared to L2 WT. This is similar to more diffuse recruitment of TMOD3 in L2 ΔCT226 as well. Our data indicates FLII may be primary host protein interacting with CT226. FLII contains leucine rich repeats in it N-terminal which mediates it interaction with the coiled-coil regions of LRRFIP1 and LRRFIP2 (Fong and de Couet 1999; Dai, et al. 2009; Kopecki, et al. 2016).

Incidentally, CT226 also has a predicted coiled-coil in its C-terminal region (Dehoux, et al. 2011). The CT226 dependent FLII recruitment to the inclusion needs to be further verified by complementing CT226 into the mutant strain.

Since its initial identification as a CT226 putative binding protein, two other inclusion proteomics studies have reported TMOD3 interaction with the *C. trachomatis* inclusion (Aeberhard, et al. 2015; Mirrashidi, et al. 2015; Dickinson, et al. 2019). TMOD3, like FLII, also contains leucine rich repeats that could mediate interaction of TMOD3 with CT226. Thus, we hypothesized that CT226 also interacts with TMOD3. Our co-immunoprecipitation data showed CT226 interacts with TMOD3. Yeast 2 hybrid analysis of CT226 and TMOD3 interaction indicated a weak interaction. However, this could in part be due to the slow growth of yeast strain expressing TMOD3. There are no homologs of TMOD3 in yeast (Yamashiro, et al. 2012) and expression of TMOD3 in this system seemed to slow yeast growth. We conclude yeast 2 hybrid may not be the optimal system to study this interaction. TMOD3 was found to enrich around the inclusion as well recruited to inclusion. Co-localization with 14-3-3β further confirmed TMOD3 recruitment to inclusion. TMOD3 recruitment was seen at least 18 hours post-infection up to 36 hours post-infection. Further, the enrichment and recruitment of CT226 was conserved among *C. trachomatis* serovar and *C. muridarum*. However, the loss of CT226 in L2 ΔCT226 did not cause loss of recruitment of TMOD3 suggesting that other Incs could be involved. As an alternative hypothesis, TMOD3 could be recruited independent of an Inc and the interaction may be occurring due to the opportunity presented by close proximity. In this scenario, the actin cage that surrounds the chlamydial inclusion may be bringing TMOD3 with it. TMOD3 is an actin capping protein that plays multifunctional

roles in regulating dynamic actin-based cellular processes (Parreno and Fowler 2018). This is highly relevant as *Chlamydia* is known to manipulate the host actin cytoskeletal system and have an actin cage around the periphery of the inclusion (Caven and Carabeo 2019). Given the enrichment and recruitment of TMOD3 at the inclusion, we originally hypothesized that TMOD3 is important for intracellular development of *C. trachomatis*. To test this hypothesis, we enumerated IFU production of *C. trachomatis* infected cells that were siRNA depleted for TMOD3. TMOD3 knockdown did not seem to affect *Chlamydia* growth resulting in only a modest decrease in IFUs. This could be due many factors. TMOD3 is a ubiquitously expressed protein that is abundant in HeLa cells (Geiger, et al. 2012; Schaab, et al. 2012) and even after siRNA knockdown there could still be sufficient TMOD3 for *Chlamydia* and the host cell to use. There are other TMODs in the cell that perform similar functions (Yamashiro, et al. 2012). A TMOD3 knockout cell line could be used to further investigate the role of TMOD3 recruitment. Also, *C. trachomatis* is known for redundancies in ways it can manipulate host cell processes.

CHAPTER V

CONCLUSIONS AND FUTURE DIRECTIONS

Chlamydia trachomatis resides in a parasitophorous vacuole, called the inclusion, inside the host cell (Abdelrahman and Belland 2005). The inclusion membrane represents a key site for host-pathogen interaction where bacterial effectors localize and recruit/interact with host proteins (Elwell, et al. 2016). While our understanding of the host-pathogen interaction at the inclusion membrane has seen rapid progress in recent years, much remains to be characterized. The goal of this study included two main areas of investigation in regard to Host-*Chlamydia* interactions. The first goal was to study role host kinases in intracellular development of *C. trachomatis*. The second goal was to investigate host interactions of *C. trachomatis* inclusion membrane protein, CT226.

5.1. Studies on host kinases PKC and PKA recruitment by *C. trachomatis*

C. trachomatis being an intracellular pathogen, relies on host cell for its replication (Bastidas, et al. 2013). Many of the host cell processes subverted by *Chlamydia* during infection are regulated by host kinases. Recent proteomics studies have indicated that host kinases may interact with bacterial effectors at the inclusion membrane (Aeberhard, et al. 2015; Mirrashidi, et al. 2015; Zadora, et al. 2019).

Chapters 2 and 3 of this study investigated *C. trachomatis* recruitment and subversion of two classes of host kinases, protein kinase C (PKC) and protein kinase A (PKA). In Chapter 2, we show that *C. trachomatis* recruits multiple isoforms of phosphorylated PKC (active) and co-localizes with src-rich microdomains on the inclusion membrane. Further, phosphorylated PKC substrates are localized all around the periphery of the inclusion membrane. Localization of phosphorylated PKC and PKC substrates was specific to *C. trachomatis* serovars and was not seen in other *Chlamydia* species tested. PKC has been implicated in apoptosis resistance of *C. trachomatis* infected cells and may have a possible role in acquisition of lipids from the host (Shivshanker, et al. 2008; Tse, et al. 2005). In our study, pharmacological inhibition of PKC resulted in a modest decrease in infectious progeny production of *C. trachomatis*. Given the diversity of PKC isoforms recruited to the inclusion, it may be difficult to target them for inhibition. Future studies should be directed towards identifying phosphorylated PKC substrates at inclusion and their role in Chlamydial development. The PKC phosphorylated proteins could represent host proteins as well as Chlamydial proteins, mainly Incs. In line with this, a recent proximity labeling based proteomics study found myristoylated alanine-rich C kinase substrate (MARCKS), a well-known substrate of PKC, associating with the inclusion (Olson, et al. 2019). Preliminary data from out lab have also shown recruitment of MARCKS as well as another PKC substrate, C-kinase potentiated protein phosphatase-1 inhibitor (CPI-17) at the inclusion microdomains. CPI-17, thus represent another target for future studies. On the other hand, targeting host proteins upstream of PKC may be a doable approach since targeting the diverse number of PKCs is problematic. Many PKC isoforms are activated via phospholipase C (PLC) mediated generation of diacylglycerol

(DAG) (Wu-Zhang and Newton 2013) and as discussed in the PKC Chapter, DAG has already been shown to be in the vicinity of the chlamydial inclusion.

Further, a recent phosphoproteomics study showed PKC was one of the host kinases that may phosphorylate Incs while also identifying phosphorylation sites on these chlamydial proteins that could be targeted by mutation analysis (Zadora, et al. 2019). It would be interesting to study what role PKC phosphorylation of Incs play in their function. These investigations will require generation of mutations at phosphorylated amino acid residues. Although, Chlamydial genetics have seen recent advancements and expansion of genetic tools available, major limitations, mainly low *C. trachomatis* transformation efficiency and laborious time-consuming nature of the whole process, remain in Chlamydial mutagenesis making such investigations challenging.

In Chapter 3, we investigated the role of another host kinase, PKA, in *C. trachomatis* development. Like PKC, PKA is also implicated in the phosphorylation of Chlamydial Incs. (Zadora, et al. 2019) We showed that the catalytic and regulatory subunits of PKC (PKA-Cα and PKA-RIIα) localized around the inclusion or in the peri-Golgi area. We further showed that these PKA subunits co-localized with Golgi marker, golgin-97, around the inclusion. Phosphorylated PKA substrates recruited to the entire periphery of the inclusion which increased during mid to late stages of infection suggesting importance in late stage events. PKA substrate phosphorylation also increased during mid to late stages *C. trachomatis* infection. Pharmacological inhibition of PKA using two different inhibitors (H89 and Rp-cAMPS) suggested a possible role for PKA in extrusion production in *C. trachomatis* infected cells. PKA inhibition using H89 almost completely halted extrusion production which appeared to be independent of myosin

phosphatase pathway that *C. trachomatis* uses for extrusion production suggesting that the regulation of the extrusion process is more complicated than previously thought.

C. trachomatis is known to cause Golgi fragmentation into mini stacks which then surrounds the inclusion (Heuer, et al. 2009). Although initially suggested to be important for Chlamydial growth, the role of Golgi fragmentation needs further characterization (Elwell, et al. 2016). Various signaling proteins localize at Golgi in the host cell including PKA (Mayinger 2011). It is possible that the Golgi may serve as a platform for usurping of PKA signaling by *C. trachomatis*. In line with this, PKA has been implicated in the phosphorylation of Incs (Zadora, et al. 2019). We also observed the recruitment of phosphorylated substrates to the entire periphery of the inclusion. How *C. trachomatis* may activate the Golgi localized PKA remains unknown. PKA is also known to regulate Golgi biogenesis and stability (Bejarano, et al. 2006). Hence, studying the role of PKA in *C. trachomatis* mediated Golgi fragmentation would be an interesting avenue of future investigation.

Pharmacological inhibition of PKA using H89 and Rp-cAMPS indicated a possible role of PKA in extrusion production in *C. trachomatis*. H89, a broad range inhibitor almost completely stopped extrusion production while Rp-cAMPS, a more specific inhibitor, caused only a modest decrease in extrusion production. Besides PKA, H89 can target various other host kinases such as mitogen- and stress-activated protein kinase 1 (MSK1), ribosomal protein S6 kinase 1 (S6K1), and Rho-associated coiled-coil containing protein kinase 2 (ROCK2) among other host kinases (Lochner and Moolman 2006). This indicates the possible involvement of these other kinases targeted by H89 in extrusion production. Further, H89 mediated extrusion inhibition was not dependent on

myosin phosphatase pathway indicating involvement other host proteins regulated by PKA or other H89 targeted kinases. Future investigations should be focused on characterizing potential roles of H89 targeted kinases in extrusion production.

5.2. Host interactions of CT226

This study was also aimed at investigating the host interactions of the Inc, CT226. CT226 is a non-core Inc that conserved in *C. trachomatis* serovars and the closely related *C. muridarum* (Lutter, et al. 2012). The prediction of leucine zipper (LZ) within coiled-coil region in the C-terminus of CT226 warrants future investigations regarding its functionality and role in interactions of CT226 with the host proteins. Given, the conservation of leucine residues of the LZ in TC0497, a homolog of CT226 in *C. muridarum*, it would be interesting to investigate if the functions and interactions are also conserved.

A previous study identified FLII, LRRFIP1, LRRFIP2, and TMOD3 as putative binding partners of CT226 (Mirrashidi, et al. 2015). Subsequent studies found FLII, LRRFIP1, and TMOD3 to be associated with *C. trachomatis* inclusion (Aeberhard, et al. 2015; Dickinson, et al. 2019; Olson, et al. 2019). CT226 was found to interact with LRRFIP1 in another study as well (Olson, et al. 2019). In this study, we observed FLII, LRRFIP1, and TMOD3 as interacting with CT226 (eGFP fusion) in co-immunoprecipitation assay. Leveraging on the recent developments in Chlamydial mutagenesis, we generated a mutant strain *C. trachomatis* L2 ΔCT226. Deletion of CT226 in *C. trachomatis* resulted in complete loss of FLII recruitment while an altered, potentially decreased, recruitment was seen with LRRFIP1 and TMOD3. LRRFIP2

recruitment was found to be independent of CT226. These data indicate that FLII may be the primary host protein interacting with CT226 while LRRFIP1 and TMOD3 probably interact indirectly. These interactions could be further verified in heterologous systems such two hybrid systems. Yeast 2 hybrid analysis of CT226 and TMOD3 interaction in our study indicated that yeast may not be the optimal system to study this interaction as TMOD3 expression caused a growth defect in yeast. Alternatively, bacterial two hybrid system may be used to further characterize these interactions. Future investigations should also be targeted towards verifying these interactions further by complementing the L2 ΔCT226. Given, the recruitment of FLII, LRRFIP1, and LRRFIP2, and TMOD3 to the inclusion, the functional importance of these host proteins in *C. trachomatis* infection will be interesting to study. TMOD3 is an actin capping (pointed end) protein that regulates several host cell processes requiring dynamic actin cytoskeletal structures (Parreno and Fowler 2018). *C. trachomatis* is known to manipulate host actin and an actin cage surround Chlamydial inclusion (Bastidas, et al. 2013; Caven and Carabeo 2019). TMOD3 knockdown using siRNA did not show a significant effect on IFU production by *C. trachomatis*. siRNA knockdown may not achieve substantial reduction of TMOD3, given its abundant expression in HeLa cells. A TMOD3 knockout cell line could be used to better characterize the role of TMOD3 in *C. trachomatis* development.

FLII interacts with LRRFIP1 and LRRFIP2 to regulate inflammation via toll-like receptor pathway (Dai, et al. 2009). FLII is also known to regulate pro-inflammatory caspases (Li, et al. 2008). LRRFIP1 has been implicated in mediating a rapid type I interferon response (Bagashev, et al. 2010). On the other hand, LRRFIP2 is known to negatively regulate NOD-, LRR- and pyrin domain-containing receptor 3 (NLRP3)

inflammasome activation (Jin, et al. 2013). *C. trachomatis* is known to modulate host inflammatory response (Elwell, et al. 2016). Inflammation is also known to contribute to the pathology of *C. trachomatis* infection (Stephens 2003). Taken together, it is likely that the recruitment of these host proteins may play a role in modulation of inflammation by *C. trachomatis*. Future studies should be focused on characterizing the functional implication of FLII, LRRFIP1, and LRRFIP2 recruitment to the *C. trachomatis* inclusion. LRRFIP1 knockdown in HeLa cells results in a slight but not significant increase in IFU production in *C. trachomatis* (Dickinson, et al. 2019; Olson, et al. 2019). A more relevant model for studying role of these host proteins include a macrophage cell line or an *in vivo* murine infection model.

REFERENCES

Abdelrahman Y, Ouellette SP, Belland RJ, Cox JV. 2016. Polarized Cell Division of *Chlamydia trachomatis*. PLoS Pathog 12:e1005822.

Abdelrahman YM, Belland RJ. 2005. The chlamydial developmental cycle. FEMS Microbiol Rev 29:949-959.

Aeberhard L, Banhart S, Fischer M, Jehmlich N, Rose L, Koch S, Laue M, Renard BY, Schmidt F, Heuer D. 2015. The Proteome of the Isolated Chlamydia trachomatis Containing Vacuole Reveals a Complex Trafficking Platform Enriched for Retromer Components. PLoS Pathog 11:e1004883.

Agaisse H, Derre I. 2013. A C. trachomatis cloning vector and the generation of C. trachomatis strains expressing fluorescent proteins under the control of a C. trachomatis promoter. PLoS One 8:e57090.

Agaisse H, Derre I. 2014a. The expression of the effector protein IncD in *C. trachomatis* mediates the recruitment of the lipid transfer protein CERT and the ER-resident protein VAPB to the inclusion membrane. Infect Immun.

Agaisse H, Derre I. 2014b. Expression of the effector protein IncD in Chlamydia trachomatis mediates recruitment of the lipid transfer protein CERT and the endoplasmic reticulum-resident protein VAPB to the inclusion membrane. Infect Immun 82:2037-2047.

Al-Zeer MA, Al-Younes HM, Kerr M, Abu-Lubad M, Gonzalez E, Brinkmann V, Meyer TF. 2014. Chlamydia trachomatis remodels stable microtubules to coordinate Golgi stack recruitment to the chlamydial inclusion surface. Mol Microbiol 94:1285-1297.

Almeida F, Borges V, Ferreira R, Borrego MJ, Gomes JP, Mota LJ. 2012. Polymorphisms in inc proteins and differential expression of inc genes among Chlamydia trachomatis strains correlate with invasiveness and tropism of lymphogranuloma venereum isolates. J Bacteriol 194:6574-6585.

Almeida F, Luis MP, Pereira IS, Pais SV, Mota LJ. 2018. The Human Centrosomal Protein CCDC146 Binds Chlamydia trachomatis Inclusion Membrane Protein CT288 and Is Recruited to the Periphery of the Chlamydia-Containing Vacuole. Front Cell Infect Microbiol 8:254.

Alzhanov DT, Weeks SK, Burnett JR, Rockey DD. 2009. Cytokinesis is blocked in mammalian cells transfected with Chlamydia trachomatis gene CT223. BMC Microbiol 9:2.

Bagashev A, Fitzgerald MC, Larosa DF, Rose PP, Cherry S, Johnson AC, Sullivan KE. 2010. Leucine-rich repeat (in Flightless I) interacting protein-1 regulates a rapid type I interferon response. J Interferon Cytokine Res 30:843-852.

Bannantine JP, Griffiths RS, Viratyosin W, Brown WJ, Rockey DD. 2000. A secondary structure motif predictive of protein localization to the chlamydial inclusion membrane. Cell Microbiol 2:35-47.

Bastidas RJ, Elwell CA, Engel JN, Valdivia RH. 2013. Chlamydial intracellular survival strategies. Cold Spring Harb Perspect Med 3:a010256.

Bastidas RJ, Valdivia RH. 2016. Emancipating Chlamydia: Advances in the Genetic Manipulation of a Recalcitrant Intracellular Pathogen. Microbiol Mol Biol Rev 80:411-427.

Bauler LD, Hackstadt T. 2014. Expression and targeting of secreted proteins from Chlamydia trachomatis. J Bacteriol 196:1325-1334.

Bejarano E, Cabrera M, Vega L, Hidalgo J, Velasco A. 2006. Golgi structural stability and biogenesis depend on associated PKA activity. J Cell Sci 119:3764-3775.

Belland R, Ojcius DM, Byrne GI. 2004. Chlamydia. Nat Rev Microbiol 2:530-531.

Belland RJ, Zhong G, Crane DD, Hogan D, Sturdevant D, Sharma J, Beatty WL, Caldwell HD. 2003. Genomic transcriptional profiling of the developmental cycle of Chlamydia trachomatis. Proc Natl Acad Sci U S A 100:8478-8483.

Betts-Hampikian HJ, Fields KA. 2010. The Chlamydial Type III Secretion Mechanism: Revealing Cracks in a Tough Nut. Front Microbiol 1:114.

Bornberg-Bauer E, Rivals E, Vingron M. 1998. Computational approaches to identify leucine zippers. Nucleic Acids Res 26:2740-2746.

Buchholz KR, Stephens RS. 2007. The extracellular signal-regulated kinase/mitogen-activated protein kinase pathway induces the inflammatory factor interleukin-8 following Chlamydia trachomatis infection. Infect Immun 75:5924-5929.

Bugalhao JN, Mota LJ. 2019. The multiple functions of the numerous Chlamydia trachomatis secreted proteins: the tip of the iceberg. Microb Cell 6:414-449.

Burton MJ, Mabey DC. 2009. The global burden of trachoma: a review. PLoS Negl Trop Dis 3:e460.

Caldwell HD, Kromhout J, Schachter J. 1981. Purification and partial characterization of the major outer membrane protein of Chlamydia trachomatis. Infect Immun 31:1161-1176.

Capmany A, Gambarte Tudela J, Alonso Bivou M, Damiani MT. 2019. Akt/AS160 Signaling Pathway Inhibition Impairs Infection by Decreasing Rab14-Controlled Sphingolipids Delivery to Chlamydial Inclusions. Front Microbiol 10:666.

Carabeo RA, Grieshaber SS, Fischer E, Hackstadt T. 2002. Chlamydia trachomatis induces remodeling of the actin cytoskeleton during attachment and entry into HeLa cells. Infect Immun 70:3793-3803.

Carpenter V, Chen YS, Dolat L, Valdivia RH. 2017. The Effector TepP Mediates Recruitment and Activation of Phosphoinositide 3-Kinase on Early Chlamydia trachomatis Vacuoles. mSphere 2.

Caven L, Carabeo RA. 2019. Pathogenic Puppetry: Manipulation of the Host Actin Cytoskeleton by Chlamydia trachomatis. Int J Mol Sci 21.

CDC. 2019. Sexually Transmitted Disease Surveillance 2018. Atlanta, GA: U.S. Department of Health and Human Services.

Chen F, Cheng W, Zhang S, Zhong G, Yu P. 2010. [Induction of IL-8 by Chlamydia trachomatis through MAPK pathway rather than NF-kappaB pathway]. Zhong Nan Da Xue Xue Bao Yi Xue Ban 35:307-313.

Chen YS, Bastidas RJ, Saka HA, Carpenter VK, Richards KL, Plano GV, Valdivia RH. 2014. The Chlamydia trachomatis type III secretion chaperone Slc1 engages multiple early effectors, including TepP, a tyrosine-phosphorylated protein required for the recruitment of CrkI-II to nascent inclusions and innate immune signaling. PLoS Pathog 10:e1003954.

Chin E, Kirker K, Zuck M, James G, Hybiske K. 2012. Actin recruitment to the Chlamydia inclusion is spatiotemporally regulated by a mechanism that requires host and bacterial factors. PLoS One 7:e46949.

Chumduri C, Gurumurthy RK, Zadora PK, Mi Y, Meyer TF. 2013. Chlamydia infection promotes host DNA damage and proliferation but impairs the DNA damage response. Cell Host Microbe 13:746-758.

Cingolani G, McCauley M, Lobley A, Bryer AJ, Wesolowski J, Greco DL, Lokareddy RK, Ronzone E, Perilla JR, Paumet F. 2019. Structural basis for the homotypic fusion of chlamydial inclusions by the SNARE-like protein IncA. Nat Commun 10:2747.

Clifton DR, Fields KA, Grieshaber SS, Dooley CA, Fischer ER, Mead DJ, Carabeo RA, Hackstadt T. 2004. A chlamydial type III translocated protein is tyrosine-phosphorylated at the site of entry and associated with recruitment of actin. Proc Natl Acad Sci U S A 101:10166-10171.

Coombes BK, Mahony JB. 2002. Identification of MEK- and phosphoinositide 3-kinase-dependent signalling as essential events during Chlamydia pneumoniae invasion of HEp2 cells. Cell Microbiol 4:447-460.

Cosse MM, Hayward RD, Subtil A. 2018. One Face of *Chlamydia trachomatis*: The Infectious Elementary Body. Curr Top Microbiol Immunol 412:35-58.

Da Ros CT, Schmitt Cda S. 2008. Global epidemiology of sexually transmitted diseases. Asian J Androl 10:110-114.

Dai P, Jeong SY, Yu Y, Leng T, Wu W, Xie L, Chen X. 2009. Modulation of TLR signaling by multiple MyD88-interacting partners including leucine-rich repeat Fli-I-interacting proteins. J Immunol 182:3450-3460.

Damiani MT, Gambarte Tudela J, Capmany A. 2014. Targeting eukaryotic Rab proteins: a smart strategy for chlamydial survival and replication. Cell Microbiol 16:1329-1338.

Dean D, Powers VC. 2001. Persistent *Chlamydia trachomatis* infections resist apoptotic stimuli. Infect Immun 69:2442-2447.

Dehoux P, Flores R, Dauga C, Zhong G, Subtil A. 2011. Multi-genome identification and characterization of chlamydiae-specific type III secretion substrates: the Inc proteins. BMC Genomics 12:109.

Delevoye C, Nilges M, Dehoux P, Paumet F, Perrinet S, Dautry-Varsat A, Subtil A. 2008. SNARE protein mimicry by an intracellular bacterium. PLoS Pathog 4:e1000022.

Derre I. 2015. Chlamydiae interaction with the endoplasmic reticulum: contact, function and consequences. Cell Microbiol 17:959-966.

Derre I, Swiss R, Agaisse H. 2011. The lipid transfer protein CERT interacts with the Chlamydia inclusion protein IncD and participates to ER-Chlamydia inclusion membrane contact sites. PLoS Pathog 7:e1002092.

Dickinson MS, Anderson LN, Webb-Robertson BM, Hansen JR, Smith RD, Wright AT, Hybiske K. 2019. Proximity-dependent proteomics of the Chlamydia trachomatis inclusion membrane reveals functional interactions with endoplasmic reticulum exit sites. PLoS Pathog 15:e1007698.

Ding H, Gong S, Tian Y, Yang Z, Brunham R, Zhong G. 2013. Transformation of sexually transmitted infection-causing serovars of chlamydia trachomatis using Blasticidin for selection. PLoS One 8:e80534.

Du K, Zheng Q, Zhou M, Zhu L, Ai B, Zhou L. 2011. Chlamydial antiapoptotic activity involves activation of the Raf/MEK/ERK survival pathway. Curr Microbiol 63:341-346.

Du K, Zhou M, Li Q, Liu XZ. 2018. Chlamydia trachomatis inhibits the production of pro-inflammatory cytokines in human PBMCs through induction of IL-10. J Med Microbiol 67:240-248.

Dumoux M, Menny A, Delacour D, Hayward RD. 2015. A Chlamydia effector recruits CEP170 to reprogram host microtubule organization. J Cell Sci 128:3420-3434.

Dumoux M, Nans A, Saibil HR, Hayward RD. 2015. Making connections: snapshots of chlamydial type III secretion systems in contact with host membranes. Curr Opin Microbiol 23:1-7.

Elwell C, Mirrashidi K, Engel J. 2016. Chlamydia cell biology and pathogenesis. Nat Rev Microbiol 14:385-400.

Elwell CA, Ceesay A, Kim JH, Kalman D, Engel JN. 2008. RNA interference screen identifies Abl kinase and PDGFR signaling in Chlamydia trachomatis entry. PLoS Pathog 4:e1000021.

Elwell CA, Czudnochowski N, von Dollen J, Johnson JR, Nakagawa R, Mirrashidi K, Krogan NJ, Engel JN, Rosenberg OS. 2017. Chlamydia interfere with an interaction between the mannose-6-phosphate receptor and sorting nexins to counteract host restriction. Elife 6.

Elwell CA, Engel JN. 2012. Lipid acquisition by intracellular Chlamydiae. Cell Microbiol 14:1010-1018.

Elwell CA, Jiang S, Kim JH, Lee A, Wittmann T, Hanada K, Melancon P, Engel JN. 2011. Chlamydia trachomatis co-opts GBF1 and CERT to acquire host sphingomyelin for distinct roles during intracellular development. PLoS Pathog 7:e1002198.

Fan T, Lu H, Hu H, Shi L, McClarty GA, Nance DM, Greenberg AH, Zhong G. 1998. Inhibition of apoptosis in *chlamydia*-infected cells: blockade of mitochondrial cytochrome c release and caspase activation. J Exp Med 187:487-496.

Faris R, Merling M, Andersen SE, Dooley CA, Hackstadt T, Weber MM. 2019. Chlamydia trachomatis CT229 Subverts Rab GTPase-Dependent CCV Trafficking Pathways to Promote Chlamydial Infection. Cell Rep 26:3380-3390 e3385.

Fields KA, Hackstadt T. 2002. The chlamydial inclusion: escape from the endocytic pathway. Annu Rev Cell Dev Biol 18:221-245.

Fields KA, Mead DJ, Dooley CA, Hackstadt T. 2003. Chlamydia trachomatis type III secretion: evidence for a functional apparatus during early-cycle development. Mol Microbiol 48:671-683.

Fischer A, Harrison KS, Ramirez Y, Auer D, Chowdhury SR, Prusty BK, Sauer F, Dimond Z, Kisker C, Hefty PS, et al. 2017. Chlamydia trachomatis-containing vacuole serves as deubiquitination platform to stabilize Mcl-1 and to interfere with host defense. Elife 6.

Fong KS, de Couet HG. 1999. Novel proteins interacting with the leucine-rich repeat domain of human flightless-I identified by the yeast two-hybrid system. Genomics 58:146-157.

Gauliard E, Ouellette SP, Rueden KJ, Ladant D. 2015. Characterization of interactions between inclusion membrane proteins from Chlamydia trachomatis. Front Cell Infect Microbiol 5:13.

Geiger T, Wehner A, Schaab C, Cox J, Mann M. 2012. Comparative proteomic analysis of eleven common cell lines reveals ubiquitous but varying expression of most proteins. Mol Cell Proteomics 11:M111 014050.

Geisler WM, Suchland RJ, Rockey DD, Stamm WE. 2001. Epidemiology and clinical manifestations of unique Chlamydia trachomatis isolates that occupy nonfusogenic inclusions. J Infect Dis 184:879-884.

Gerbase AC, Rowley JT, Mertens TE. 1998. Global epidemiology of sexually transmitted diseases. Lancet 351 Suppl 3:2-4.

Grieshaber SS, Grieshaber NA, Hackstadt T. 2003. Chlamydia trachomatis uses host cell dynein to traffic to the microtubule-organizing center in a p50 dynamitin-independent process. J Cell Sci 116:3793-3802.

Gross A, Bouaboula M, Casellas P, Liautard JP, Dornand J. 2003. Subversion and utilization of the host cell cyclic adenosine 5'-monophosphate/protein kinase A pathway by Brucella during macrophage infection. J Immunol 170:5607-5614.

Gurumurthy RK, Chumduri C, Karlas A, Kimmig S, Gonzalez E, Machuy N, Rudel T, Meyer TF. 2014. Dynamin-mediated lipid acquisition is essential for Chlamydia trachomatis development. Mol Microbiol 94:186-201.

Gurumurthy RK, Maurer AP, Machuy N, Hess S, Pleissner KP, Schuchhardt J, Rudel T, Meyer TF. 2010. A loss-of-function screen reveals Ras- and Raf-independent MEK-ERK signaling during Chlamydia trachomatis infection. Sci Signal 3:ra21.

Hackstadt T, Scidmore-Carlson MA, Shaw EI, Fischer ER. 1999. The Chlamydia trachomatis IncA protein is required for homotypic vesicle fusion. Cell Microbiol 1:119-130.

Heuer D, Rejman Lipinski A, Machuy N, Karlas A, Wehrens A, Siedler F, Brinkmann V, Meyer TF. 2009. Chlamydia causes fragmentation of the Golgi compartment to ensure reproduction. Nature 457:731-735.

Hooppaw AJ, Fisher DJ. 2015. A Coming of Age Story: Chlamydia in the Post-Genetic Era. Infect Immun 84:612-621.

Hussain SK, Broederdorf LJ, Sharma UM, Voth DE. 2010. Host Kinase Activity is Required for *Coxiella burnetii* Parasitophorous Vacuole Formation. Front Microbiol 1:137.

Hybiske K, Stephens RS. 2007. Mechanisms of host cell exit by the intracellular bacterium Chlamydia. Proc Natl Acad Sci U S A 104:11430-11435.

Igietseme JU, Omosun Y, Stuchlik O, Reed MS, Partin J, He Q, Joseph K, Ellerson D, Bollweg B, George Z, et al. 2015. Role of Epithelial-Mesenchyme Transition in Chlamydia Pathogenesis. PLoS One 10:e0145198.

Jewett TJ, Dooley CA, Mead DJ, Hackstadt T. 2008. Chlamydia trachomatis tarp is phosphorylated by src family tyrosine kinases. Biochem Biophys Res Commun 371:339-344.

Jin J, Yu Q, Han C, Hu X, Xu S, Wang Q, Wang J, Li N, Cao X. 2013. LRRFIP2 negatively regulates NLRP3 inflammasome activation in macrophages by promoting Flightless-I-mediated caspase-1 inhibition. Nat Commun 4:2075.

Johannes FJ, Prestle J, Eis S, Oberhagemann P, Pfizenmaier K. 1994. PKCu is a novel, atypical member of the protein kinase C family. J Biol Chem 269:6140-6148.

Johnson CM, Fisher DJ. 2013. Site-specific, insertional inactivation of incA in Chlamydia trachomatis using a group II intron. PLoS One 8:e83989.

Kalamidas SA, Kuehnel MP, Peyron P, Rybin V, Rauch S, Kotoulas OB, Houslay M, Hemmings BA, Gutierrez MG, Anes E, et al. 2006. cAMP synthesis and degradation by phagosomes regulate actin assembly and fusion events: consequences for mycobacteria. J Cell Sci 119:3686-3694.

Kall L, Krogh A, Sonnhammer EL. 2004. A combined transmembrane topology and signal peptide prediction method. J Mol Biol 338:1027-1036.

Kari L, Goheen MM, Randall LB, Taylor LD, Carlson JH, Whitmire WM, Virok D, Rajaram K, Endresz V, McClarty G, et al. 2011. Generation of targeted Chlamydia trachomatis null mutants. Proc Natl Acad Sci U S A 108:7189-7193.

Kaul R, Wenman WM. 1986. Cyclic AMP inhibits developmental regulation of Chlamydia trachomatis. J Bacteriol 168:722-727.

Keb G, Hayman R, Fields KA. 2018. Floxed-Cassette Allelic Exchange Mutagenesis Enables Markerless Gene Deletion in Chlamydia trachomatis and Can Reverse Cassette-Induced Polar Effects. J Bacteriol 200.

Keranen LM, Dutil EM, Newton AC. 1995. Protein kinase C is regulated in vivo by three functionally distinct phosphorylations. Curr Biol 5:1394-1403.

Kim JH, Jiang S, Elwell CA, Engel JN. 2011. Chlamydia trachomatis co-opts the FGF2 signaling pathway to enhance infection. PLoS Pathog 7:e1002285.

Kokes M, Dunn JD, Granek JA, Nguyen BD, Barker JR, Valdivia RH, Bastidas RJ. 2015. Integrating chemical mutagenesis and whole-genome sequencing as a platform for forward and reverse genetic analysis of Chlamydia. Cell Host Microbe 17:716-725.

Kopecki Z, Ludwig RJ, Cowin AJ. 2016. Cytoskeletal Regulation of Inflammation and Its Impact on Skin Blistering Disease Epidermolysis Bullosa Acquisita. Int J Mol Sci 17.

Koskela P, Anttila T, Bjorge T, Brunsvig A, Dillner J, Hakama M, Hakulinen T, Jellum E, Lehtinen M, Lenner P, et al. 2000. Chlamydia trachomatis infection as a risk factor for invasive cervical cancer. Int J Cancer 85:35-39.

Krogh A, Larsson B, von Heijne G, Sonnhammer EL. 2001. Predicting transmembrane protein topology with a hidden Markov model: application to complete genomes. J Mol Biol 305:567-580.

Kumar Y, Valdivia RH. 2008. Actin and intermediate filaments stabilize the Chlamydia trachomatis vacuole by forming dynamic structural scaffolds. Cell Host Microbe 4:159-169.

Kun D, Xiang-Lin C, Ming Z, Qi L. 2013. Chlamydia inhibit host cell apoptosis by inducing Bag-1 via the MAPK/ERK survival pathway. Apoptosis 18:1083-1092.

Kurihara Y, Itoh R, Shimizu A, Walenna NF, Chou B, Ishii K, Soejima T, Fujikane A, Hiromatsu K. 2019. Chlamydia trachomatis targets mitochondrial dynamics to promote intracellular survival and proliferation. Cell Microbiol 21:e12962.

LaBrie SD, Dimond ZE, Harrison KS, Baid S, Wickstrum J, Suchland RJ, Hefty PS. 2019. Transposon Mutagenesis in Chlamydia trachomatis Identifies CT339 as a ComEC Homolog Important for DNA Uptake and Lateral Gene Transfer. mBio 10.

Lane BJ, Mutchler C, Al Khodor S, Grieshaber SS, Carabeo RA. 2008. Chlamydial entry involves TARP binding of guanine nucleotide exchange factors. PLoS Pathog 4:e1000014.

Li J, Yin HL, Yuan J. 2008. Flightless-I regulates proinflammatory caspases by selectively modulating intracellular localization and caspase activity. J Cell Biol 181:321-333.

Lochner A, Moolman JA. 2006. The many faces of H89: a review. Cardiovasc Drug Rev 24:261-274.

Lutter EI, Barger AC, Nair V, Hackstadt T. 2013. Chlamydia trachomatis inclusion membrane protein CT228 recruits elements of the myosin phosphatase pathway to regulate release mechanisms. Cell Rep 3:1921-1931.

Lutter EI, Martens C, Hackstadt T. 2012. Evolution and conservation of predicted inclusion membrane proteins in chlamydiae. Comp Funct Genomics 2012:362104.

Macdonald LJ, Graham JG, Kurten RC, Voth DE. 2014. Coxiella burnetii exploits host cAMP-dependent protein kinase signalling to promote macrophage survival. Cell Microbiol 16:146-159.

MacDonald LJ, Kurten RC, Voth DE. 2012. Coxiella burnetii alters cyclic AMP-dependent protein kinase signaling during growth in macrophages. Infect Immun 80:1980-1986.

Madeira F, Park YM, Lee J, Buso N, Gur T, Madhusoodanan N, Basutkar P, Tivey ARN, Potter SC, Finn RD, et al. 2019. The EMBL-EBI search and sequence analysis tools APIs in 2019. Nucleic Acids Res 47:W636-W641.

Malhotra M, Sood S, Mukherjee A, Muralidhar S, Bala M. 2013. Genital Chlamydia trachomatis: an update. Indian J Med Res 138:303-316.

Matsumoto A, Bessho H, Uehira K, Suda T. 1991. Morphological studies of the association of mitochondria with chlamydial inclusions and the fusion of chlamydial inclusions. J Electron Microsc (Tokyo) 40:356-363.

Mavillard F, Hidalgo J, Megias D, Levitsky KL, Velasco A. 2010. PKA-mediated Golgi remodeling during cAMP signal transmission. Traffic 11:90-109.

Mayinger P. 2011. Signaling at the Golgi. Cold Spring Harb Perspect Biol 3.

Mehlitz A, Banhart S, Hess S, Selbach M, Meyer TF. 2008. Complex kinase requirements for Chlamydia trachomatis Tarp phosphorylation. FEMS Microbiol Lett 289:233-240.

Mehlitz A, Banhart S, Maurer AP, Kaushansky A, Gordus AG, Zielecki J, Macbeath G, Meyer TF. 2010. Tarp regulates early Chlamydia-induced host cell survival through interactions with the human adaptor protein SHC1. J Cell Biol 190:143-157.

Meinkoth JL, Ji Y, Taylor SS, Feramisco JR. 1990. Dynamics of the distribution of cyclic AMP-dependent protein kinase in living cells. Proc Natl Acad Sci U S A 87:9595-9599.

Mirrashidi KM, Elwell CA, Verschueren E, Johnson JR, Frando A, Von Dollen J, Rosenberg O, Gulbahce N, Jang G, Johnson T, et al. 2015. Global Mapping of the Inc-Human Interactome Reveals that Retromer Restricts Chlamydia Infection. Cell Host Microbe 18:109-121.

Mital J, Hackstadt T. 2011a. Diverse requirements for SRC-family tyrosine kinases distinguish chlamydial species. mBio 2.

Mital J, Hackstadt T. 2011b. Role for the SRC family kinase Fyn in sphingolipid acquisition by chlamydiae. Infect Immun 79:4559-4568.

Mital J, Lutter EI, Barger AC, Dooley CA, Hackstadt T. 2015. Chlamydia trachomatis inclusion membrane protein CT850 interacts with the dynein light chain DYNLT1 (Tctex1). Biochem Biophys Res Commun 462:165-170.

Mital J, Miller NJ, Dorward DW, Dooley CA, Hackstadt T. 2013. Role for chlamydial inclusion membrane proteins in inclusion membrane structure and biogenesis. PLoS One 8:e63426.

Mital J, Miller NJ, Fischer ER, Hackstadt T. 2010. Specific chlamydial inclusion membrane proteins associate with active Src family kinases in microdomains that interact with the host microtubule network. Cell Microbiol 12:1235-1249.

Mohammad I, Arora PD, Naghibzadeh Y, Wang Y, Li J, Mascarenhas W, Janmey PA, Dawson JF, McCulloch CA. 2012. Flightless I is a focal adhesion-associated actin-capping protein that regulates cell migration. FASEB J 26:3260-3272.

Moulder JW. 1991. Interaction of chlamydiae and host cells in vitro. Microbiol Rev 55:143-190.

Mueller KE, Plano GV, Fields KA. 2014. New frontiers in type III secretion biology: the Chlamydia perspective. Infect Immun 82:2-9.

Mueller KE, Wolf K, Fields KA. 2016. Gene Deletion by Fluorescence-Reported Allelic Exchange Mutagenesis in Chlamydia trachomatis. mBio 7:e01817-01815.

Nguyen BD, Valdivia RH. 2012. Virulence determinants in the obligate intracellular pathogen Chlamydia trachomatis revealed by forward genetic approaches. Proc Natl Acad Sci U S A 109:1263-1268.

Nguyen PH, Lutter EI, Hackstadt T. 2018. Chlamydia trachomatis inclusion membrane protein MrcA interacts with the inositol 1,4,5-trisphosphate receptor type 3 (ITPR3) to regulate extrusion formation. PLoS Pathog 14:e1006911.

Nicholson TL, Olinger L, Chong K, Schoolnik G, Stephens RS. 2003. Global stage-specific gene regulation during the developmental cycle of Chlamydia trachomatis. J Bacteriol 185:3179-3189.

Nishizuka Y. 1995. Protein kinase C and lipid signaling for sustained cellular responses. FASEB J 9:484-496.

Nishizuka Y. 2001. The protein kinase C family and lipid mediators for transmembrane signaling and cell regulation. Alcohol Clin Exp Res 25:3S-7S.

Olive AJ, Haff MG, Emanuele MJ, Sack LM, Barker JR, Elledge SJ, Starnbach MN. 2014. *Chlamydia trachomatis*-induced alterations in the host cell proteome are required for intracellular growth. Cell Host Microbe 15:113-124.

Olson MG, Widner RE, Jorgenson LM, Lawrence A, Lagundzin D, Woods NT, Ouellette SP, Rucks EA. 2019. Proximity Labeling To Map Host-Pathogen Interactions at the Membrane of a Bacterium-Containing Vacuole in Chlamydia trachomatis-Infected Human Cells. Infect Immun 87.

Omsland A, Sager J, Nair V, Sturdevant DE, Hackstadt T. 2012. Developmental stage-specific metabolic and transcriptional activity of *Chlamydia trachomatis* in an axenic medium. Proc Natl Acad Sci U S A 109:19781-19785.

Parreno J, Fowler VM. 2018. Multifunctional roles of tropomodulin-3 in regulating actin dynamics. Biophys Rev 10:1605-1615.

Patel AL, Chen X, Wood ST, Stuart ES, Arcaro KF, Molina DP, Petrovic S, Furdui CM, Tsang AW. 2014. Activation of epidermal growth factor receptor is required for Chlamydia trachomatis development. BMC Microbiol 14:277.

Paul B, Kim HS, Kerr MC, Huston WM, Teasdale RD, Collins BM. 2017. Structural basis for the hijacking of endosomal sorting nexin proteins by Chlamydia trachomatis. Elife 6.

Paumet F, Wesolowski J, Garcia-Diaz A, Delevoye C, Aulner N, Shuman HA, Subtil A, Rothman JE. 2009. Intracellular bacteria encode inhibitory SNARE-like proteins. PLoS One 4:e7375.

Pearce LR, Komander D, Alessi DR. 2010. The nuts and bolts of AGC protein kinases. Nat Rev Mol Cell Biol 11:9-22.

Peterman EE, Taormina P, 2nd, Harvey M, Young LH. 2004. Go 6983 exerts cardioprotective effects in myocardial ischemia/reperfusion. J Cardiovasc Pharmacol 43:645-656.

Pettengill MA, Lam VW, Ojcius DM. 2009. The danger signal adenosine induces persistence of chlamydial infection through stimulation of A2b receptors. PLoS One 4:e8299.

Rahnama M, Fields KA. 2018. Transformation of Chlamydia: current approaches and impact on our understanding of chlamydial infection biology. Microbes Infect 20:445-450.

Rajalingam K, Sharma M, Lohmann C, Oswald M, Thieck O, Froelich CJ, Rudel T. 2008. Mcl-1 is a key regulator of apoptosis resistance in Chlamydia trachomatis-infected cells. PLoS One 3:e3102.

Resnikoff S, Pascolini D, Etya'ale D, Kocur I, Pararajasegaram R, Pokharel GP, Mariotti SP. 2004. Global data on visual impairment in the year 2002. Bull World Health Organ 82:844-851.

Reyland ME. 2009. Protein kinase C isoforms: Multi-functional regulators of cell life and death. Front Biosci (Landmark Ed) 14:2386-2399.

Rockey DD, Heinzen RA, Hackstadt T. 1995. Cloning and characterization of a Chlamydia psittaci gene coding for a protein localized in the inclusion membrane of infected cells. Mol Microbiol 15:617-626.

Rockey DD, Scidmore MA, Bannantine JP, Brown WJ. 2002. Proteins in the chlamydial inclusion membrane. Microbes Infect 4:333-340.

Rzomp KA, Moorhead AR, Scidmore MA. 2006. The GTPase Rab4 interacts with Chlamydia trachomatis inclusion membrane protein CT229. Infect Immun 74:5362-5373.

Sah P, Nelson NH, Shaw JH, Lutter EI. 2019. Chlamydia trachomatis recruits protein kinase C during infection. Pathog Dis 77.

Sahni SK, Rydkina E. 2009. Host-cell interactions with pathogenic Rickettsia species. Future Microbiol 4:323-339.

Sahni SK, Turpin LC, Brown TL, Sporn LA. 1999. Involvement of protein kinase C in *Rickettsia rickettsii*-induced transcriptional activation of the host endothelial cell. Infect Immun 67:6418-6423.

Schaab C, Geiger T, Stoehr G, Cox J, Mann M. 2012. Analysis of high accuracy, quantitative proteomics data in the MaxQB database. Mol Cell Proteomics 11:M111 014068.

Schachter J. 1999. In R. S. Stephens (ed.),Chlamydia: intracellular biology, pathogenesis, and immunity. Washington, DC: ASM Press.

Scidmore-Carlson MA, Shaw EI, Dooley CA, Fischer ER, Hackstadt T. 1999. Identification and characterization of a Chlamydia trachomatis early operon encoding four novel inclusion membrane proteins. Mol Microbiol 33:753-765.

Scidmore MA, Hackstadt T. 2001. Mammalian 14-3-3beta associates with the Chlamydia trachomatis inclusion membrane via its interaction with IncG. Mol Microbiol 39:1638-1650.

Sharma M, Rudel T. 2009. Apoptosis resistance in Chlamydia-infected cells: a fate worse than death? FEMS Immunol Med Microbiol 55:154-161.

Shaw EI, Dooley CA, Fischer ER, Scidmore MA, Fields KA, Hackstadt T. 2000. Three temporal classes of gene expression during the Chlamydia trachomatis developmental cycle. Mol Microbiol 37:913-925.

Shaw JH, Key CE, Snider TA, Sah P, Shaw EI, Fisher DJ, Lutter EI. 2018. Genetic Inactivation of Chlamydia trachomatis Inclusion Membrane Protein CT228 Alters MYPT1 Recruitment, Extrusion Production, and Longevity of Infection. Front Cell Infect Microbiol 8:415.

Shivshankar P, Lei L, Wang J, Zhong G. 2008. Rottlerin inhibits chlamydial intracellular growth and blocks chlamydial acquisition of sphingolipids from host cells. Appl Environ Microbiol 74:1243-1249.

Siegl C, Prusty BK, Karunakaran K, Wischhusen J, Rudel T. 2014. Tumor suppressor p53 alters host cell metabolism to limit Chlamydia trachomatis infection. Cell Rep 9:918-929.

Sixt BS, Bastidas RJ, Finethy R, Baxter RM, Carpenter VK, Kroemer G, Coers J, Valdivia RH. 2017. The Chlamydia trachomatis Inclusion Membrane Protein CpoS Counteracts STING-Mediated Cellular Surveillance and Suicide Programs. Cell Host Microbe 21:113-121.

Sixt BS, Nunez-Otero C, Kepp O, Valdivia RH, Kroemer G. 2019. Chlamydia trachomatis fails to protect its growth niche against pro-apoptotic insults. Cell Death Differ 26:1485-1500.

Sixt BS, Valdivia RH. 2016. Molecular Genetic Analysis of Chlamydia Species. Annu Rev Microbiol 70:179-198.

Skalhegg BS, Tasken K. 2000. Specificity in the cAMP/PKA signaling pathway. Differential expression,regulation, and subcellular localization of subunits of PKA. Front Biosci 5:D678-693.

Stanhope R, Flora E, Bayne C, Derre I. 2017. IncV, a FFAT motif-containing Chlamydia protein, tethers the endoplasmic reticulum to the pathogen-containing vacuole. Proc Natl Acad Sci U S A 114:12039-12044.

Stephens RS. 2003. The cellular paradigm of chlamydial pathogenesis. Trends Microbiol 11:44-51.

Stephens RS, Kalman S, Lammel C, Fan J, Marathe R, Aravind L, Mitchell W, Olinger L, Tatusov RL, Zhao Q, et al. 1998. Genome sequence of an obligate intracellular pathogen of humans: Chlamydia trachomatis. Science 282:754-759.

Su H, McClarty G, Dong F, Hatch GM, Pan ZK, Zhong G. 2004. Activation of Raf/MEK/ERK/cPLA2 signaling pathway is essential for chlamydial acquisition of host glycerophospholipids. J Biol Chem 279:9409-9416.

Subbarayal P, Karunakaran K, Winkler AC, Rother M, Gonzalez E, Meyer TF, Rudel T. 2015. EphrinA2 receptor (EphA2) is an invasion and intracellular signaling receptor for Chlamydia trachomatis. PLoS Pathog 11:e1004846.

Suchland RJ, Rockey DD, Bannantine JP, Stamm WE. 2000. Isolates of Chlamydia trachomatis that occupy nonfusogenic inclusions lack IncA, a protein localized to the inclusion membrane. Infect Immun 68:360-367.

Sun Q, Yong X, Sun X, Yang F, Dai Z, Gong Y, Zhou L, Zhang X, Niu D, Dai L, et al. 2017. Structural and functional insights into sorting nexin 5/6 interaction with bacterial effector IncE. Signal Transduct Target Ther 2:17030.

Tam JE, Davis CH, Wyrick PB. 1994. Expression of recombinant DNA introduced into Chlamydia trachomatis by electroporation. Can J Microbiol 40:583-591.

Tasken K, Aandahl EM. 2004. Localized effects of cAMP mediated by distinct routes of protein kinase A. Physiol Rev 84:137-167.

Toth A, Kiss E, Gergely P, Walsh MP, Hartshorne DJ, Erdodi F. 2000. Phosphorylation of MYPT1 by protein kinase C attenuates interaction with PP1 catalytic subunit and the 20 kDa light chain of myosin. FEBS Lett 484:113-117.

Tse SM, Mason D, Botelho RJ, Chiu B, Reyland M, Hanada K, Inman RD, Grinstein S. 2005. Accumulation of diacylglycerol in the Chlamydia inclusion vacuole: possible role in the inhibition of host cell apoptosis. J Biol Chem 280:25210-25215.

Verbeke P, Welter-Stahl L, Ying S, Hansen J, Hacker G, Darville T, Ojcius DM. 2006. Recruitment of BAD by the Chlamydia trachomatis vacuole correlates with host-cell survival. PLoS Pathog 2:e45.

Verma A, Maurelli AT. 2003. Identification of two eukaryote-like serine/threonine kinases encoded by Chlamydia trachomatis serovar L2 and characterization of interacting partners of Pkn1. Infect Immun 71:5772-5784.

Wang T, Chuang TH, Ronni T, Gu S, Du YC, Cai H, Sun HQ, Yin HL, Chen X. 2006. Flightless I homolog negatively modulates the TLR pathway. J Immunol 176:1355-1362.

Wang Y, Kahane S, Cutcliffe LT, Skilton RJ, Lambden PR, Clarke IN. 2011. Development of a transformation system for Chlamydia trachomatis: restoration of glycogen biosynthesis by acquisition of a plasmid shuttle vector. PLoS Pathog 7:e1002258.

Ward NE, O'Brian CA. 1992. Kinetic analysis of protein kinase C inhibition by staurosporine: evidence that inhibition entails inhibitor binding at a conserved region of the catalytic domain but not competition with substrates. Mol Pharmacol 41:387-392.

Weber MM, Bauler LD, Lam J, Hackstadt T. 2015. Expression and localization of predicted inclusion membrane proteins in Chlamydia trachomatis. Infect Immun 83:4710-4718.

Weber MM, Lam JL, Dooley CA, Noriea NF, Hansen BT, Hoyt FH, Carmody AB, Sturdevant GL, Hackstadt T. 2017. Absence of Specific Chlamydia trachomatis Inclusion Membrane Proteins Triggers Premature Inclusion Membrane Lysis and Host Cell Death. Cell Rep 19:1406-1417.

Wesolowski J, Weber MM, Nawrotek A, Dooley CA, Calderon M, St Croix CM, Hackstadt T, Cherfils J, Paumet F. 2017. Chlamydia Hijacks ARF GTPases To Coordinate Microtubule Posttranslational Modifications and Golgi Complex Positioning. mBio 8.

Wickstrum J, Sammons LR, Restivo KN, Hefty PS. 2013. Conditional gene expression in Chlamydia trachomatis using the tet system. PLoS One 8:e76743.

Wolf K, Rahnama M, Fields KA. 2019. Genetic Manipulation of Chlamydia trachomatis: Chromosomal Deletions. Methods Mol Biol 2042:151-164.

Wong W, Scott JD. 2004. AKAP signalling complexes: focal points in space and time. Nat Rev Mol Cell Biol 5:959-970.

Wu-Zhang AX, Newton AC. 2013. Protein kinase C pharmacology: refining the toolbox. Biochem J 452:195-209.

Wyrick PB. 2000. Intracellular survival by *Chlamydia*. Cell Microbiol 2:275-282.

Xiao Y, Zhong Y, Greene W, Dong F, Zhong G. 2004. *Chlamydia trachomatis* infection inhibits both Bax and Bak activation induced by staurosporine. Infect Immun 72:5470-5474.

Xu S, Battaglia L, Bao X, Fan H. 2013. Chloramphenicol acetyltransferase as a selection marker for chlamydial transformation. BMC Res Notes 6:377.

Yamashiro S, Gokhin DS, Kimura S, Nowak RB, Fowler VM. 2012. Tropomodulins: pointed-end capping proteins that regulate actin filament architecture in diverse cell types. Cytoskeleton (Hoboken) 69:337-370.

Yang C, Starr T, Song L, Carlson JH, Sturdevant GL, Beare PA, Whitmire WM, Caldwell HD. 2015. Chlamydial Lytic Exit from Host Cells Is Plasmid Regulated. mBio 6:e01648-01615.

Zadora PK, Chumduri C, Imami K, Berger H, Mi Y, Selbach M, Meyer TF, Gurumurthy RK. 2019. Integrated Phosphoproteome and Transcriptome Analysis Reveals Chlamydia-Induced Epithelial-to-Mesenchymal Transition in Host Cells. Cell Rep 26:1286-1302 e1288.

Zhu H, Shen Z, Luo H, Zhang W, Zhu X. 2016. Chlamydia Trachomatis Infection-Associated Risk of Cervical Cancer: A Meta-Analysis. Medicine (Baltimore) 95:e3077.

Zuck M, Hybiske K. 2019. The Chlamydia trachomatis Extrusion Exit Mechanism Is Regulated by Host Abscission Proteins. Microorganisms 7.

VITA

Prakash Sah

Candidate for the Degree of

Doctor of Philosophy

Dissertation: HOST KINASES IN CHLAMYDIA TRACHOMATIS DEVELOPMENT AND INTERACTIONS OF INCLUSION MEMBRANE PROTEIN CT226

Major Field: Microbiology, Cell and Molecular Biology

Biographical:

Education:

Completed the requirements for the Doctor of Philosophy in Microbiology, Cell and Molecular Biology at Oklahoma State University, Stillwater, Oklahoma in December, 2020.

Completed the requirements for the Master of Science in Microbiology at Tribhuvan University, Kathmandu, Nepal in 2012.

Completed the requirements for the Bachelor of Science in Microbiology at Tribhuvan University, Kathmandu, Nepal in 2007.

Experience:

1. Research Assistant/Teaching Assistant in the Department of Microbiology and Molecular Genetics, Oklahoma State University, August 2015- December 2020
2. Lecturer in the Department of Microbiology, Universal College of Medical Sciences, Bhairahawa, Nepal, December 2011- June 2015

Professional Memberships:

American Society of Microbiology (2016-present)